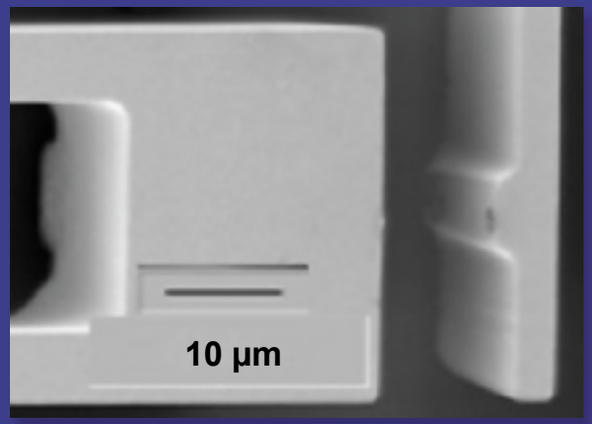

A large range of microsystems is being used or investigated for a variety of implantable applications. The bi-stable micro electro mechanical switch targeted at implantable programmable electrode application as described in this thesis has a contact resistance of 5Ω, a breakdown voltage between the two contact members in OFF state of 300V, and only needs 0.2nJ to change state. The accompanying hermetic wafer level glass silicon stack with feedthroughs bonded at 250N, 230V, 365°C pass thermal and mechanical stress tests according to MIL-STD-883. Contact measurements carried out in an N_2 atmosphere inside the wafer level package demonstrate that ruthenium covered contacts are robust for 10^6 cycles. MEMS reliability is treated in the context of a general framework for quantitative reliability. The electrical method to measure resonance is applicable for automated reliability screening during manufacturing. A 125µs pulse is sufficient to switch from OFF to ON state. The required pulse amplitude is not influenced by the pulse width. The bi-stable MEMS switch has advantages in comparison to a FET switch in the area of power consumption, DC breakdown voltage, leakage current and contact resistance.

R.A.M. Receveur Implantable MST: MEMS Switch 2007

R.A.M. Receveur

Micro System Technologies for Implantable Applications:

Bi-Stable MEMS Switch

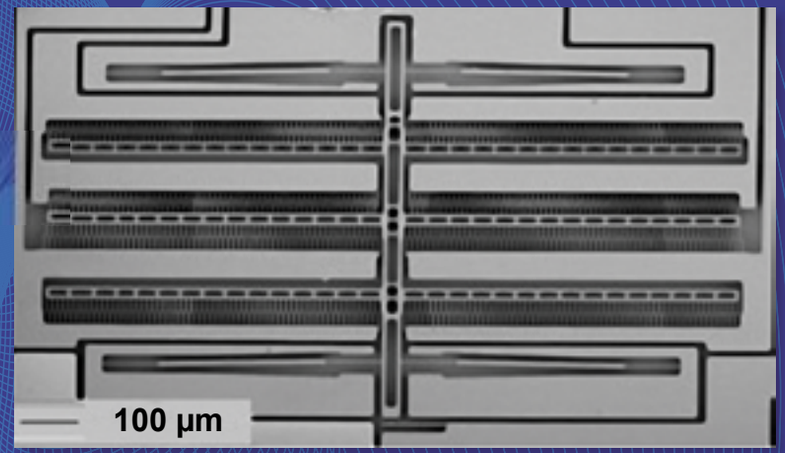

Institute of Microtechnology (IMT)
University of Neuchâtel
Switzerland

Front cover: Scanning Electron Microscope (SEM) picture of the bi-stable MEMS switch. Back cover: SEM picture of the two contact members of the bi-stable MEMS switch.

Micro System Technologies for Implantable Applications: Bi-Stable MEMS Switch

Dissertation

submitted to the Faculty of Sciences of the University of Neuchâtel in fulfillment of the requirements for the degree of Doctor of Science

by

Rogier Alphons Maurice Receveur
Ir. Delft University of Technology, Applied Physics

Institute of Microtechnology
University of Neuchâtel
Rue Jaquet-Droz 1
2007 Neuchâtel
Switzerland

2007

Université de Neuchâtel uni

FACULTE DES SCIENCES
Secrétariat-Décanat de la faculté
- Rue Emile-Argand 11
- CP 158
- CH-2009 Neuchâtel

IMPRIMATUR POUR LA THESE

Micro System Technologies for Implantable Applications : Bi-Stable MEMS Switch

Rogier RECEVEUR

UNIVERSITE DE NEUCHATEL

FACULTE DES SCIENCES

La Faculté des sciences de l'Université de Neuchâtel,
sur le rapport des membres du jury

MM. N. de Rooij (directeur de thèse), H. Hügli, W. Noell,
H. Shea (EPF Lausanne),
F. Lindemans (Medtronic Bakken Research Center, Maastricht, NL)
et P. Weiss (Colibrys SA, Neuchâtel)

autorise l'impression de la présente thèse.

Neuchâtel, le 23 août 2007

Le doyen :
T. Ward

UNIVERSITE DE NEUCHATEL
FACULTE DES SCIENCES
Secrétariat-décanat de la faculté
Rue Emile-Argand 11 - CP 158
CH-2009 Neuchâtel

■ Téléphone : +41 32 718 21 00 ■ Fax : +41 32 718 21 03 ■ E-mail : secretariat.sciences@unine.ch ■ www.unine.ch/sciences

Abstract

Typical properties of micro systems like small size and low power consumption are advantageous for implantable applications. An overview from literature is given as an extended introduction to the MEMS switch portion of the thesis. A large range of microsystems is being used or investigated for a variety of implantable applications. The major technology-market combinations are Sensors for Cardiovascular-, Drug Delivery for Drug Delivery- and Electrodes for Neurological- and Ophthalmologic-applications. Together these form 51% of all end items. Packaging, interconnection, coatings, power supply, communication and material aspects are described. Electrical stimulation therapies require precisely targeted stimulation, ability to do so during the lifetime of a patient and a simple therapy delivery procedure. Adding electrodes using existing technology would increase the size of the connector block, the lead-diameter and -stiffness. The core of this thesis deals with a novel bi-stable MEMS switch that is proposed for electrode multiplexing. Basic device- and micro contact properties are measured and compared to theory. The Au/Ni coated bi-stable MEMS switch has a contact resistance of 5Ω, can handle a current of 250mA, has a breakdown voltage between the two contact members in OFF state of 300V and only needs 0.2nJ to change state. All the measured results were within 10% of the theoretical expectations. A wafer level process for hermetic sealing of the switch with feedthroughs is presented. This package enables fragile MEMS structure protection, electrical connection, stabilization of switch properties, small size and low cost at the same time. Wafer level glass silicon stacks bonded at 250 kg, 230 V, 365 ºC pass thermal and mechanical stress tests according to MIL-STD-883 and meet the requirements for biomedical applications. Contact measurements carried out in an N_2 atmosphere inside the wafer level package demonstrate that ruthenium covered contacts are robust for 10^6 cycles. A literature review of existing MEMS switches (mono and bi stable) as well as the available wafer level packaging options is given. MEMS reliability is treated in the context of a general framework for quantitative reliability. The measured dynamical switch properties are compared to theory and the relation to switch reliability is discussed. The electrical method to measure resonance is applicable for automated reliability screening during manufacturing. A 125µs pulse is sufficient to switch from OFF to ON state. The required pulse amplitude is not influenced by the pulse width. The bi-stable MEMS switch has advantages in comparison to a FET switch in the area of power consumption, DC breakdown voltage, leakage current and contact resistance. Further possible future developments could be in the area of MEMS control, chip scale implantable medical devices and micro electrodes.

Table of Contents

Abstract

1 Introduction

1.1 Electrical stimulation 1
1.2 Bi-Stable MEMS switch 3
1.3 Outline of the thesis 4

2 Micro System Technologies for Implantable Applications

2.1 Introduction 7
2.2 Overview of implantable microsystems 10
2.2.1 Sensors 11
2.2.2 Electrical Stimulation and Sensing 26
2.2.3 Micromachined drug and gene delivery devices 33
2.2.4 Micromachined ultrasound transducers 35
2.2.5 Micro Opto Electro Mechanical Systems (MOEMS) 36
2.2.6 Other Micro System Devices for Implantable Applications 37
2.2.7 Summary of Implantable Microsystems 38
2.3 Overview of basic technological building blocks 52
2.3.1 Processing 52
2.3.2 Packaging 53
2.3.3 Power 55
2.3.4 Communication 56
2.3.5 Materials 57
2.4 Implantable Microsystems: a case study 58
2.4.1 Sick Sinus Syndrome 58
2.4.2 Implantable Microsystems for Sick Sinus Syndrome 59
2.5 Discussion 61
2.6 Summary 63
2.7 References 66

3 Laterally Moving Bi-Stable MEMS DC-Switch
3.1 Introduction 103
3.2 Materials and methods 111
3.2.1 Fabrication Process 111
3.2.2 Design 113
3.2.3 Experimental setup 116
3.3 Theory 119
3.3.1 Electrostatic actuators 119
3.3.2 Mechanical system 119
3.3.3 Dynamics 121
3.3.4 Micro contact 122
3.4 Results and discussion 124
3.4.1 Design choices 124
3.4.2 Verification of basic properties 125
3.4.3 Bi-stable switch properties 129
3.4.4 Micro contact properties 132
3.5 Conclusion and outlook 134
3.6 References 135

4 Wafer level hermetic package and device testing of the bi-stable MEMS switch
4.1 Introduction 138
4.2 Packaging and interconnect 141
4.2.1 Hermetic seal 142
4.2.2 Hermiticity 143
4.2.3 Hermetic feedthrough 144
4.3 Materials and methods 145
4.3.1 Design and fabrication process 145
4.3.2 Experiment, theory and simulation 147
4.4 Results and discussion 148
4.4.1 Bond quality 149
4.4.2 Micro contact properties 155
4.5 Conclusion 159
4.6 References 160

5 Analysis of the dynamics of the bi-stable MEMS switch
5.1 Reliability 164
5.1.1 Reliability Theory 164
5.1.2 Essential Requirements Active Implantable Medical Devices 166
5.1.3 MEMS reliability 167
5.1.4 Micro contact failure mechanisms 169
5.2 Switch dynamics 171
5.2.1 Bi-stable MEMS switch 171
5.2.2 Resonance 175
5.2.3 Bouncing 177
5.2.4 Numerical Simulation 178
5.3 Results 181
5.3.1 Resonance 181
5.3.2 Bouncing 190
5.4 Discussion 190
5.5 Conclusion 192
5.6 References 193
6 Discussion and Outlook of the Bi-Stable MEMS switch
6.1 MEMS switch versus FET 196
6.1.1 Power consumption 196
6.1.2 DC Breakdown 197
6.1.3 Electrostatic Discharge (ESD) 197
6.1.4 Leakage current 198
6.1.5 MEMS switch vs. FET switch 198
6.1.6 Recommendations 199
6.2 MEMS control 200
6.2.1 MEMS IC interconnect 200
6.2.2 High Voltage MEMS control 204
6.3 System level aspects 206
6.4 Conclusion 206
6.5 References 207
7 Final Conclusions 214
Acknowledgements
Bibliography, Biography

1 Introduction

1.1 Electrical stimulation

Electrical stimulation therapies can alleviate pain, restore health and/or extend life for a large range of clinical conditions. In general an electrical stimulus is generated inside an Implantable Pulse Generator (IPG) and delivered to a specific anatomical location through a stimulation electrode. The electrode is connected to the IPG via a lead that contains lead conductors. The electrical pulse thus delivered creates a desired clinical effect. Successful examples of implantable electrical stimulation devices are cardiac pacemakers for slow beating hearts, cardiac resynchronization devices for heart failure (HF), implantable cardioverter defibrillators (ICD) for sudden cardiac death prevention, Implantable Neuro Stimulators (INS) to treat chronic pain (Spincal Cord Stimulation, SCS), essential tremor (Deep Brain Stimulation, DBS) or urinary incontinence and cochlear stimulation to restore hearing. Implantable devices for electrical stimulation represent a multi billion dollar value for the healthcare system.

In general it can be stated that all electrical stimulation therapies require precisely targeted stimulation of a specific anatomical site. Secondly, there is a need to maintain the ability to do so during the lifetime of a patient. This includes dealing with changes in patient condition (possibly due to the therapy itself) or changes in the device condition like displacements of the electrodes. Finally, the therapy delivery procedure should be as simple as possible. This will reduce the risk of errors and minimize the burden on the scarce physician time, thus increasing the acceptance and the range of patients that can

benefit. In this work it is proposed to address these needs by adding more electrodes to the implantable device.

There are certain constraints that make the addition of many more electrodes difficult when using existing technology. The size of the connector block that provides the interface between IPG and lead would increase, while it already forms a significant part of the total volume of the IPG with the current number of electrodes. Likewise adding lead conductors to the leads to address the additional electrodes would increase the lead diameter and stiffness. These trends are against the general drive of reducing size of the implantable devices to minimize impact on the patient. A possible solution that is not limited by the constraints just described is to incorporate an electrode multiplexer in the stimulation system.

An electrode multiplexer has the ability to direct a single incoming stimulation pulse from the IPG to a plurality of electrodes at the stimulation site (see Figure 1.1). When incorporated into a lead, such a system would typically consist of a power source, logic, packaging and switches.

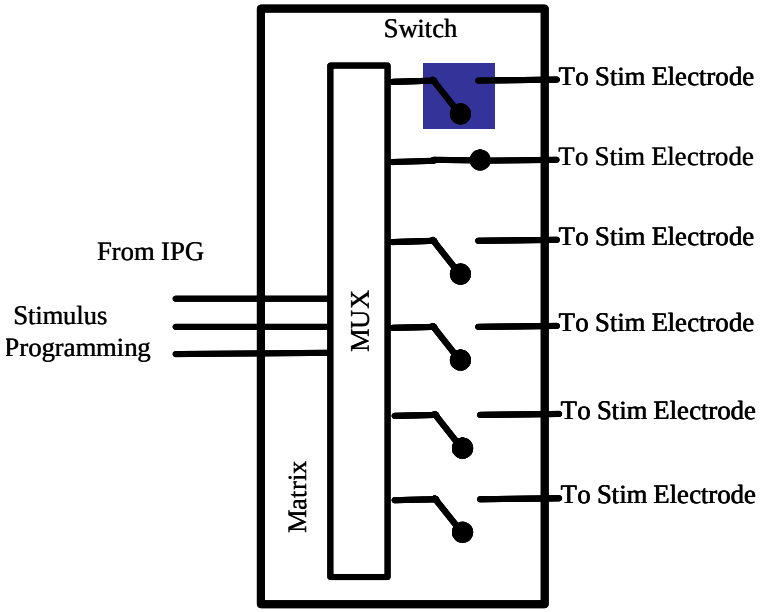

Figure 1.1 Schematic of the use of multiplexing (MUX) to address a multitude of Stim Electrodes from a limited number of Stimulus wires coming from the Implantable Pulse Generator (IPG). Programming information to set the status of the switches is also coming from the IPG. The top switch is indicated by the filled circle, the second switch from the top is drawn in closed position.

1.2 Bi-Stable MEMS switch

In the preceding section it has been explained that switches are an enabling ingredient for a multiplexed electrical stimulation system. Typical requirements for such switches are low power consumption, small size, low resistance, high reliability, biocompatibility and hermetic packaging possibility. Low power consumption relates to the fact that most implanted devices today are operating on a limited energy supply, and hence the lower the power consumption, the longer the device longevity. This is of course beneficial to the patient. As stated already above, the

smaller the size of the implant, the better for the patient. High reliability is very important, especially in cases where the patient's life depends on the device, but in general also because replacing a defective device submits the patient to a surgical procedure. A low resistance will keep the energy dissipated in the switch to a minimum, leaving most of the energy for the therapy.

Bi-stable MEMS (Micro Electro Mechanical System) switches are stable in the ON and in the OFF state. Once brought in a specific state, they stay in that state without using any energy. To change the state, a small amount of energy is required. This type of switches offer advantages precisely on the points mentioned above in comparison to Field Effect Transistor (FET) switches. The development and subsequent experiments with a novel bi-stable MEMS switch and related aspects targeted at the described application form the core of this thesis.

1.3 Outline of the thesis

The overall structure of this thesis is graphically illustrated in Figure 1.2.

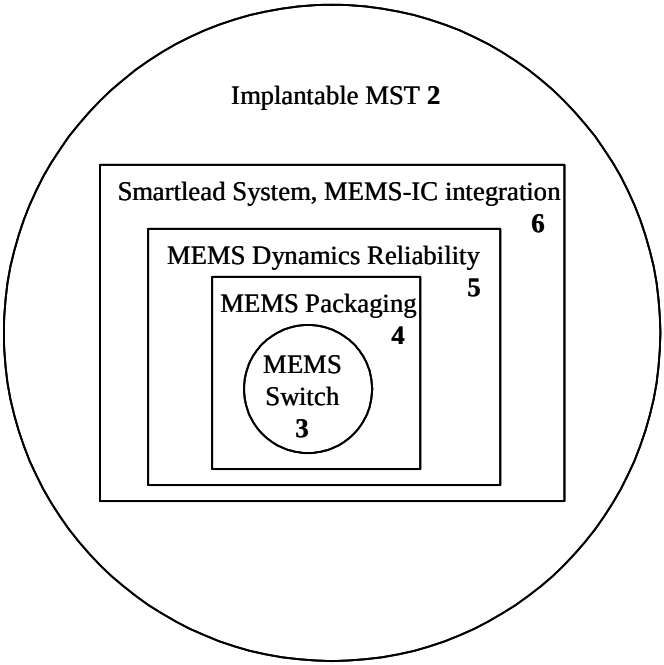

Figure 1.2 Schematic graphical representation of the thesis structure. The various blocks represent chapters of this thesis, indicated by an abbreviated chapter name and chapter number in bold. Chapter 2 can be read as an extended introduction to this thesis. The smartlead system as introduced in this chapter is then build up in a bottom up fashion, starting from the core bi-stable MEMS switch and proceeding towards the total system. See text below for more introductory text.

Since small size and low power consumption are typical characteristics of micro systems and since these are also typical requirements for implantable applications, this switch is not the only example of implantable microsystems. On the contrary, the field has taken of in the early eighties and has been growing ever since, resulting in hundreds of examples in various states in the product life cycle at the present time. To place the work on the

MEMS switch in perspective, Chapter 2 provides a general and broad overview of the literature on implantable microsystems.

The bi-stable MEMS switch is described in Chapter 3. The design, operating principle, theory and manufacturing process will be presented as well as experimental results. This chapter also includes an overview of MEMS switches (mono- and bi-stable) as described in literature.

The design, manufacture and experiments with hermetic sealing and feedthroughs of the switch at wafer level are presented in Chapter 4, including a brief review of available packaging options as described in literature. Results of device tests carried out inside these packages are given as well in that chapter.

Besides low power and small size, reliability is a major requirement for medical devices, especially for life saving applications. A lot of work exists about MEMS reliability, but every MEMS structure is unique and needs its own approach. Chapter 5 provides a theoretical basis for a quantitative approach towards reliability, provides typical reliability requirements for Active Implantable Medical Devices (AIMD), provides a discussion on reliability issues typical for MEMS and then treats the bi-stable MEMS switch failure mechanisms. The chapter ends with a more detailed experimental and theoretical treatment of the dynamics of the switch.

In the discussion and outlook chapter (chapter 6) the advantages of the bi-stable MEMS switch in comparison to a FET switch are recapitalized. The outlook reviews options for MEMS control at various levels of integration and comments on system level aspects of the Smartlead. Final conclusions are given in chapter 7.

2 Micro System Technologies for Implantable Applications

In this chapter a general and broad overview of micro systems for implantable applications as found in literature will be provided. Sensors, micro electrodes, drug and gene delivery devices, micro machined ultrasound transducers, MOEMS, micro actuators, surgical tools, micro surface topology, micro fabricated bio degradable scaffolds and others are being used or investigated in a wide range of clinical areas including cardiology, neurology, ophthalmology, orthopedics, drug delivery (for various clinical areas), surgery, endocrinology, tissue engineering etcetera. The information will be ordered by applying a classification scheme. A general overview of packaging, communication, power and materials -the major underlying technical blocks needed to produce implantable micro devices- will also be provided.

2.1 Introduction

Micro System Technologies have become the basis of a large industry with total sales of MST manufacturers exceeding US$5B, continuous growth for the past 10 years and main applications in automotive and communication markets. The field was firmly established in the early eighties with the first mass produced micro machined pressure sensor, an international conference and a review paper and it was pioneered in the early seventy's [1]. There have been an increasing number of publications in MST journals with the keyword "medical" taking off from a rather constant (low) level around 1985.

This chapter has been published for the most part in the Journal of Micromechanics and Microengineering authored by Rogier A M Receveur, Fred W Lindemans and Nico F de Rooij [304]

Advantages of MST compared to other technologies provide opportunities for application in implantable biomedical devices. Developments in these devices are driven by the desire to better mimic normal physiology and to improve quantity and quality of life. Major healthcare challenges like the aging population, patient centered care and affordable costs can be well addressed by MST [2,3,4,5].

According literature, MST offers opportunities ranging from extending human functions [6] to using it as a disruptive technology with enormous commercial potential[7]. Advantages of MST for biomedical applications are small size[8,9,10,11,1,7,4,5,2]; low weight[8,10,11,1]; high reliability[8,1,12]; low power[8,11,7,12]; low cost[8,9,2,11,1,7,12]; superior functionality or performance [9,1,7,12,4,2,11,10] and MST can be combined with biotechnology and molecular biology[13]. In other words, MST provide unique opportunities and will have major impact on domains including medicine[9,3,1,4,14].

Products made with microtechnology now exist in all phases of the development cycle, including volume manufacturing and they are being used in lots of medical applications that are on the market already [15]. There are numerous examples of Micro System Technologies for Biomedical Applications in almost all areas of medicine including diagnostics and monitoring [14,8,5,7], drug delivery [14,8,16], neurology [14,3,7], surgery [14,8,15], audiology [8] and cardiology [8,7].

There are also many challenges for (micro fabricated) biomedical devices including reliability [8,17,2], packaging[2,18,19,1,7,4], bio-compatibility and –stability [20,18,19,7,17,9,1], the absence of a mass market driver [1,7,4] and long development times [21,4,1].

The opportunities sketched above have led to the idea to perform a literature review of MST for implantable applications in order to investigate what is reality and what is promise. A number of excellent literature reviews exists focusing on specific technological categories or clinical areas [22,23,14,24,25,26,27,28,29,30]. This chapter provides a general and broad overview of implantable MST as reported in the literature. It is focused on the technical domain but it is not a comprehensive guide on "how to design and manufacture an implantable microsystem", it does not provide a detailed clinical background and it is not a business analysis. The overview ends with a table were all applications are classified and a description of the observations that can be made from this table. To deal with the enormous amount of technical aspects of microsystems for a variety of applications and still stay within the scope of a thesis chapter the following approach has been chosen. The key technological concepts for specific applications have been summarized as briefly as possible in the body text of section 2.2. Technological aspects common to a complete class of microsystems are presented in general terms at the start of each section dealing with that class (see Table 2.1). Basic technological building blocks relevant for all implantable applications of microsystems are described in a separate section (section 2.3, see Table 2.1). Finally a case study of one clinical condition is presented and the role that microsystems play in treating that disease (section 2.4).

Table 2.1 Graphical representation of the description of technological aspects of implantable microsystems in this chapter. The MST class forms the main structure of section 2.2. Technological aspects that are specific for a complete MST class (indicated as Specific Technology on the left side of the first column) are described in section 2.2. Technologies that are relevant for all MST classes (indicated as Building Blocks on the left side of the first column) are presented in general terms in section 2.3.

		MST class					
		Sensors	Electrical	Drug Delivery	MOEMS	Ultrasound	Other
Specific Technology	Sensors	V					
	Electrical		V				
	Drug Delivery			V			
	MOEMS				V		
	Ultrasound					V	
	Other						V
Building Blocks	Processing	V	V	V	V	V	V
	Packaging	V	V	V	V	V	V
	Communication	V	V	V	V	V	V
	Power	V	V	V	V	V	V
	Materials	V	V	V	V	V	V

2.2 Overview of implantable microsystems

An implantable medical device is considered any device that is intended to function inside the body for some time (further defined in section 2.2.7). Literature gives various definitions of what a microsystem is [31,1,4]. In this chapter, a micro system is loosely defined as a device that contains at least one part that is made using IC-like fabrication technology with dimensions in the order of micrometers. The aim of this section is to give a global overview of which microsystems are being used and how they are clinically applied. The focus is on the micro fabricated part of the total microsystem. Therefore the information presented in this section is grouped according to corresponding types of micro fabricated parts. The focus is also on implantable micro systems not enclosed by a hermetic metal can. The clinical need for these microsystems is mentioned and the solution is placed in historical context. At the end of this section a summary and overall analysis of the information is provided.

2.2.1 Sensors

Implantable micro fabricated sensors are for example used to facilitate diagnosis or to provide a means to generate closed loop control of therapy. The following subsections are grouped per sensor type. Some products or concepts use multiple sensors at the same time. These are presented in the section 'other sensors'.

The most common type among pressure sensors is made using surface micromachining processes. A suspended thin mechanical membrane is created by etching a sacrificial layer. Membrane deflection caused by environmental pressure variations can be transduced with help of piezoresistors on the high strain areas of the membrane or conductors on both sides of the gap and appropriate electronic circuitry. Complementary Metal Oxide Semiconductor CMOS (CMOS) compatible micromachining processes allow integration of read out circuitry close to the sensor. Operating pressure ranges can be tuned towards the desired range by changing layer thickness and diameter. Accelerometers have a suspended mass that moves relative to its mechanical support by external acceleration. The same transducer versions as for pressure sensors (capacitive or piezoresistive) are used. Both bulk micromachining in combination with wafer bonding and surface micromachining techniques are used to manufacture accelerometers. The use of these two types of sensors for implantable applications can leverage the knowledge acquired by the Micro Electro Mechanical System (MEMS) industry from the high volume markets that exist today (millions of MEMS pressure- and acceleration- sensors are sold each year for non implantable applications). A variety of other less common sensors will be described. Power consumption, size, sensitivity, specificity, accuracy and stability are important design parameters for most implantable applications of sensors.

2.2.1.1 Pressure Sensors

Intra Ocular Pressure Sensors

Long term (continuous) intra ocular pressure (IOP) measurements offer new perspectives for patients suffering from glaucoma. Glaucoma is the loss of vision due to damage of the optic nerve for which elevated IOP is one of the risk factors. An implantable miniature pressure transensor was proposed in 1967[32] followed by a miniature pressure sensor system intended to fit in an artificial lens in 1990[33]. In 1998 an intraocular pressure sensor consisting of a coil on flex, flip chip pressure sensor and IC embedded in a lens was introduced [34,11]. Such a system is currently being commercialized. Another principle is to use a distributed parallel-resonant inductive-capacitive circuit, with a pressure-dependent resonance frequency. The high Q inductor is deposited by electro deposition of copper on a micromachined chip incorporating a pressure-sensitive diaphragm [35].

Intra Cranial Pressure Sensors

Patients suffering from head injury or diseases such as chronic hydrocephalus, brain tumors or abscesses may show an increase in intra cranial pressure (ICP). Continuous measurement using a wireless implanted system offers the advantage of increased mobility over catheter based systems [36], can reduce the mortality risk of intensive care patients[37] and allows to monitor ICP of patients after surgery to treat obstructive hydrocephalus [38]. In 1979 several patients were implanted with a differential pressure sensor incorporated with a shunt valve system using a resonant circuit in the sensor and a radio frequency detector outside the body for telemetry [39]. Eleven years later the same system was used to determine the quantitative relationship between changes in body position and ventricular fluid pressure in normal subjects and subjects with shunts [38]. In 1983 a long term monitoring technique was

presented [40]. A one-chip implanted device with micro coil operating through inductive coupling for both powering and read/write operation was used with success to read intra cranial pressure values in 1988 [41].

In 1995 an Implantable Telemetric Endo System (ITES) was developed by an interdisciplinary consortium of industrial and non-industrial partners[42]. Further developments used surface micromachined polysilicon membranes for capacitive absolute pressure detection and monolithic integrated circuitry. The sensor system was tested in vitro in 0.9% NaCl solution, showing excellent results compared to a commercially available reference sensor[37]. Eggers et al [43] made an argument for a non integrated approach, using a surface micro-machined capacitive absolute pressure sensor fabricated in an eight-mask Metal Oxide Semiconductor (MOS) - like process and two low-power Application Specific Integrated Circuits (ASICs) for capacitance change read-out and telemetric data and energy transmission. They used flip-chip mounting on a flexible substrate. The same system is also proposed for intraocular pressure[44]. In 1997 a fully implantable CMOS compatible pressure and temperature sensor on flex with ASIC with on chip coil for telemetry protected with silicone was made based on prior experience with catheter versions. This system used a switch between the sampling rates in order to capture special signal components in an emergency situation.[36,45].

An implantable telemetric pressure sensor system for long-term monitoring of therapeutic implants is currently being developed in the frame work of the European project Healthy Aims[46]. One of the clinical application areas mentioned is measurement of ICP. Other applications include measurement of IOP (see above) and monitoring pressure outside an aortic stent-graft placed to exclude aneurysms from blood flow (see below). The implanted part of the system consists of a measuring head made

of a pressure sensor and an interface IC connected to a telemetry unit by a conducting lead. The telemetry unit contains a transponder chip, micro controller and antenna coil [47]. An ICP system using a miniature strain gauge pressure sensor mounted in a titanium case at the tip of a 100cm flexible nylon tube is commercially available[48] and was clinically evaluated in 1998[49].

Cardio Vascular Pressure Sensors

The heart pumps blood through the body's vascular system and blood pressure at various anatomical positions contains clinically relevant information. Pressure proximal and distal to an occlusion can be measured to quantify its severity in terms of flow reserve [50]. It is also measured before and after a balloon catheter operation [51]. Pulmonary wedge pressure measured downstream of a temporarily occluded pulmonary artery is used to monitor patients with heart failure. This section starts by describing micro fabricated pressure sensors on catheters that have been proposed or developed to address these temporary needs and then progresses to examples of microsystems for continuous monitoring of cardiovascular pressure as found in literature.

Microfabricated pressure sensors on catheters offer advantages over fluid filled catheters with external transducers and are used on a regular basis in the clinic or for animal research [52]. They are not suffering from catheter whip, limited frequency response and resonance and due to their small size they can reach small places while yielding pressure readings comparable to reference sensors. In 1973 a patent was issued describing miniature strain gauges for measuring pressure variations at the tip of a catheter [53]. Other patents describe the use of piezo-resistive material [54]; a differential pressure measurement [55] and a miniature catheter tip measurement device with a pressure sensor of 0,4mm

x 0,9mm x 0,15mm (width x length x height) that is determining the total diameter [56]. This company is currently making pressure-conductance catheters used for mouse experiments. Another company produces conductance catheters with pressure sensors. The transducer consists of a miniature strain gauge pressure sensor mounted in a titanium case at the tip of a 100cm flexible nylon tube [49]. Two multiplexed pressure sensors operated via two wires for differential pressure measurements were presented in 1992. A hermetic cavity is made using anodic bonding of silicon to a glass substrate and a dissolved wafer process. Conductors pass into the cavity through a recessed area that is later sealed with plasma enhanced chemical vapor deposition (PECVD) of silicon nitride or oxide. CMOS circuitry is mounted in a recessed area in the glass and connected to the diaphragm using wirebonding [57]. An integrated circuit (IC) piezo resistive pressure sensor mounted on the tip of a catheter was already proposed by this group in 1973 [58]. A reference to a capacitive pressure sensor dates from 1980 [59]. A guide wire with a pressure sensor at the tip also exists that uses a tiny 100µm x 150 µm x 1300 µm chip incorporating a piezo resistor attached to the side of a thin surface micromachined membrane that hermetically seals a cavity in which a vacuum exists. The membrane deflects under pressure, causing stress in the piezo material. The change in resistance is measured using a wheatstone bridge. A passive piezo resistor is provided to compensate for temperature effects [51,60]. The same group describes a tip pressure catheter using an optical technique to detect a resonance frequency which is changed by the pressure [51,61] or using a cantilever that moves due to the pressure, thus changing the amount of reflected light [62]. Drawbacks are in the optical connections and production packaging limitations [51]. Another company describes an optical pressure sensor that is based on detecting a pressure sensitive interference pattern in a cavity with a photo detector [63]. Since everything is happening

in the tip there is no need for special measures to correct for influences of catheter bending [64,65]. Capacitive pressure sensors have a high pressure sensitivity, low temperature drift but need onsite detection electronics if capacitance is very small [51]. A surface micro machined capacitive pressure sensor (0.7mm x 5mm) on a 1mm catheter is described in [11]. It has a 120μm membrane with 1μm gap, on board amplification and pulse width modulated output at a power consumption of 5mW. This pressure sensor has already been described for an invasive measurement of blood pressure in 1990[66] and for use on a catheter in 1991 [67]. In that same year another catheter-tip capacitive pressure sensor was presented [68]. The size of this sensor is 0.7mm x 3.5mm x 0.8 mm and the spacing between the capacitor electrodes is 1.0μm. A capacitance detection IC is placed close to the diaphragm and only two wires are needed for the sensor. Eight years earlier the same group was presenting work on buried piezo resistors for catheter tip and side wall biomedical applications [69,70]. Very recently they have developed a fiber-optic Fabry-Perot interferometric pressure sensor of 125μm in diameter and a detection system [71]. This same principle is used by another company and dates from 1993[72,73]. The sensor has two optical fibers polished perpendicular to the transmission line and coated with a thin layer to form the mirrors placed at a distance from each other to form the cavity. This yields a precise, stable, fast and inexpensive sensor.

Continuous monitoring of pressure for cardiovascular applications using wireless implantable microsystems offers additional opportunities for better therapies and increased quality of life for a number of conditions that are presented below.

Coronary artery disease

Atherosclerosis is the forming of plaques inside arteries which can lead to reduction or obstruction of blood flow, ultimately causing chest pain, myocardial infarction (MI), arrhythmias and/or heart failure if this happens in the coronary arteries of the heart. A stent can be placed in the occluded area via percutaneous technique (coronary angioplasty). Researchers have proposed to use pressure sensors on stents to be able to monitor restenosis of the stent (reoccurrence of occlusion after the procedure) [74]. The backbone of this stent is fabricated from a 50 μm thick stainless steel foil using micro-electro-discharge forming two 50 nH coils, coupled to two micromachined capacitive pressure sensors. Each coil-capacitor (LC) circuit can be wirelessly probed. The use of a permanently implanted pressure sensor for ambulatory left atrial pressure monitoring may detect heartfailure and help confirm successful revascularization [75]. This device is also used to optimize therapy for heart failure ([76], see below). To improve the recovery of damaged heart muscle, the circulation of patients arriving in the emergency room with an acute MI is sometimes temporarily assisted by a catheter based cardiac assist device. There is a need for pump control, for example to detect correct placement or obstruction, that can be provided by a pressure sensor. One cardiac assist device has an pump head with sensors using an integrated full bridge piezo resistive pressure sensor[77]. The same company has a completely implantable version that also incorporates pressure sensors.

Heart failure

When the heart muscle weakens due to prior infarction or muscle disease, the heart loses part of its capacity to pump blood, leading to an enlarged heart, which causes symptoms like fatigue and shortness of breath. A permanently implanted pressure sensor may function as a means of optimizing a cardiac

resynchronization/defibrillator system [76]. Frequent, noninvasive, monitoring of pulmonary artery diastolic pressure (PADP) may provide necessary direction for therapy in ambulatory patients with heart failure [78]. Implantable hemodynamic monitoring using right heart pressures provides diagnostic, therapeutic, and prognostic information that may have a significant impact on health care delivery in congestive heart failure (CHF) [79].

One implantable hemodynamic monitoring system contains a power source, integrated circuitry, a piezoelectric activity sensor and a radiofrequency transmission coil hermetically sealed in a titanium can. A modified pacemaker lead containing an absolute capacitive pressure sensor is positioned in the right ventricular outflow tract, requiring correction for ambient atmospheric pressures[79]. First experiments using this system to measure maximum rate of rise of right ventricular pressure for rate adaptive pacemakers were reported in 1992[80] followed by clinical studies for heart failure[81,82,83,79].

A fully implantable device that can sense direct left atrial pressure, core temperature and intra-cardiac electrocardiogram using external radio-frequency power via a telemetry coil has the sensor placed across the inter-atrial septum. The sensor device has been tested in animal models with good evidence that it is impervious to full thickness tissue coverage, still delivering accurate left atrial pressure signals [76].

A permanent implantable device placed percutaneously in the right pulmonary artery via the internal jugular vein for the noninvasive monitoring of PADP is used in a clinical setting for HF therapy as well. Using ultrasonic signals, it generates the PADP waveforms on a desktop system [78]. This device is also being used for abdominal aortic aneurysm (AAA) sac pressure monitoring ([84], see below). A major challenge for all sensors placed in the left side of the circulation is that blood clots may develop on their surface that, when released, may cause stroke.

Aneurysm

An aneurysm is a bulging of a weakened vessel wall. The success of AAA repair by placing a stent graft is expressed in terms of AAA sac shrinkage, most probably caused by excluding the sac from the systemic pressure [84]. The non invasive detection of sac pressure may allow a change in the current follow-up strategy [85]. Currently lifelong monitoring typically using computed tomography (CT) scans is indicated[86]. A miniaturized pressure monitoring device (3 x 9 x 1.5 mm) using an ultrasound-based system that allows for pressure measurements in a noninvasive, transcutaneous fashion was implanted in an animal model and yielded almost identical results compared to catheter based pressure readings. The efficacy of identifying pressure changes in an excluded aneurysm sac with endoleaks was demonstrated [85]. The implant contains a piezoelectric membrane that energizes a capacitor when actuated by ultrasound waves from a hand-held probe. Once charged, a transducer within the device measures ambient pressure and then generates an ultrasound signal that is relayed to the hand-held probe. First human clinical experience with this device was reported in the same year [87] and work is continuing [84]. In an alternative concept an external magnetic loop puts a signal on an implanted loop containing coil and micro fabricated pressure sensitive capacitor using RF energy. The change in capacitance can be read out on the external side as a change in resonance frequency [86]. The device has recently been approved by the Food and Drug Administration for acute implantation [88].

Hypertension, arrhythmias

Permanent recordings of intravascular pressure may also improve the diagnosis and treatment of hypertension or might be used to detect pulse rate and amplitude for assessing

haemodynamic effects of arrhythmia. The pressure gradient between two positions at different depth in the myocardium is very well correlated with ventricular pressure under various cardiac rhythms, preventing the need to measure inside the left circulation [89].

A completely implantable, tined silicone capsule[90] containing a telemetric sensor chip and a ferrite coil to be anchored in a branch of a vessel is currently under investigation[91]. The sensor chip uses a surface micro machined capacitive pressure sensor[66] - also mentioned above for temporary use on catheters - that can be designed to operate at a specific pressure range by adapting the diameter of the membrane. The read-out electronics are integrated on the same chip using standard CMOS process. The chip contains an additional temperature sensor, readout and calibration electronics, a micro controller based digital unit, and an RF-transponder front end [34].

In 1990 a miniaturized capacitive pressure sensor has been developed for implantation in the human heart. The pressure signal modulates the current in the power line resulting in a two-wire approach, with low output impedance, in total absence of any direct current (DC) components. The device is mounted in a needle extending a certain length off a base plate under an angle for reaching a specific depth inside the myocardium [89].

Pressure Sensors for Urology

Urodynamic investigations to diagnose urinary problems involve interventions in the bladder and simultaneous measurements. Typically these are catheter based tools that use miniature pressure sensors at the tip. Totally implantable pressure measurement systems would enable measurements under close to normal life circumstances for the patients [92,93]. In 1984 such a device has been proposed. A thick film substrate serves as a carrier and interconnecting device for the

components. The entire circuit is protected with a micro-machined ceramic package, with a removable container for the disposable battery. The system can transmit pressure data over at least 4 m, with an autonomy of half a week [92,94,95]. A pressure sensitive telemetry device consisting of pressure sensor, amplifier and voltage controlled oscillator (VCO) has also been reported. The device was able to transmit pulses of radio waves which pulsing rate is a function of the pressure [93]. In 1987 a closed loop control of the unstable bladder has been proposed. It relies on a biofeedback system, which makes use of the bladder pressure as a parameter for functional stimulation. The key element consists of an implantable bladder pressure telemetry device that relies on a radio frequency (RF) power link. To close the biofeedback system, an independent programmable stimulator has been developed that is triggered by the pressure data [96]. The combination of micro fabricated sensors and actuators to form a closed loop control system is currently still under investigation. An artificial sphincter and sphincter sensor is being developed in the European project Healthy Aims [97].

Pressure Sensors for Other applications

A small pill shaped bio-telemeter to be used for monitoring the health of a fetus during and after in-utero fetal surgery was presented in 1998. The fully implantable, miniaturized sensing device is linked to a remote receiver through a wireless radio frequency link. It is small enough to be introduced to the uterine cavity through a 10 mm trocar during endoscopic fetal surgery [98]. Solid-state-pressure-sensor-catheters are also used in gastroenterology for measurements in the gastro intestinal tract (GIT). Another GIT application uses a stimulus sensitive hydrogel at the core of a sensor to measure the partial pressure of carbon dioxide in the stomach for patients with gastrointestinal ischemia. Briefly, CO_2 goes through a membrane, mixes with an electrolyte and changes the pH causing the hydrogel to

swell/crimp which changes the pressure that is measured by a pressure sensor [99,100].

A miniaturized micro structured measurement cell covered by a semi permeable diaphragm to be implanted micro invasively into the anterior chamber of the eye has been proposed as a glucose sensor. Osmotic pressure within this cell depends on the intraocular glucose concentration and is translated into deformation of the diaphragm which is measured using white light interferometry [101]. In a similar sort of concept a thin membrane is deflected using a glucose-sensitive hydrogel which exhibits swelling when immersed in a glucose-containing solution [102].

2.2.1.2 Acceleration sensors

Many modern pacemakers contain accelerometers that monitor the activity of the patient and adapt the pacing rate accordingly [103]. One company has developed an accelerometer in the tip of a lead [104]. Another device uses an accelerometer and telemetry system for the detection of hip prosthesis loosening by vibration analysis [105]. The same group already used injectable accelerometers for animal monitoring in 1993 [106].

2.2.1.3 Amperometric sensors

An amperometric principle (measuring current) is for example used to measure glucose. Glucose oxidase (GOx) is immobilized in some way on a microfabricated electrode. GOx is an enzyme (a catalyst in biological systems), that facilitates the oxidation of glucose. This reaction produces hydrogen peroxide that takes part in the corresponding reduction reaction at another electrode. Micro machined electrodes have the advantages of low cost, mass production, fast response time and high reliability. However the output current is very low because of the small size and it is difficult to immobilize GOx on the electrode surface. Therefore the main technological challenges of these sensors are

in the charge transfer mechanism, the GOx immobilization using various methods (glutaraldehyde cross linking, bovine serum albumin cross linking, electro polymerization, sol-gel) or self assembling mono layers and electrode material issues (Au, Pt, carbon). The largest portion of these sensors is for use outside the body. Here implantable devices that use microfabrication to add functionality to amperometric glucose sensors with micro electrodes are presented. One group presents a surface micromachined needle-shaped structure for in-situ glucose monitoring. The Ti/Pt and Ag/AgCl electrodes are located at the tip of the needle. The needle shape and windows in the cells are created using wet and dry etching [107]. Others have used cleanroom processing techniques to mass-produce flexible, electroenzymatic glucose sensors designed for implantation in subcutaneous tissue for continuous glucose monitoring [108]. Currently this system is market released and feasibility studies of a combination with insulin pump therapy are being performed [109].

2.2.1.4 Other sensors

Under this heading flow-, ac conductance-, magnetic-, strain-, force- and other sensors for a variety of clinical applications will be presented.

Measurement of blood flow can be relevant for the diagnosis of cardiovascular disease, for monitoring restenosis in stents [110] or for optimizing settings of pacemakers. Some techniques for measuring flow are based on the differential hot film anemometer. One implementation of this principle uses a bulk micromachined 5 μm thick membrane with two temperature sensitive diodes and polysilicon heating resistor [11]. Another one proposes the use of distributed thermistor thin film on a catheter to measure flow [111]. A flow sensor based on a micro-opto-mechanical principle is described in [112]. The position of a micro machined part that is packaged between two glass wafers

is dependend on the flow and is measured by a light emitting diode (LED) and a photodiode on opposite sides of the two glass plates. It uses a 30 μm thick silicon on insulator (SOI) layer with 3 μm oxide where the carrier layer is completely etched away. An electromagnetic principle to detect wrong probe placement by an unbalance in flow is presented in [113]. An electric field is measured perpendicular to the flow and a magnetic field created by a dual magnet set up. For flow based on the Doppler effect using micro machined ultrasound transducers see section 2.2.4.

Alternating Current (AC) conductance can be correlated to the hematocrit value of the blood and can be measured with a 4 point measurement from Pt electrodes made using a lift off technique [11].

Magnetic sensors are used to facilitate navigation during clinical procedures. One such system has three dimensional (3D) magnetic sensor on a catheter [114,115].

Strain sensors are used in dental care and orthopedics to monitor the status of implants. A low power miniaturized autonomous datalogger capable of measuring, compensating and processing 18 different strain gauges simultaneously is presented in [116]. Hip and knee joint prosthesis are modified to enclose strain gauges and electronics [117].

Force sensors are used in minimally invasive robotic surgery. One sensor is based on a flexible titanium structure fabricated using electrodischarge machining of which the deformations are measured through reflective measurements with three optical fibers. It has a range of 2.5N in axial direction and 1.7N in radial direction [118]. The addition of MEMS tactile sensors on tools for minimal invasive surgery is described in [119].

Information from multiple sensors located on the tip of a catheter generates more data that will be available to the doctor to improve diagnosis, monitor the procedure and assess the effectiveness of therapy during minimal invasive transvenous cardiological or neurological procedures[120]. Measuring

pressure, flow and temperature at the same time assists in diagnosing small vessel disease[121]. A multiple parameter blood sensor for simultaneous pressure, flow and oxygen saturation is presented in [18,120]. The pressure sensor has a 4 μm thick polysilicon membrane with polysilicon piezoresistive readout; the flow velocity sensor has a polysilicon heater with aluminum-polysilicon thermopiles on either side and the oxygen saturation sensor uses two stacked diodes with the top one being sensitive to 660nm and 800nm and the bottom one only to 800nm. Another catheter tip chip measures pressure, flow and temperature simultaneously. Pressure is measured using piezo resistive elements on a flexible membrane. Flow is measured using the hot wire method or temperature dilution. Temperature is measured using the temperature sensitivity of the piezo resistor [121].Another contribution describes a silicon chip with a pressure and a temperature sensor with a total catheter size of about 1.5 to 2 mm diameter [4].

There are a number of other examples involving other types of sensors that are made using micro fabrication technology. One research project is developing miniscule subcutaneous sensors, that can be used to monitor, for example, the function of the heart or prosthetic joints over long periods of time [122]. Others are aiming at the development of an implantable glucose sensor [123,124].

Finally there are some implantable applications of sensors for continuous long term animal monitoring that will be mentioned here. One company has a whole range of products for animal use (blood pressure, heart rate, electro cardiogram (ECG), electro encephalogram (EEG) and activity) and also a human clinical division. [125]. A European research project yielded a device that monitors heart sounds. The electronics are housed in a polyallomer tube (dimensions 75 mm x 17 mm) including a piezoelectric sensor [126]. Even though storing an identification number is not really sensing something, two chronically

implantable radio frequency identification devices (RFID) chips for animal use will be mentioned here. One consists of a passive chip and antenna sealed in inert glass capsule implanted under the skin and only activated when scanner is placed over it [127] and the other is implanted using an injection pistol [128].

2.2.2 Electrical Stimulation and Sensing

A large portion of implantable clinical applications of micro system technology is dealing with electrical stimulation and/or sensing and has a long history starting in the 1950's[25]. Examples of current devices and therapies are cardiac pacemakers, cardiac resynchronization devices, implantable cardioverter defibrillators, cochlear stimulators, neurological pulse generators for spinal, deep brain or sacral nerve stimulation[129,130] and there are options for other clinical areas [131]. Generally speaking, an electrical stimulus is generated by an implantable pulse generator (IPG) and electrically conducted to an electrode positioned at the therapy delivery site.

This section provides a general overview of the various electrical stimulation/sensing devices using micro fabricated electrodes including complete stimulators made using micro system technologies (microstimulators) for implantable applications. The term micro electrode is also used for single electrodes with a diameter in the order of 1 μm made of glass or etched metal needles applied for intra-cellular potential recordings. In this chapter only micro electrodes made using IC-like fabrication technologies will be considered, offering the advantage of exact electrode positions, small size, multiple electrodes, improved electrode tissue interface and active circuitry [132,133,131,134] that can lead to adaptable therapy [135].

Micro electrodes are made on a flat substrate with thin film techniques (2D array), plating (electroplating or electroless) creating 2.5D or with combinations of various processing steps to

create poles with the possibility to have multiple electrodes along the length of each pole (3D array). The electrode materials are Pt/Au/Ir/IrOxide/Ag/TiNi/C. These materials have optimum charge transfer properties for electrical stimulation in combination with electrochemical properties that lead to long term stability. There are several concepts in which the electrodes are made on top of electronic circuitry providing some form of intelligence (multiplexing/current sources). The substrates can be thinned or processed to the extent that they become flexible, or can be made of a flexible material from the start.

2.2.2.1 Micro Electrodes for Ophthalmic Applications

In some diseases of the eye like retina pigmentosa or age related macula degeneration, only the rods and cones that transform incoming light into electrical signals are affected while the optic nerve fibers are still intact. Electrical stimulation of the nerve cells in the retina [136,137], in order to generate visual sensation in these patients, is being investigated by several groups. In general terms, the stimulation pattern is either based on wirelessly received information generated by a camera system, data processing algorithm and transmitter unit or directly received from photosensitive elements attached to the electrodes. Other approaches use electrical stimulation of the optical nerve or in the visual part of the cortex [138]

Epiretinal Stimulation

In this case electrodes are place in contact with the ganglion cells that are located at the inner surface of the retina. An intraocular prosthesis that could electrically stimulate the inner retina to provide vision has been postulated in 1994[139]. Since then this system has gone through animal [140] and human testing[141]. It consists of an implantable stimulator and a 4*4 array of 460-micron diameter platinum disks positioned on the retina. The implantable part of another system consists out of a

coil on flex with decoder IC and stimulation IC with electrodes [34,142,19,11]. This work started in 1995[143] and has been extensively tested in animals [144]. Authors involved in the above projects have published the actor component of the retina implant stimulator, which is a flexible active silicon multielectrode used for electrostimulation of the retinal ganglion cells [142]. A similar system is being developed in the context of the European project Heatlhy Aims [145]. First acute human trials with part of the system are being done [146]. In 1996 another group reported on stimulation of ganglion cells using conventional electrodes or a neural prosthesis [147]. The retina is electrically stimulated using Iridium Oxide electrodes on a flexible substrate [148].

Subretinal Stimulation

In this case electrodes are placed under the surface of the retina and receive their signals from photosensitive elements. Subretinal electrical stimulation of the rabbit retina with a bipolar strip electrode consisting of two pieces of Au foil on both sides of a polymer foil was reported in 1997 [149]. The same authors are involved in a company that makes an "artificial silicon retina," a microchip with 5,000 solar cells that stimulates remaining functional retinal cells[150,151] which is currently in clinical trial[152]. Feasibility of a similar concept investigated by another group is presented in 1999 [153]. Long term stability and biocompatibility of the subretinal implants has been studied extensively [153,154,155] using wired prototypes and a silicon-based micro-photodiode array that closely resembled the design and composition of the final prosthesis [156]. 3-dimensional micro-fabrication substrate-integrated microelectrodes show an improved charge transfer capacity [157]. This group has also published a survey of subretinally implanted microphotodiode arrays [158] and visual prostheses in general [159].

Optical nerve stimulation

Visual information received in the eye is transmitted in electrical form through the optical nerve to the visual cortex. Appropriately encoded electrical stimulation of the optical nerve could restore vision in blind patients. A first system was implanted in 1998[160] and patients are still being followed [161]. It is experimentally determined which stimulus causes which phosphenes, and this information is used to transform images into a stimulation pattern.

Visual cortex stimulation

Electrical stimulation of the medial occipital cortex can produce visual sensations [138]. One system includes a video camera, external signal processing equipment, and a brain implant that gives blind people with totally non-functional retinas the ability to have some kind of vision [162,163]. Research into an array of penetrating electrodes that can form the basis of a visual prosthesis centered around electrical stimulation of the visual cortex was reported in 1988 and is ongoing[164,165,166]. The system is also being used for chronic recording of the neuronal activity in the visual cortex [167,168]. These studies can aid in the development of implantable electrical stimulation systems to restore vision [168]. The evolution of the electrode array manufacturing and design is extensively described in literature [169,165,170,171]. Another group uses an array of thirty-eight microelectrodes spaced 500 microns apart[172]. Yet another group uses a miniaturized visual implant containing a micro electrode array[173,174,175].

2.2.2.2 Micro electrodes for auditory applications

Along similar principles as applied in the ophthalmic case described above, electrical stimulation can restore “hearing” in patients who have an intact nervous system but irreversible conduction hearing loss like damaged hair cells in the inner ear.

Electrical stimulation of the auditory nerve can be applied in the cochlear nerve in the inner ear, in the midbrain or in the brain[176].

The use of microfabrication for better field distribution, using addressable electrodes and well-timed electrical pulses for field steering can improve the therapeutic effect [177]. Microtechnologies for this application are being investigated in the context of a European project[178,179]. Topics include active electrodes for implantation in the cochlea; polyimide- and integrated silicon based electrodes for implantation in the modiolis nerve bundle and microconnectors and microelectrodes [178,176]. An example from another group is an entirely flexible micro electrode array (40mm long, 4 μm thick) that is made using a boron / ethylenediamine-pyrocatechol (EDP) approach designed for insertion into the cochlea. The shape and position can be monitored by sensors on the probe [133].

2.2.2.3 Micro electrodes to restore motor function

Restoration of motor function in paralyzed limbs due to damaged nerve fibers may be realized by electrical stimulation. Recording of signals from nerves may be used as feedback or input to form neuroprosthetic devices[180].

There are many examples of restoring motor function by electrical stimulation that are not using micro electrodes but that do use micro fabrication techniques in other parts of the implant [181,182,183,184,185,186]. Most of these have a history of over 25 years. In 1991 an injectable microstimulator contained in a hermetically sealed glass capsule receiving power and command signals by inductive coupling for use at neuromuscular sites was described [187,188,189]. In the same year another group performed a study with a 45 μm thick tip-shaped silicon substrate containing twelve platinum electrode sites (10 μm x 50 μm and 50 μm distance) with a Si_3N_4 insulating layer [190]. Four years later a 3D multi-electrode array manufactured using a sawing

procedure in combination with a reactive ion etching (RIE) process was presented. A flip-chip technique to connect the array to (de)multiplexing circuitry,in which current sources and buffer amplifiers are also integrated, is being studied[191]. Later, a two-dimensional 24-channel array using 25um-diameter NiCr wires was used to achieve the desired level of redundancy [192].

A microstimulator that can be implanted through a gauge-10 hypodermic needle was developed in 1996. It uses a glass silicon anodic bond and polysilicon feedthroughs [193,194,195,196]. The same microelectrode arrays that have been described above for visual cortex stimulation and recording have been proposed as a means to enable patients with severe neuromuscular disease to more effectively interact with their environment [197,166,180]. Another group describes platinum electrodes fabricated with a lift off technique on a 5 μm polyimide carier to be placed around a nerve. A top layer of polyimide is deposited for mechanical support and isolation, the electrode areas are opened by RIE [198]. Mutiplexer circuitry is connected to the electrodes using a specially developed interconnect technique to reduce the number of cables needed to address the electrodes [13,17,10,131,199]. Special electrode designs using similar fabrication techniques are intended to promote nervous regeneration through holes in the structure [13,200]. More recently, the development of an all plastic implant including electronics and conductors for improved flexibility has been presented [200,201]. Another implantable microstimulator system for neuromuscular stimulation is described in [202,203]. In 1987 an implantable stimulator packaged in a ceramic cylinder for long-term muscle stimulation was reported [204,205].

2.2.2.4 Micro electrodes for brain research

Penetrating neuro probes for recording of brain activity offer the advantage that signals can be collected from within the brain. The examples mentioned in this section are mainly used to study

the functioning of the brain at a fundamental level. They enable discovering correlations between electrical activity in the central nervous system and externally applied psychophysical stimuli [206,207]. Mostly, the long term outcome of this fundamental research is targeted towards a specific clinical application. For example, brain activity during a developing epileptic seizure was measured inside the brain before it was measurable on the surface [22] and its use for closed-loop control of neural prostheses was studied[208]. Although they are aimed at these applications, we feel that the concepts presented here fit best under this heading of brain research. There are several ways to fabricate such electrical probing devices using micro technology. One example uses a silicon carrier (3mmx50umx15um) that supports an array of polysilicon or tantalum thin-film conductors. Silicon nitride and silicon dioxide are used to define the electrode openings. The process allows inclusion of circuitry for signal amplification and multiplexing [208]. More recently this group presented silicon ribbon cables for implantable neural probes [209]. Another multiple electrode probe is produced by means of thin-film techniques. Silicon dioxide and silicon nitride are used as insulation layer. Gold, Platinum or Silver that can be chlorodized at the surface are used for recording [22]. Others have proposed to treat chronic pain in a closed-loop scheme of electrical recording and stimulation in the brain. The probe substrate structure is obtained from a thinned silicon wafer. Each recording probe has 10 TiW/Au recording sites [207].Yet another penetrating neural probe for neuro biological research has 16 Iridium electrodes on each tip that are made in three phases using a combination of dry and wet etching [132]. One implant has three shanks with five recording sites (20 μm x 20 μm) and two via holes (40 μm x 40 μm) to promote tissue attachment on each shank. The electrodes have a 5-10 μm thick silicon backbone layer at the tip that is rigid enough to penetrate the pia and a 1mm flexible segment without a silicon backbone layer.

[210,211]. A multifunctional probe allowing both electrical and chemical recording and stimulation for fundamental brain research is being developed in the context of a European project[212]. Another example is the use of a three dimensional array of microneedles that penetrates the outer skin layer for electroencephalography. The spikes are etched in silicon by deep reactive ion etching and are subsequently covered with a silver-silverchloride (Ag-AgCl) double layer [213]. A device that allows the stimulation electrodes to be configured and thereby reduces side effects for deep brain stimulation is under investigation by another group [214].

2.2.3 Micromachined drug and gene delivery devices

Drugs can improve the life of patients for a wide range of clinical conditions and can be administered in a number of ways. Microsystems are aiming at improving the control over the release of the drug at the appropriate time and site and in appropriate dosage. Four different sorts of microsystems in this area are distinguished: implantable pumps, smart pills, micro porous materials and microneedles (considering skin penetration as implantable).

The basic ingredients of a membrane type of pump are a fluid inlet, a pumping chamber and a fluid outlet. The volume of the pumping chamber is controlled by a deflectable membrane. One stroke of the membrane moves a controlled volume of fluid. Valves on the in- and out-let ensure flow in the correct direction. Important design characteristics for delivery of substances to the body are accuracy, resolution, safety and control. Therefore additional features on such pumps are integrated-pressure sensors, -flow restrictors and -fluid filters [215].

One completely microfabricated pump opens the way to implantation of the pump at various anatomical positions [216,217]. Another company is progressing towards first market introduction of a micro pump [218]. Implantable biosensors and

micropumps also work together as a closed loop control system for personal pharmaceutical delivery [219]. Other pumps contain micromachined parts or sensors for pump control.

An ingestible capsule that signals a remote receiver and releases a dosage of medicament when triggered is described in [220]. A similar concept is a micro pill containing drug reservoirs and microelectronics for the controlled release of the drug using wireless technology [221,222]. Another variation of this concept is the timed release of single doses from within a large array of dose reservoirs [223].

Some drug delivery concepts are based on porous materials or nanoporous membranes [216]. There are also various examples of microneedles being used for transdermal drug delivery. [216,224,225,124]. One concept includes pumping, liquid storage, liquid dosing and anti clogging measures [226,227,228].

Microneedles have also been used for transdermal gene delivery. One technique is based on a set of oscillating solid microneedles driven by a modified tattooing device that results in plasmid DNA delivery directly to the target cells. This technique is more efficient than single injection and particle-mediated gene transfer [229]. Arrays of silicon projections ranging in height from 50 to 200 μm have been fabricated using isotropic potassium hydroxide etch techniques on $1cm^2$ microchips. When these micro structures were placed in contact with DNA solution and then moved laterally over the skin they were able to breach the skin barrier [230]. There is one example of a stent with micro needles covered with a nanoporous layer that contains the therapeutic agent like DNA. The needles are designed to penetrate the internal elastic lamina of a vessel leading to an effective delivery. The translamina stent has been successfully deployed in vivo in rabbit femoral arteries [27].

2.2.4 Micromachined ultrasound transducers

Micromachined ultrasound transducers are used to measure flow based on the Doppler effect[110] or provide images based on echos [231,232,233] for vascular or endoscopic[234] applications. The implantable ultrasound transducers mentioned here are designed to fit on a tool in the shape of a catheter or guidewire for use in transvenous or minimally invasive procedures. Individual element dimensions in the order of micrometers are achieved with “non standard” micro fabrication techniques out of bulk lead zirconium titanate (PZT) material, and are needed to fit the transducers on the implant tools. More recently, capacitive micromachined ultrasound transducers (cMUT) were introduced manufactured by means of surface micromachining, offering the advantage of higher integration levels for improved quality.

cMUT consist of a sealed cavity beneath a membrane with electrodes on both sides of the membrane. An electrostatic force between the plates of the capacitor causes the membrane to vibrate and emit acoustic energy. A 16x16 cMUT array that fits through a 5mm lumen is proposed for two dimensional (2D) real-time volumetric imaging in [234]. The silicon substrate on which the cMUT are made can also be thinned down and bent [235]. Another group has used cMUT for forward looking intravascular ultrasound [236,237,232].

The devices based on PZT all realize a large number of interconnects in a small space. One group creates the transducers on a flexible circuit that is rolled up to fit into a 1.2 mm diameter guide wire which puts very high requirements on flip chip, chip thinning, dicing accuracy and number of interconnects [238]. Likewise, a 112 channel two-dimensional array constructed on a six layer flexible polyimide interconnect circuit is mounted on a catheter with 2.33 mm outside diameter [239,240] or a 1 mm diameter intravascular probe involving a bended flex circuit with connections to a multiplexer and cable [233].

2.2.5 Micro Opto Electro Mechanical Systems (MOEMS)

Endoscopes are used to visualize the interior of a hollow organ or to provide vision during minimally invasive surgery. Endoscopy started with the use of rigid tubes with fixed lenses until the 1970's. Multicore fibre optics enabled flexible endoscopes in the 1980's [4]. Further miniaturization led to the development of endoscopes with a video camera at the distal end [241]. Microsystem technology can further enhance the functionality of next generation endoscopes. Examples are a diagnostic endo laser scanner with optical components realized using lithographic methods and microscanning mirrors to avoid the spectral limitations of conventional image guides [242], a miniature endoscopic confocal optical scanning microscope with a scanning head including an electrostatic 2D MEMS scanner [243] and an optical coherence tomography endoscope based on a microelectromechanical mirror [244].

Endoscopy can be uncomfortable for the patient, has to be done in the hospital and does not allow optimal view in difficult areas of the anatomy. A capsule endoscope attempts to address these limitations. Two examples of capsule endoscopes are a camera pill containing an optical lens, CMOS imager, battery and radio transmitter that travels through the GIT while sending video images out and an intracorporeal videoprobe that uses a CMOS camera and micro mechanical tilting mechanism. [245,246,247].

A glucose sensor for implantation in the subcutaneous tissue of the human body is being investigated. The optical characteristics of glucose in the near infrared spectrum are used for concentration measurement by absorbance of fluid in a micro fabricated chamber [248]. Finally there is a miniature implantable telescope with two glass fabricated micro lenses that can project a magnified image over a large area of the retina [249,250].

2.2.6 Other Micro System Devices for Implantable Applications

Micro actuators are used for making smart catheters for minimally invasive (transvascular) procedures. They involve the use of 3D lithography, electronics and shape memory[251]; distributed microactuators made of shape memory alloys[26,252] and a catheter that can be heated locally via distributed electrical contacts [253].

Micro machined cutting tools have sharper edges then conventional needles and can be combined with ultrasonic energy or sensors [254,255]. They can be used when very fine and precise surgery is needed, for example in ophthalmology[254,256]. One device consists of two silicon ultrasonic horns bonded with a channel along the length to form a needle [254]. Later devices are silicon needles with integrated piezoresistive pressure sensors fabricated using bulk micromachining technology and bonded PZT-4 plates for ultrasonic energy [255,256].

Nano or micro structured surface topologies may provoke a desired tissue response in urological, cardiological or orthopedical implants [257,258,259]. Likewise, nano reinforced materials might have suitable properties for neural or orthopaedic prosthetic devices [260].

A subset of micro fabricated scaffolds used for tissue engineering is made implantable by using biodegradable material. Several types of polymers have been described. Closed micro fluidic channels at the capillary size-scale have been manufactured of poly-lactic-co-glycolic acid using a micro molding process. The process is high resolution, fast, inexpensive, reproducible, and scalable [261]. Likewise, microstructures with simple fluidic channels have been fabricated of poly-(ε-caprolactone-dl-lactide) tetraacrylate using a fast and flexible soft-lithography process. Microstructures down to 50μm suitable for liver reconstructs were fabricated [262]. Polyglycerol sebacate is another biocompatible and

biodegradable elastomer that can be used as a material for fabricating microfluidic vascular scaffolds or nerve guides. Three dimensional structures are created from this material by a micromolding process in combination with multilayer bonding. Controlling the cellular microenvironment (concentration of oxygen, fluid shear forces) within scaffolds is critical for eliciting desirable biological responses such as proliferation, migration, and maturation. The scaffold is suitable for incorporating multiple cell types and integration with existing biomaterial systems and technologies for tissue-specific applications [263]. There is one company that uses nanostructured porous silicon as a biodegradable material, which can be easily micromachined in the form of scaffolds [264].

A system for continuous glucose monitoring during dialysis involves a microneedle array to sample interstitial fluid and an electrochemical enzyme-based glucose sensor. The microneedles contain an integrated porous polysilicon dialysis membrane that separates the interstitial fluid from dialysis fluid, which is pumped through the microneedles. Glucose can diffuse through this membrane into the system. The glucose sensor involved in this system is an integrated enzyme-based microsystem fabricated on wafer-level using in-device immobilization which is located outside the body [265].

2.2.7 Summary of Implantable Microsystems

In the previous sections, a wide range of microsystems for implantable applications has been presented with a focus on its micro part. As a first observation it can be stated that a large range of microsystems is being used or investigated. A variety of sensors, numerous micro electrodes, drug delivery devices, micro machined ultrasound transducers, MOEMS, micro actuators, surgical tools and micro surface topology have been presented (see Figure 2.1).

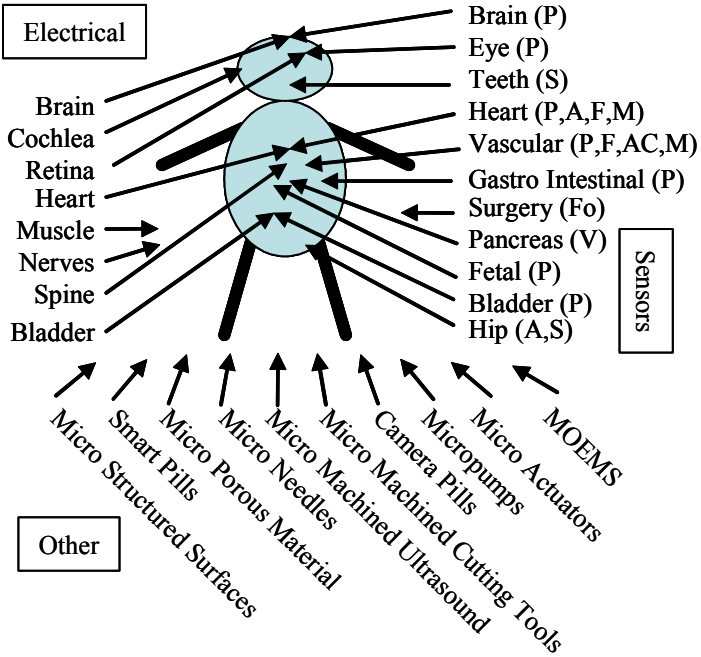

Figure 2.1 Micro System Technologies for implantable applications. Electrical means MST for electrical stimulation and sensing and includes micro stimulators. Sensors: P = Pressure, A = Acceleration, Fl = Flow, AC = AC conductance, M = Magnetic, S = Strain, Fo = Force, M = Multiple, V = Viscosity. Other is the collection of other types of MST. MOEMS = Micro Opto Electro Mechanical System.

To further analyze the information each "end item" has been classified on a number of aspects. End item is meant to identify the total 'product'. This term is introduced because the micro system is frequently just a part of a product. 'Product' is between 'quotes' because the end item can have various states of development (see below).

End items are categorized by:

- MST class and -part
  - Class according to paragraph headings used in this section **(**E = Electrical**,** S = Sensor**,** D = Drug delivery**,** M = MOEMS**,** U = Ultrasound**,** O = Other**)**
  - Part to further specify detail per class
- Duration of implant
  - Transient (< 1 day, TR); Temporary (1 day < duration < 30 days, TE); Chronic (> 30 days, CH)
- Type of organization
  - Academic (A);Commercial (C)
- Status of end item
  - Idea (ID); Proto (OTO); Animal (AN); Clinical (CL); Product (ODU)
- Clinical Field
  - Animal (An), Auditory (Aud), Cardiology (Car), Dentology (Dent), Drugdelivery (Drug), Endocrinology (Endo), Fetal (Fetal), Gastroenterology (Gastro), Neurology (Neuro), Oncology (Onco), Ophthalmology (Oph), Orthopedics (Orth), Surgery (Surg), Tissue Engineering (Tis), Urology (Uro) and Various (Var)
- Activity
  - Active (A) if publication or webpage update in year 2000 or later, Passive (P) otherwise.

Classification is based on the references mentioned in this chapter; fields are filled out as unknown if it is not clear how to classify based on the available information. As with every classification, there is never a perfect match for all, therefore there is always a category “Other”. There are many examples of

end items that are being realized in the context of government funded programs. An end item is classified as commercial if there is an industrial partner driving the application and as academic otherwise. Besides the classifications, the name of the end item, name of the organization, reference to internet address and year/author of oldest and most recent paper are given. Note that only a couple of implantable micro-fabricated parts contained in a "classic" hermetically sealed metal casing are mentioned. An overview is given in Table 2.2.

Table 2.2 (page 42-46) Overview of end items with classification and additional information. End Item refers to the total product. Organization is the main organization that is driving the development. Part is an abbreviated indication of the actual microsystem part of the end item. In this column AC Cond = alternating current conductance, CMUT = capacitive micromachined ultrasound transducer, PZT = lead zirconium titanate and the remaining abbreviations should be self apparent. Dur. is the duration of implant (Transient (< 1 day, TR); Temporary (1 day < duration < 30 days, TE); Chronic (> 30 days, CH)). Type is the type of organization (Academic (A);Commercial (C)). Stat. is the development status of the end item (Idea (ID); Proto (OTO); Animal (AN); Clinical (CL); Product (ODU)). Clin. is the clinical field of application (Animal (An), Auditory (Aud), Cardiology (Car), Dentology (Dent), Drugdelivery (Drug), Endocrinology (Endo), Fetal, Gastroenterology (Gastro), Neurology (Neuro), Oncology (Onco), Ophthalmology (Oph), Orthopedics (Orth), Surgery (Surg), Tissue Engineering (Tis), Urology (Uro) and Various (Var)). Act. is the activity (Active (A) if most recent reference published in year 2000 or later or internet, Passive (P) otherwise). Then the publishing year and first author of the most recent reference followed by the publishing year and first author of the oldest reference (if applicable). Full reference can be found in the reference list of this chapter. The final column contains a reference to the internet. Rows are first ordered per MST class Sensors; Electrical Stimulation and Sensing; Micromachined drug and gene delivery devices; micromachined ultrasound transducers; micro opto electro mechanical systems and other micro system devices for implantable applications that correspond to the major sub sections in this section. Rows are then ordered alphabetically on Part, Activity and Duration.

End Item	Organization	Part	Dur.	Type	Stat.	Clin.	Act.	Year	Author	Year	Author	Internet
Sensors												
Hematocrit sensor	RWTH Aachen	AC Cond.	TR	A	OTO	Car	P	1998	Mokwa			iwe1.rwth-aachen.de
Hip prosthesis loosening	Leuven, Katholic University	Accelero.	CH	A	AN	Orth	A	2000	Puers			esat.kuleuven.be/micas
Accelerometer	Sorin Biomedica	Accelero.	CH	C	ODU	Car	P	1998	Langenfeld			elamedical.com
Injectible AN Monitor	Leuven, Katholic University	Accelero.	CH	A	OTO	An	P	1997	Puers	1993	Vergrote	esat.kuleuven.be/micas
CGMS	Medtronic	Ampero.	TE	C	ODU	Endo	A	2006	Mastro.	1992	Johnson	medtronic.com
Needle glucose sensor	Electr. Telecom. Res. Inst.	Ampero.	TE	A	OTO	Endo	P	1999	Kim			cadvax.etri.re.kr
Flow catheter	Verimetra	Flow	TR	C	AN	Car	A					verimetra.com
Flow sensor on catheter	Millar	Flow	TR	C	ID	Car	P	1979	Millar			millarinstruments.com
Flow sensor on catheter	RWTH Aachen	Flow	TR	A	OTO	Car	P	1998	Mokwa			iwe1.rwth-aachen.de
Force sensor	Leuven, Katholic University	Force	TR	A	OTO	Surg	A	2004	Peirs			esat.kuleuven.be/micas
3D cath. nav. sys.	Delft Uni. of Technology	Magnetic	TR	A	OTO	Car	A	2003	Tanase	2002	Tanase	http://ei.et.tudelft.nl
Pressure, temp and flow	Radi	Other	TR	C	ID	Car	A	2001	Smith			radi.se
Multiple parameter sensor	Delft Uni. of Technology	Other	TR	A	OTO	Var	A	2000	Goosen	2000	Goosen	http://ei.et.tudelft.nl
MEMS tactile sensors	Verimetra	Other	TE	C	OTO	Surg	A	2003	Rebello			verimetra.com
Bloodglucose	Thera Sense	Other	TE	C	ID	Endo	A	2005	Heller			http://abbottdiabetescare.com
Implantable CO2 sensor	Twente, Technical Uni.	Other	TE	A	CL	Gastro	A	2004	Herber	2003	Herber	mesaplus.utwente.nl
Wireless TULE	Tampere Uni Tech	Other	CH	A	OTO	Car	A	2004	Ristama			cs.uta.fi/hci/wfpc/groups.html
Animal monitor	Transoma	Other	CH	C	ODU	An	P	1997	Gelzer			datasci.com
Transdermal ECG monitor	Tras-os-Montes Alto Douto	Other	CH	A	AN	An	P	1997	Torres-Pereira			utad.pt
PV catheter	CDLeykom	Pressure	TR	C	ODU	Car	A					cdleycom.com
Pressure catheter	Millar	Pressure	TR	C	ODU	Car	A	1999	Millar	1973	Millar	millarinstruments.com
PressureWire, Piezo	Radi, KTH	Pressure	TR	C	ODU	Car	A					radi.se
Pressure catheter	Samba	Pressure	TR	C	ODU	Car	A	2001	Engstrom			samba.se
Catheter	Unisensor	Pressure	TR	C	ODU	Var	A					unisensor.ch
Catheter (optical)	Radi	Pressure	TR	C	ODU	Car	A	2000	Stemme	1993	Tenerz	radi.se
Bladder pressure	Wisconsin, Uni.of -Madison	Pressure	TR	A	CL	Uro	A	2002	Siwapornsathain			wisc.edu
Catheter (Fabrit Perot)	Tohoku University	Pressure	TR	A	AN	Car	A	2005	Kentaro			mems.mech.tohoku.ac.jp
Impella	Abiomed/ Impella	Pressure	TE	C	ODU	Car	A	2006	Siess			abiomed.com
ICP, catheter based	Codman Neurosciences	Pressure	TE	C	ODU	Neuro	A					codman.com
ICP	SICAN / TU Berlin	Pressure	TE	C	OTO	Neuro	A	2000	Flick			tu-berlin.de
ICP telemetric (ITES)	Bremen Uni	Pressure	TE	C	AN	Neuro	A	2000	Eggers	1995	Zacheja	imsas.uni-bremen.de/
IOP, telemetric (ITES)	Bremen Uni	Pressure	TE	C	AN	Oph	A	2000	Marschner			imsas.uni-bremen.de/
Wireless Sensor	ISSYS	Pressure	CH	C	AN	Neuro	A	2005	Rich			mems-issys.com
IOP Sensor	Mesotec	Pressure	CH	C	CL	Oph	A	1998	Mokwa			mesotec.de

End Item	Organization	Part	Dur.	Type	Stat.	Clin.	Act.	Year	Author	Year	Author	Internet
Sensors (Continued)												
HeartPod	Savacor	Pressure	CH	C	CL	Car	A	2005	Walton			savacor.com
Pressure Sensor	CardioMEMS	Pressure	CH	C	ODU	Car	A	2005	Allen			cardiomems.com
ICP Sensor	Campus Micro Tech.	Pressure	CH	C	OTO	Neuro	A					campus-micro-technologies.com
Remon AAA	Remon	Pressure	CH	C	CL	Car	A	2006	Ellozy	2004	Milner	remonmedical.com
Remon CHF	Remon	Pressure	CH	C	CL	Car	A	2006	Parikh			remonmedical.com
Chronicle	Medtronic	Pressure	CH	C	CL	Car	A	2006	Braunsch.	1992	Bennett	medtronic.com
HeartPod	Savacor	Pressure	CH	C	CL	Car	A	2006	Ritzema-Carter			savacor.com
Stent	Michigan, University of	Pressure	CH	A	OTO	Car	A	2004	Takahata			eecs.umich.edu
IOP	Leuven, Katholic University	Pressure	CH	A	OTO	Oph	A	2000	Puers			esat.kuleuven.be/micas
Occular glucose sensor	Karlsruhe, University	Pressure	CH	A	OTO	Endo	A	2004	Rawer			itiv.uni-karlsruhe.de
Glucose sensitive hydrogel	Illinois Urbana-Champaign	Pressure	CH	A	OTO	Endo	A	2005	Mariserla			mse.uiuc.edu
Multiplexed catheter	Michigan, University of	Pressure	TR	A	OTO	Car	P	1992	Ji	1973	Sauman	eecs.umich.edu
Pressure catheter	RWTH Aachen	Pressure	TR	A	OTO	Car	P	1998	Mokwa	1990	Kandler	iwe1.rwth-aachen.de
Catheter (capacitive)	Tohoku University	Pressure	TR	A	OTO	Car	P	1990	Esashi			mems.mech.tohoku.ac.jp
Catheter (Piezo)	Tohoku University	Pressure	TR	A	OTO	Car	P	1982	Esashi			mems.mech.tohoku.ac.jp
Bladder pressure	Leuven, Katholic University	Pressure	TE	A	OTO	Uro	P	1987	Sansen	1984	Sansen	esat.kuleuven.be/micas
Valve and sensor	Healthy Aims	Pressure	CH	C	OTO	Uro	P	2004	Tooley			healthyaims.org
Fetal Monitor	NASA	Pressure	CH	A	OTO	Fetal	P	1998	Mundt			nasa.gov/centers/ames
Telesensor	Radionics	Pressure	CH	C	CL	Neuro	P	1990	Chapman	1979	Cosman	http://hms.harvard.edu
ICP Sensor	Texas Instruments	Pressure	CH	C	OTO	Neuro	P	1988	Talamonti			ti.com
"Swimmer"	RWTH Aachen	Pressure	CH	A	AN	Car	P	2001	Mokwa	1990	Kandler	iwe1.rwth-aachen.de
Pressure Sensor	Leuven, Katholic University	Pressure	CH	A	OTO	Car	P	1990	Puers			esat.kuleuven.be/micas
Pressure monitoring	Uppsala Institute of Tech.	Pressure	CH	A	OTO	Oph	P	1990	Backlund			uu.se
IOP	Smith-Kettlewell Ins.	Pressure	CH	A	AN	Oph	P	1967	Collins			ski.org
Dental Implant	Leuven, Katholic University	Strain	CH	A	ID	Dent	A	2002	Claes			esat.kuleuven.be/micas
Prosthesis, electronics	Stanmore Orthop. Hosp.	Strain	CH	A	OTO	Orth	A	2003	Canham			rnoh-stanmore.org.uk
Glucose Sensor	Sensile Medical	Viscosity	CH	C	OTO	Endo	A					sensile-medical.com
Electrical Stimulation and Sensing												
Electrodes	Royal Institute of Tech.	Electr.	CH	A	CL	Neuro	A	2001	Griss			s3.kth.se/mst
Penetrating Neural Probe	Michigan, University of	Electr.	CH	A	CL	Neuro	A	2004	Lisby	1985	Najafi	eecs.umich.edu
Retina stim photodiodes	Tuebingen, University	Electr.	CH	C	CL	Oph	A	2005	Sachs	1997	Zrenner	eye-chip.com
Artificial Silicon Retina	Second Sight	Electr.	CH	C	CL	Oph	A	2005	Weiland	1994	Humayun	2-sight.com
Configurable stimulation	Medtrode	Electr.	CH	C	OTO	Neuro	A	2004	Capaldi			medtrode.com
Artificial Silicon Retina	Optobionics	Electr.	CH	C	CL	Oph	A	2004	Chow	1993	Chow	optobionics.com

End Item	Organization	Part	Dur.	Type	Stat.	Clin.	Act.	Year	Author	Year	Author	Internet
Electrical Stimulation and Sensing (Continued)												
Brain implant	Artificial Ophthalmology	Electr.	CH	C	CL	Oph	A	2000	Dobelle	1974	Dobelle	artificialvision.com
Neuroprobes	Imec	Electr.	CH	C	ID	Neuro	A	2006	Neves			neuroprobes.org
Smart Electrode	Cochlear	Electr.	CH	C	ID	Aud	A	2006	Humbeeck			healthyaims.org
Neuroprobe	Cochlear	Electr.	CH	C	OTO	Aud	A	2006	Humbeeck			healthyaims.org
Intra Occular Stimulation	IIP	Electr.	CH	C	OTO	Oph	A	2005	Hornig			iip-tec.com
Polymer neural probes	Foster Miller	Electr.	CH	C	OTO	Neuro	A	2005	Farrel			foster-miller.com
Smart Electrode	IBMT	Electr.	CH	A	AN	Neuro	A	2006	Koch	1995	Stieglitz	ibmt.fraunhofer.de
EPI-RET	RWTH Aachen	Electr.	CH	A	AN	Oph	A	2006	Mokwa	1995	Eckmiller	iwe1.rwth-aachen.de
Micro Intra Cortical Probe	Arizona State University	Electr.	CH	A	AN	Neuro	A	2004	Lee			asu.edu
Visual Neurostimulator	Montreal, Ecole Polytech.	Electr.	CH	A	AN	Oph	A	2004	Trepanier	1996	Harvey	polystim.ca/
MeCFES	Polytechnico di Milano	Electr.	CH	A	CL	Neuro	A	2001	Thorsen			cbi.polimi.it
Optical Nerve	Leuven, Universite Cath.	Electr.	CH	A	CL	Oph	A	2006	Delbeke	1998	Veraart	md.ucl.ac.be/gren
Retina stimulation	Harvard Medical School	Electr.	CH	A	CL	Oph	A	2003	Rizzo			meei.harvard.edu
Drop Foot Stimulator	FineTech Medical	Electr.	CH	C	CL	Neuro	P	2004	Spensley	2002	van der Aa	salisburyfes.com
Freehand	NeuroControl Corp	Electr.	CH	C	ODU	Neuro	P	1995	Scott			neurocontrol.com
Cochlea stimulation	Michigan, University of	Electr.	CH	A	AN	Aud	P	1997	Bell			eecs.umich.edu
Penetrating Neural Probes	Case Western Reserve Uni.	Electr.	CH	A	AN	Neuro	P	1986	Prohaska			cwru.edu
Neurology prostheses	MRC	Electr.	CH	A	CL	Neuro	P	1994	Perkin	1979	Brindley	mrc.ac.uk
Intracortical stimulation	Nat.Ins.Neur.Disorders	Electr.	CH	A	CL	Oph	P	1996	Schmidt			ninds.nih.gov
Neural Microprobe	Leuven, Katholic University	Electr.	CH	A	OTO	Neuro	P	1991	Peeters			esat.kuleuven.be/micas
Electrical Stimulator	Montreal, Ecole Polytech.	Electr.	CH	A	OTO	Neuro	P	1999	Arabi	1997	Arabi	polystim.ca/
Utah Electrode Array	Utah, University of	Needles	CH	A	AN	Neuro	A	2005	Patterson	1993	Nordhausen	ece.utah.edu
Utah Electrode Array	Utah, University of	Needles	CH	A	AN	Neuro	A	2005	Patterson	1998	Rousche	ece.utah.edu
Utah Electrode Array	Utah, University of	Needles	CH	A	AN	Oph	A	2003	Normann	1988	Campbell	ece.utah.edu
3D multi electrode array	Twente, Technical Uni.	Needles	CH	A	AN	Neuro	P	1999	Smit	1991	Rutten	bmti.utwente.nl
Penetrating neural probes	Stanford, University	Needles	CH	A	AN	Neuro	P	1997	Kewley			http://cis.stanford.edu
Bion micro stimulator	Alfred Mann Foundation	Stim.	CH	C	CL	Neuro	A	2005	Baker	1991	Loeb	http://ami.usc.edu
Microstimulator	Michigan, University of	Stim.	CH	A	AN	Neuro	A	2004	Dokmeci	1996	Ziaie	wimserc.org
Implantable Stimulator	Leuven, Katholic Uni.	Stim.	CH	A	AN	Neuro	P	1991	Callewaert	1987	Callewaert	esat.kuleuven.be/micas
Micromachined drug and gene delivery devices												
Drug delivery system	ChipRX	Drugdel.	CH	C	OTO	Drug	A	2003	Deo			chiprx.com
Micropump	Sarcos	Drugdel.	CH	C	OTO	Drug	A					sarcos.com
SimpleChoice	SpectRX	Drugdel.	TE	C	ODU	Drug	A					spectrx.com
Enterion	Pharmaceutical Profiles	Drugdel.	TE	C	ODU	Drug	A	2005	Clewlow	2004	Clewlow	enterion.co.uk

End Item	Organization	Part	Dur.	Type	Stat.	Clin.	Act.	Year	Author	Year	Author	Internet
Micromachined drug and gene delivery devices (Continued)												
Porous silicon	PSimedica	Drugdel.	TE	C	OTO	Drug	A					psimedica.co.uk
Transdermal Interfaces	Royal Institute of Tech.	Drugdel.	TE	A	OTO	Drug	A	2005	Roxhed	2003	Griss	s3.kth.se/mst
Implantable Pump	Codman Neurosciences	Drugdel.	CH	C	OTO	Drug	A					codmanjnj.com
Array of drug reservoirs	MicroChips	Drugdel.	CH	C	AN	Drug	A	2006	Presscot			mchips.com
Nanoporous drug delivery	Debiotech	Drugdel.	CH	C	ID	Drug	A	2003	Maillefer			debiotech.ch
Mircomachined pump	Debiotech	Drugdel.	CH	C	OTO	Drug	A	2003	Maillefer	1998	Leung Ki	debiotech.ch
Ingestible capsule	GastroTarget Corp.	Drugdel.	TE	C	ID	Gastro	P	1994	Schentag			
Transdermal drug delivery	Debiotech / KTH	Needles	TE	C	OTO	Drug	A	2003	Maillefer			debiotech.ch
Microtrans	BioValve	Needles	TE	C	ODU	Drug	A					biovalve.com
Micro needles	Micronit	Needles	TE	C	OTO	Drug	A	2003	Gardeniers	2002	Gardeniers	micronit.com
Microneedles stent	Virginia, University of	Needles	CH	A	AN	Car	A	2004	Reed			http://bme.virginia.edu
Microenhancer	BD Technologies	Needles	TR	C	AN	Gene	A	2002	Mikszta			bd.com
Microseeding	Brigham Hospital Boston	Needles	TR	A	AN	Gene	P	1998	Eriksson			brighamandwomens.org
Micromachined ultrasound transducers												
Ultrasound	Sensant, Stanford	CMUT	TR	C	ODU	Onco	A	2003	Wong	2002	Johnson	sensant.com
Ultrasound	Georgia Tech	CMUT	TR	A	OTO	Car	A	2005	Degertekin	2002	Knight	me.gatech.edu
CardioQTM	Deltex	PZT	TR	C	ODU	Car	A					deltexmedical.com
Flowire	Volcano	PZT	TR	C	ODU	Car	A	2000	Schulze-Clewing			volcano.com
Ultrasound	Duke University	PZT	TR	A	AN	Car	A	2004	Lee	2000	Light	bme.duke.edu
Ultrasound	Imperial College	PZT	TR	A	CL	Surg	A	2004	Dickinson			imperial.ac.uk/biomedeng
Micro Opto Electro Mechanical Systems												
Conf. Opt. Scan. Micr.	Olympus	MOEMS	TR	C	OTO	Var	A	2005	Murakami			olympus.co.jp/en/
Camera Pill	Given Imaging	MOEMS	TE	C	ODU	Gastro	A	2005	Panescu			givenimaging.com/
Endoscope	Pittsburgh, University of	MOEMS	TE	A	AN	Onco	A	2001	Pan			engr.pitt.edu/bioengineering
Flow Sensor	IZM, Fraunhofer	MOEMS	TE	A	OTO	Fetal	A	2003	Keoschkerjan			izm-m.fraunhofer.de/
Implantable telescope	Opthalmic Technologies	MOEMS	CH	C	CL	Oph	A	2004	Lane	2002	Peli	visioncareinc.net
BioInfoMicro Interface	Brown University	MOEMS	CH	A	OTO	Neuro	A	2005	Anderson			brown.edu
Near IR glucose sensor	Iowa University	MOEMS	CH	A	OTO	Endo	A	2006	Kanukurthy			ece.engineering.uiowa.edu
IVP	IMS-CHIPS	MOEMS	TR	A	OTO	Gastro	P	2005	Arena	2000	Neidlinger	http://ivp.ims-chips.de/
DELAS	Laser- und Medizin Tech	MOEMS	TR	C	OTO	Surg	P	1997	Schutz			lmtb.de
Other Micro System Devices for Implantable Applications												
Smart Catheters	Tohoku University	Actuators	TR	A	OTO	Var	A	2001	Mineta			mems.mech.tohoku.ac.jp
Smart Catheters	Delft Uni.of Technology	Actuators	TR	A	OTO	Var	A	2005	Langelaar			dimes.tudelft.nl
Smart Catheters	Sarcos	Actuators	TE	C	OTO	Var	A					sarcos.com/medicalproj.html

End Item	Organization	Part	Dur.	Type	Stat.	Clin.	Act.	Year	Author	Year	Author	Internet
Other Micro System Devices for Implantable Applications (Continued)												
Micro Surgical Tools	Wisconsin, Uni. -Madison	Cutting	TR	A	OTO	Surg	A	2001	Chen	2001	Son	wisc.edu
Cutting Tools	Berkeley, Uni. of California	Cutting	TE	A	OTO	Surg	P	1995	Lal			berkeley.edu/
Stent with nanobumps	Purdue University	Bumps	CH	A	OTO	Car	A	2005	Palin	2003	Thalpa	purdue.edu
Polymer with nano tubes	Purdue University	Nanotubes	CH	A	OTO	Var	A	2004	Webster			purdue.edu
Microdialysis	Berkeley, Uni. of California	Needles	TE	A	OTO	Endo	A	2004	Zimmerman			me.berkeley.edu
RFID	Verichip	Other	CH	C	AN	An	A					adsx.com
AN Identification	Destron Fearing	Other	CH	C	ODU	An	A					destronfearing.com
Biodegr. Scaffold	MIT	Scaffold	TE	A	OTO	Tis	A	2002	King			mit.edu
Biodegr. Scaffold	Inst. Industr. Science Tokyo	Scaffold	TE	A	OTO	Tis	A	2004	Leclerc			iis.u-tokyo.ac.jp
Biodegr. Scaffold	Charles Stark Draper Lab	Scaffold	TE	A	OTO	Tis	A	2006	Bettinger			draper.com/business/biomed
BioSilicon	pSiwida	Scaffold	TE	C	OTO	Tis	A					psiwida.com

Although there are more then 140 micro systems for implantable applications listed in Table 2.2 it is not claimed that this overview is complete. Nevertheless some observations will be based on this data. In Figure 2.2 and Figure 2.3, the distributions of the publication dates of the references that have been included in Table 2.2 are examined. Thirty-three percent (15 of 45) of the end items with both most recent and oldest reference originate from the year 2000 or later. Thirty-two percent of the end items have both a most recent and oldest reference. Table 2.3-Table 2.6 provide various ways of ordering the data using the classification scheme. Further commenting on the numbers is done in the table captions.

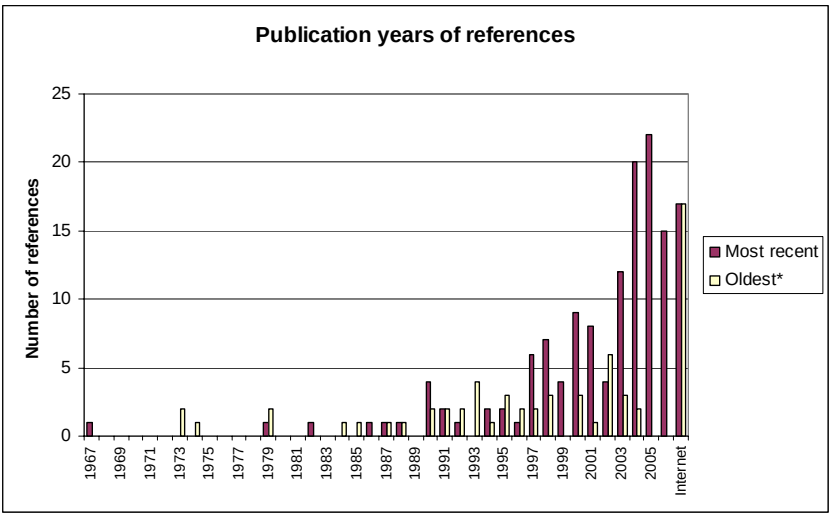

Figure 2.2 Number of references per year of publication for all end items mentioned in Table 2.2. Purple bars are the most recent publications. Yellow are the oldest publications (*excluding end items that only have a most recent reference). Internet references are placed in a separate category since no additional investigations into the publishing date was done.

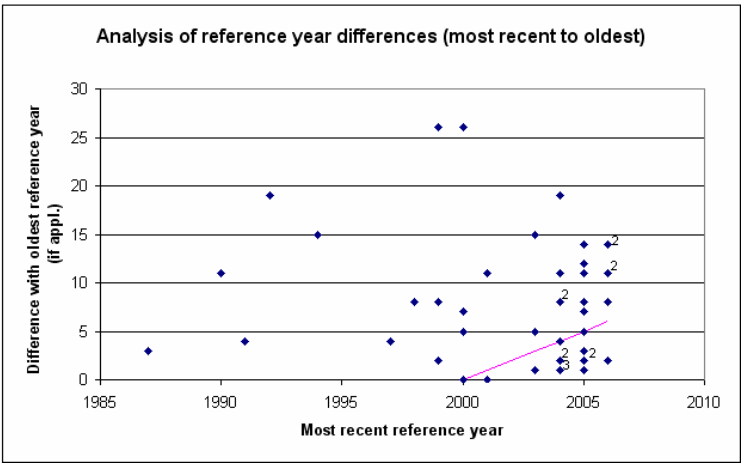

Figure 2.3 Difference between most recent and oldest reference as function of most recent reference year (only those references that have most recent and oldest reference). The small numbers next to a data point (number is placed at upper right corner of data point) indicate doubles or triple. End items below or on the purple line are from the year 2000 or more recent. End items above the purple line are from 1999 or earlier. In formula Diff = Yrec – Yco, were Diff is the difference between oldest and most recent, Yrec is the most recent year of publication and Yco is the desired 'cut off' year. In this case Yco = 2000.

Table 2.3 Number of end items as a function of Duration of implant (Transient (< 1 day, TR); Temporary (1 day < duration < 30 days, TE); Chronic (> 30 days, CH)); as function of Status of development of the end item (Idea (ID); Proto (OTO); Animal (AN); Clinical (CL); Product (ODU)); as function of Activity (Active (A) if most recent reference published in year 2000 or later or internet, Passive (P) otherwise) and as function of the Type of organization (Academic (A);Commercial (C)). There are 142 end items in total (1) of which 105 are active (2) and 70 are commercial (6). The majority of passive end items (25 of 37) have a status of prototype or animal research and are created by academic type of organizations. From the 105 active end items 18 (13% of total number of end items) are classified as product (3) all made by commercial type of organizations, as is to be expected for products. Note also that from these 18 products, there are only 2 for chronic use. There is still considerable potential for chronic implantable micro system products to come, judged by the number of end items in clinical, animal and proto phase in this category (4). However the path from academic research to commercialization, clinical trials and market introduction of chronically implantable products is long (more then 12 to 13 years) as indicated by the average year of first publication of end items that are still in the animal or clinical phase (5).

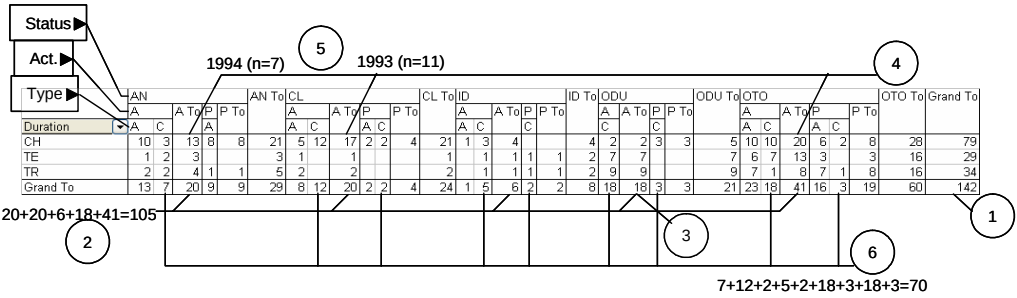

	AN					AN To	CL					CL To	ID					ID To	ODU					ODU To	OTO					OTO To	Grand To
	A		A To	P	P To		A		A To	P	P To		A		A To	P	P To		A		A To	P	P To		A		A To	P	P To		
Duration	A	C		A			A	C		A	C		A	C		C			C			C			A	C		A	C			
CH	10	3	13	8	8	21	5	12	17	2	2	4	21	1	3	4			4	2	2	3	3	5	10	10	20	6	2	8	28	79
TE	1	2	3			3	1		1				1		1	1	1	1	2	7	7			7	6	7	13	3		3	16	29
TR	2	2	4	1	1	5	2		2				2		1	1	1	1	2	9	9			9	7	1	8	7	1	8	16	34
Grand To	13	7	20	9	9	29	8	12	20	2	2	4	24	1	5	6	2	2	8	18	18	3	3	21	23	18	41	16	3	19	60	142

Table 2.4 Classical technology-market matrix with MST Class on the vertical axis and Clinical Field on the horizontal axis (Animal (An), Auditory (Aud), Cardiology (Car), Dentology (Dent), Drugdelivery (Drug), Endocrinology (Endo), Fetal, Gastroenterology (Gastro), Neurology (Neuro), Oncology (Onco), Ophthalmology (Oph), Orthopedics (Orth), Surgery (Surg), Tissue Engineering (Tis), Urology (Uro) and Various (Var)). The table entries are the number of end items. The major technology market combinations are Sensors for Cardiovascular, Drug Delivery for Drug Delivery and Electrodes for Neurology and Ophthalmology. Together these form 51% of all end items. Sensors for Cardiovascular are further detailed in Table 2.5 and Electrodes for Neurology are further detailed in Table 2.6.

Class	An	Aud	Car	Dent	Drug	Endo	Fetal	Gastro	Neuro	Onco	Oph	Orth	Surg	Uro	Var	Gene	Tis	Total
Drugdelivery			1		13			1								2		17
Electrodes		3							21		11							35
MOEMS						1	1	2	1	1	1		1		1			9
Other	2		1			1							2		4		4	14
Sensor	3		28	1		6	1	1	7		5	2	2	3	2			61
Ultrasound			4							1			1					6
Total	5	3	34	1	13	8	2	4	29	2	17	2	6	3	7	2	4	142

Table 2.5 Sensors for cardiovascular application as function of status and duration for all types of organizations (academic and commercial) and activities (active and passive). On the vertical axis the type of sensor is classified. On the horizontal axis the status of development (Idea (ID); Proto (OTO); Animal (AN); Clinical (CL); Product (ODU)) and the duration of implant (1 day < duration < 30 days, TE); Chronic (> 30 days, CH)) are classified. The table entries are the number of end items. From this table it can be seen that the majority of cardiovascular pressure sensors are pressure sensors (20 of 28). A relatively large portion of the pressure sensors are product (7 of 20, or 35%). Most of these cardiovascular pressure sensors products are for transient use (5 of 7, or 71%).

	AN		AN To	CL	CL To	ID	ID To	ODU			ODU To	OTO		OTO To	Total
Part	CH	TR		CH		TR		CH	TE	TR		CH	TR		
AC Conductance													1	1	1
Accelerometer								1			1				1
Flow		1	1			1	1						1	1	3
Magnetic													1	1	1
Other						1	1					1		1	2
Pressure	1	1	2	5	5			1	1	5	7	2	4	6	20
Total	1	2	3	5	5	2	2	2	1	5	8	3	7	10	28

Table 2.6 Electrical Stimulation and Sensing for neurological applications (involving implantable Microsystems) as a function of status and duration for all types (academic and commercial) and activities (active and passive). On the vertical axis the main MST Part of the end item is classified. On the horizontal axis the status of development (Idea (ID); Proto (OTO); Animal (AN); Clinical (CL); Product (ODU)) and the duration of implant (1 day < duration < 30 days, TE); Chronic (> 30 days, CH)) are classified. The table entries are the numbers of end items. From this table it can be seen that there is just one product (considered to be an implantable micro system) in the neurological area. It can also be seen that all applications are for chronic use and that the majority has to do with micro fabricated electrodes (14 of 21, or 67%).

	AN	AN Total	CL	CL Total	ID	ID Total	ODU	ODU Total	OTO	OTO Total	Total
Part	CH		CH		CH		CH		CH		
Electrodes	3	3	5	5	1	1	1	1	4	4	14
Needles	4	4									4
Stimulator	2	2	1	1							3
Total	9	9	6	6	1	1	1	1	4	4	21

2.3 Overview of basic technological building blocks

In this section the information will be restructured in the form of the underlying technical blocks needed to produce the end items.

- Processing
- Packaging
- Communication
- Power
- Materials

To treat these building blocks in detail would take a separate review for each of them. Therefore, the aim of this section is to provide a general overview of what type of technologies are used, regardless of the classification as presented above. Figure 2.4 provides a schematic representation of an implantable system.

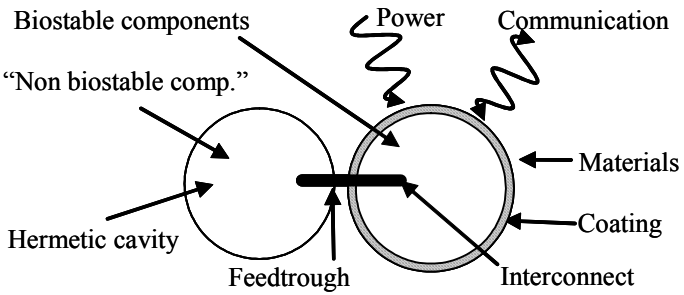

Figure 2.4 Schematic representation of technological aspects of an implantable (micro) system.

2.3.1 Processing

In this section micro fabrication processes that form the basic manufacturing technologies used to produce the end items

reviewed in this chapter are briefly described. Surface micro machining involving thin layer deposition, sacrificial layer etching, photolithographic patterning and etching are used. Processes compatible with CMOS allow integration with electronic circuitry. Bulk micro machining involving both dry and wet etching of silicon, and stacking of wafers is shown. Some devices use soft materials made using polymer micro machining technologies like micro molding or hot embossing. Laser micro machining is used to drill holes or cut material. Sometimes 'non traditional' fabrication processes coming from disciplines like chemistry or biology are used for example for amperometric sensors or coatings. Many of the papers referenced in this review contain details of the micro processing steps used to manufacture the design. A number of introductory texts on micro fabrication technologies exist, for example [31,266,267].

2.3.2 Packaging

This section is dealing with the packaging for implantable applications. The body is (fortunately) a very hostile environment for foreign bodies that enter it, due to our active immune system. Delicate parts of micro systems are therefore often protected by a hermetic package, traditionally a metal casing. Electrical communication with the outside of a hermetic cavity is possible by means of hermetic feedthroughs. Electrical conductors and interconnections outside a hermetic cavity will have to be biostable. Coatings used to improve the properties of the implant can be seen as a special way of packaging.

2.3.2.1 Hermetic protection, electrical -feedthrough, -interconnect and -conductors

The focus is on presenting the examples found in literature of electrical interconnects outside an hermetic cavity (if there is one) and on how electrical signals are fed into the hermetic cavity (feedthroughs) assuming that once inside the hermetic

cavity packaging can be achieved. First it is described how hermitic protection is realized.

Hermetic housings are traditionally made of titanium, tantalum, niobium [268] or stainless steel. Micro machined ceramic packages [204] [205] [92] [95] [94] glass sealed packages [127] and polymer encapsulations[116,126] are also used. One package uses a glass silicon anodic bond which has a mean time to failure of 177 years at 37°C, estimated from saline soak tests[193,194,195,196].

Glass to metal seals made of sodium free borosilicate glass are used for feedthroughs [268]. Interconnection techniques used in the semiconductor packaging and assembly industry are also used for manufacturing implantable devices[239,233,238]. Flip chip is frequently used [10] [11,98] with Au-Au thermo compression bonding [269] on a flex circuit [34,145,43] or on top of a MEMS chip [175]. Wirebonding on flex with globtop [36] or on printed circuit board (PCB) with two component glue for isolation [99,100,270] has also been applied. A hybrid interconnect technique based on ball wedge bonding that survives 4 years in saline solution and 10 months implantation in rats has been developed [271,17,10,131]. A three dimensional chip scale package based on ultra violet (UV) curable polymer with integrated conductors is under investigation [272]. Conductive glue has also been proposed [74].

In general, DC potential on conductors should be avoided [20] or conductors should be hermetically sealed [268], because of the risk of failure due to electrochemical corrosion or the creation of conductive pathways when salt crystals form (dendrite growth). To minimize this risk, metal parts should not differ in electrochemical contact voltage, alloys are to be avoided and welding is preferred [268]. Corrosion products should have low solvability and corrosion should be controlled also by the shape of the design [4]. One concept uses liquid crystal polymer films

with metal traces on top of it [273] and another one silicon ribon cables [209].

2.3.2.2 Coatings

Coatings are used to improve the interface of the implant with the body organs [274]. Criteria for an excellent coating are edge covering, peel resistance and integrity of the regular coating film [37]. Polymer is the most common coating material with silicone rubber probably being number one [275,56,90,37,276] [11,34,45,275]. The implant can be completely injection molded in this substrate [90]. Other polymer coatings are parylene [74] [131]; epoxy [10] or others [192,277]. Electrografting yields highly covering, highly versatile polymer coatings especially on complex shapes [278]. A polymer coating can also be used to promote cell growth [127] [19].

Other coating materials are metal coatings [279], ultrananocrystalline diamond prepared by plasma chemical vapor deposition [280], calcium phosphate deposited by pulsed laser ablation[281] or hydroxyapatite (HA)-TiO_2 created by micro-arc oxidation of a predeposited HA layer on titanium[282]. This last one is primarily used to improve osseointegration of the implant with hard tissue (bone). Surface (topology) modifications can also provoke the desired response of the body [283,1].

2.3.3 Power

For implantable products that have physical connection to the outside world, power consumption is generally not a problem since an “unlimited” supply can be accessed. Autonomous implants that operate on a primary battery need to have sufficient longevity. Especially for chronic implants this places an important requirement on the power consumption of the device. Since device functions are steadily progressing and since size should be kept as small as possible, much development effort has been invested in implantable batteries. Recently, implantable

devices with rechargeable batteries [284,285] were introduced. The examples that will be briefly presented in this section are ongoing (long term) developments aiming at autonomous power and concepts in which energy is provided from the outside.

Inductive coupling uses changing electro magnetic fields outside the body that are picked up by an implant inside the body[11,34]. Pick up coils can be micro machined on chip [43,36] or on flex[276]. The coupling range is limited [10]. To overcome this problem, a distributed implant system connected via cables powered via a central coil that is close under the skin has been proposed [13]. Efficiency can also be improved by a self-tuning system [286,287].

Autonomous power could be delivered by electrostatic conversion of mechanical vibrations. A capacitance change due to external vibrations causes current to flow and has generated 0.2uW [288]. Thousands of thermocouples on chip have been developed for an implantable biothermal battery [289]. The use of ultrasound at 1.7 Mhz with PZT discs has been described in [290]. Implantable bio fuel cells are also being investigated [291]. Other concepts use solar energy or pressure variations[292].

2.3.4 Communication

Most of the time, communication with the implantable device is desirable to either receive data concerning the device status or patient condition or to send data to the device to (re)program it. Most of the time this is done using an inductive link, which is sometimes also used for transmitting power (see 2.3.3) [127,19,98,173,277]. Advances in RF engineering have enabled detection from deep within the lossy medium of the body [86]. Thick magnetic materials on silicon support higher magnetic flux for higher power density and longer coupling distance [293].

Entirely passive circuits that can be wirelessly probed to detect a property that changes value in response to for example flow have been described [74]. Others describe a special protocol

which enables both powering and signal transfer to be done via two leads only [207]. An optical telemetry link to transmit data to an external controller is also an option [202].

2.3.5 Materials

The choice of materials for implantable applications is limited by both biostability and biocompatibility requirements. Biostability means that the material must withstand the attacks of the body. Biocompatibility means that the material must not cause any unwanted reactions by the body. A list of biocompatible and biostable materials does not exist, since the mechanisms involved depend on many details, like material processing, shape, finish, post treatment and impurities but also on the place and duration of use. Nevertheless it makes sense to present the various materials that have been described in the literature on implantable microsystems. The materials include silicon[154,18,7], silicon dioxide [154,18,133,51], silicon nitride[18,133,51], silicon carbide [294], titanium nitride [154], poly-silicon[193,194,195,196], parylene [74,131], epoxy [74,10,131], polyimide [17,131,13,10,3], polyester [3], silicon rubber [9,131,3], gold [131], platinum [131,20,25], iridium [131,20,25], titanium [18,3,7], tantalum [133], stainless steel [74] and shape memory alloys [3].

While it is beyond the scope of this section to fully discuss material properties and issues here, the material aspects relating to their use in implantable applications will be briefly described. Silicon can be made in very pure form which is good for high reliability applications of silicon micro mechanical systems due to stable mechanical properties. Apart from material properties this has to do with the highly developed infrastructure related to silicon micro fabrication processes. In addition silicon is the dominant material for IC manufacturing, offering the opportunity for MEMS IC integration, often leading to superior characteristics. Silicon carbide for example is ideal for

application in harsh environments (like the human body) because of its high chemical resistance. Silicon dioxide is a very effective insulator and is often used in combination with silicon nitride for its ability to prevent impurity diffusion and ionic contamination. Many of the metals described are used as electrical interface to the body; see section 2.2.2 for a brief discussion. Titanium is the preferred material for hermetic housings of chronically implantable devices because it is in the passive region of the electrochemical anodic polarization curve (it forms an oxide so fast that it protects the metal from further corrosion). The same is true for stainless steel which is commonly used as conductor in non hermetic environments for chronic implantable applications. Polymers are soft and flexible which minimizes the chance of damage to the body and they are advantageous for applications in which the device has to be able to adapt to the shape of the human anatomy. Polyimide is often used because of its low moisture uptake and because of its well developed fabrication processes.

2.4 Implantable Microsystems: a case study

Since a general and broad overview is per definition very general and broad, one small case study which shows in more detail the successful role that micro systems can play in a clinical setting is presented. This case study is presented in the form of 1) What is the physiology of the clinical condition and how can it be treated and 2) How do microsystems play a role (historical perspective and outlook). Sick Sinus Syndrome is selected because this is a disease which uses implantable micro systems as therapy of choice.

2.4.1 Sick Sinus Syndrome

During exercise the metabolic need of the body rises. Part of this increased need can be met by upregulating the supply of

oxygen. This is done by increasing cardiac output (CO, amount of blood that is pumped through the circulation expressed in liters per minute) and/or the amount of oxygen that is taken from the arterial blood. The cardiac output is the product of heart rate (HR) and stroke volume (SV, volume of blood pumped per heartbeat) that both can be increased. In total the body has the ability to increase the oxygen supply by a factor of approximately twenty compared to the resting state (HR x3.3; SV x1.7 and Oxygen uptake x3.5).

Heart rate is determined by the sinus node. The cardiac cells in the sinus node function as a natural pacemaker, initiating an electrical activation wave that is conducted over the heart and results in contraction of the heart muscle. While other heart cells have a constant membrane potential as a function of time when at rest, the cells in the sinus node depolarize spontaneously at a certain rate, until a threshold voltage is reached that triggers the rapid depolarization of the cell that initiates an action potential. The depolarization rate of the sinus cells (and thus the heart rate) is regulated by adrenaline and under direct control by the nervous system.

People with Sick Sinus Syndrome have a degenerated sinus node that no longer responds properly to the control mechanisms that dictate its depolarization rate. That is, the heart beats at an inappropriately low rate. Therefore these people are limited in the amount of exercise they can perform since they only have change in stroke volume and oxygen uptake left to adapt the oxygen supply.

2.4.2 Implantable Microsystems for Sick Sinus Syndrome

Electrical stimulation by an implanted electrode in contact with heart cells can also initiate electrical activation followed by mechanical contraction. Therefore, sick sinus syndrome can be well treated with an implantable pulse generator (IPG) if there is a way to determine at which rate it must pace. The literature of

rate adaptive pacing starts around 1978. Until that time there were only fixed rate pacemakers that started in 1958 with the first fully implantable battery operated fixed rate pacemaker [295]. Of course, in patients requiring a pacemaker because of atrio-ventricular block who have maintained normal sinus node function, the natural atrial rate, originating in the sinus node, is the best initiator of the optimal ventricular pacing rate. Several ways have been described to control heart rate in patients with sick sinus syndrome based on measuring a property that is a measure for the actual metabolic need. Examples are the QT interval in the cardiac electrogram [296], the pH [297]; oxygen saturation [298,299]; activity [103,300]; right ventricular pressure [80]; respiratory frequency [301] and temperature [302]. Oxygen saturation is sensed on the basis of colorimetric principles. The sensor contains a light sensitive photo diode that detects reflected light alternatively emitted from an infrared (IR)- or red (R)-LED also contained in the sensor. Each LED emits until a predefined amount of light energy is collected by the photo diode. The oxygen saturation is calculated from the ratio between the two ON times and two calibration constants that come with the sensor [299]. The first tests have been performed with an external system [298]. Patient activity causes pressure waves in the body that result in bending of the metal shield of the implanted device. A piezo electric sensor mounted on the inside of the shield transforms this bending into an electrical signal and together with appropriate algorithms can be used for rate response [103]. First experiments with pressure sensors were using an externally closed loop. A signal proportional to the rate of change of the right ventricular pressure (dP/dt) was generated by a piezoelectric bender sensor positioned on the inside of a deformable portion of a hermetically sealed capsule located on the distal end of a lead [80]. Temperature is measured with a thermistor incorporated in the tip of a lead [302]. In the end, most modern pacemakers today use acceleration sensors for rate

control because they are relatively simple (it does not have to interface with the outside) and because they can provide appropriate rate response. These sensors are typically micro machined accelerometers, present in the majority of the about 500,000 pacemakers that are implanted worldwide each year.

There is some room to improve the exercise performance of patients with sick sinus syndrome by finding more advanced ways to control the heart rate for maximum metabolic demand, but the impact on daily life would not be very great. The main emphasis of developments that are building on the use of sensors as described above is in other areas then heart rate control. It is in automatic programming of devices and expanding it to other clinical areas like detection of unstable arrhythmias[303] or heart failure management[79].

2.5 Discussion

This section highlights the perspectives and challenges of microsystems related to the areas reviewed. Power consumption, size, sensitivity, specificity, accuracy and stability are important design parameters for most implantable applications of sensors. Since many sensors have to interface to the environment in order to function, and since the body is an active system trying to control this interface, achieving the requirements on these aspects is often challenging especially for chronic implantation. The clinical advantages are driving the efforts aimed at overcoming these challenges: relevant information is made available on a continuous basis, quality of life can be increased, patient compliance is guaranteed, diagnosis is quantified or even enabled (no prior means to perform the diagnosis), therapy is improved for example by adapting the therapy according to the sensors input (close loop system), disease status can be continuously monitored, implantation procedure can be

facilitated and sensors based on implantable microsystem have improved performance compared to existing technology.

Micro electrodes made using IC like fabrication technologies offer the advantage of exact electrode positions, small size, multiple electrodes, improved electrode tissue interface and active circuitry. Main challenges are in optimizing the charge transfer properties needed for electrical stimulation in combination with electrochemical properties that lead to long term stability. For wireless applications the transmission speed is sometimes a limitation. Flexible electrodes offer advantages compared to the (generally) more rigid silicon structures in certain applications. Micro electrodes can provide improved therapy due to the ability to better target electrical stimulation energy to a specific region. It can be more challenging to determine which region this is then to provide the hardware to do it.

Important design characteristics for delivery of substances to the body are accuracy, resolution, safety and control which can be realized by micro machined components with order of magnitude improvements compared to conventional technology. Transdermal gene delivery using micro fabricated structures is more efficient than single injection and particle-mediated gene transfer. The use of microneedles designed to penetrate diffusion barriers for DNA material lead to a more effective delivery. Miniaturized imaging tools enabled by micro machined components are used in minimal access surgery which greatly reduces the impact of the treatment to the patient and allows improved diagnosis on the basis of superior or completely new images. Micro actuators are being developed for making smart catheters to expand the applicability of minimally invasive (transvascular) procedures. Smart micro machined cutting tools with sharper edges then conventional needles could be used when very fine and precise surgery is needed. Tissue response to implants can be modified by surface topology in the micrometer range and high resolution, fast,

inexpensive, reproducible and scalable micro fabricated biodegradable scaffolds are being investigated for in vivo tissue engineering of capillary structures or liver reconstructs.

In general, the perspectives that microsystems for implantable applications have to offer are low cost, small size, low weight, high reliability, low power and superior functionality or performance. Micro systems can be combined with biotechnology and molecular biology. The reliability requirements are at the same time also a challenge, since new technologies generally present new failure mechanisms. The realization of low cost can also be difficult in practice due to the lack of real mass volumes (in the order of millions) in many implantable applications. Other challenges include long development times, packaging and bio-compatibility and -stability. Success factors of new products depend on more then technical characteristics alone.

2.6 Summary

A general and broad overview of micro systems for implantable applications as found in literature has been provided. The focus has been on implantable micro-fabricated parts not contained in “classic” hermetically sealed metal casings, including transient and temporary use. Although this chapter lists more then 140 examples, it is not claimed that this overview is complete. As a first observation it is stated that a large range of microsystems is being used or investigated. Sensors, micro electrodes, drug and gene delivery devices, micro machined ultrasound transducers, MOEMS, micro actuators, surgical tools, micro surface topology, micro fabricated bio degradable scaffolds and others have been presented. These micro systems find application in a wide range of clinical areas including cardiology, neurology, ophthalmology, orthopedics, drug

delivery (for various clinical areas), surgery, endocrinology, tissue engineering etcetera.

To further analyze the information, a classification scheme has been introduced consisting of MST-class and –part, duration of implant, type of organization, status of end item, clinical field and activity. Besides the classifications, name of the end item, name of the organization, reference to internet address and year/author of oldest and most recent paper are given. Classification is based on the information available to the authors. There are 105 active and 70 commercial end items from a total of 142. The majority of the 37 passive end items (25 of 37) are prototypes or animal research devices created by academic organizations. From the 105 active end items, 18 (13% of total number of end items) are classified as products, all made by commercial organizations. Note also that from these 18 products, there are only 2 for chronic use. There is still considerable potential for permanent implantable micro system products to come, judged by the number of end items in clinical- (17), animal- (13) and proto- (20) phase in this category. The path from academic research to commercialization, clinical trials and market introduction of permanently implantable products is long, however, as indicated by the average year of first publication of end items that are still in the animal- (1994, n=7) or clinical- (1993, n=11) phase. The major technology-market combinations are Sensors for Cardiovascular, Drug Delivery for Drug Delivery and Electrodes for Neurology and Ophthalmology. Together these form 51% of all end items. The majority of sensors are pressure sensors and there is just one product (considered to be an implantable micro system) in the neurological area.

A general overview of packaging, communication, power and materials -the major underlying technical blocks needed to produce end items- has been provided regardless of the classification. Hermetic housings are traditionally made from

titanium, tantalum or niobium. Micro machined ceramic packages, glass sealed packages and polymer encapsulations are also used. Glass to metal seals are used for feedthroughs. Interconnection techniques like flip chip, wirebonding or conductive epoxy as used in the semiconductor packaging and assembly industry are also applied for manufacturing implantable devices. Coatings are used to improve the interface of the implant with the body organs with polymers or metal as coating material. Longevity for chronic implants not connected by wires to the outside places an important requirement on the power consumption of the device. Since device functions are steadily progressing and size should be kept as small as possible, much development effort is put in implantable batteries. As an alternative, rechargeable batteries were introduced or concepts in which energy is provided from the outside based on inductive coupling. Long term developments aiming at autonomous power are for example based on electrostatic conversion of mechanical vibrations. Most of the time, communication with the implantable device is desirable to either receive data concerning the device status or patient condition or to send data to the device to (re)program it. This is usually done through an inductive link although optical means also have been reported. Entirely passive circuits that can be wirelessly probed to communicate information from inside to outside the body have been described. The choice of materials for implantable applications is limited by both biostability and biocompatibility requirements. A list of biocompatible and biostable materials does not exist, since the mechanisms involved depend on many details, like material processing, shape, finish, post treatment and impurities but also on the place and duration of use. There is a large range of materials commonly used in micro fabrication used for implantable microsystems including silicon, polymers and metals.

2.7 References

[1] Kovacs, G 1998 *Micromachined Transducers Sourcebook* WCB/McGraw-Hill 0-07-290722-3

[2] Audet, S 2003 Medical Applications of Microsystems *Micro System Technologies* pp 37-43

[3] Nexus Medical Devices User-Supplier Club (USC) 2003 *Nexus Product Technology Roadmap 2003*

[4] Wilkinson, M and Hitchings, D 2003 *Microsystems in Biomedical Engineering* FSRM Swiss Foundation for Research in Microtechnology

[5] Weiss, Ch 2005 *Microsystems for Medical Technology* MSTNews pp 24-25

[6] van Est, R 2004 *Om het kleine te waarderen* Rathenau Instituut 90-77364056

[7] Technology for Industry 2005 *Micro & Nanotechnology in Healthcare & Life Sciences Market Sector Report* Technology for Industry Ltd

[8] FSRM, VDI/VDE-IT, and Yole Developpement 2003 *World of Microsystems* 2-88238-004-6

[9] Ziaie, B, Baldi, A, Lei, M, Gu, Y, and Siegel, R A 2004 Hard and soft micromachining for BioMEMS: Review of techniques and examples of applications in microfluidics and drug delivery *Advanced Drug Delivery Reviews* **56** 145-172

[10] Stieglitz, T 2001 *Implantable Microsystems for Monitoring and Neural Rehabilitation, Part I* Medical Device Technology vol 2001, pp 2-4

[11] Mokwa, W and Schnakenberg, U 1998 On-Chip Microsystems for medical applications *Microsystem Symposium* Delft

[12] Emmerzaal, J P 2005 MicroNed: samenwerken voor en met het MKB *MST: De trein raast verder!* Mikrocentrum

[13] Stieglitz, T 2002 *Implantable Microsystems for Monitoring and Neural Rehabilitation, Part II* Medical Device Technology vol 2002, pp 2-6
[14] Dario, P, Carrozza, M C, Benvenuto, A, and Menciassi, A 2000 Micro-systems in biomedical applications *Journal of Micromechanics and Microengineering* **10** 235-244
[15] Technology for Industry 2002 *Microsystems & Nanotechnology in the Medical and Biomedical Markets*
[16] Noble, R, Cox, T, and Wilkinson, A-S 2004 *Silicon-based MEMS & Medical Applications* Advanced Microsystems Engineering Group, QinetiQ, Malvern Technology Centre
[17] Schneider, A, Stieglitz, T, Haberer, W, Beutel, H, and Meyer, E 2001 Flexible Interconnects for Biomedical Microsystems Assembly *IMAPS Conference*
[18] Goosen, J F L, Tanase, D, and French, P J 2000 Silicon sensors for use in catheters *1st Annual International IEEE-EMBS Special Topic Conference on Microtechnologies in Medicine & Biology* vol 2000 pp 152-155
[19] Mokwa, W 2004 MEMS technologies for epiretinal stimulation of the retina *Journal of Micromechanics and Microengineering* **14** 12-16
[20] Sivard, A, Bradley, P, Chadwick, P, and Higgins, H 2004 *The challenge of designing in-body communications* Embedded.com vol 2004,
[21] Rakhorst, G 2006 Medische productontwikkeling binnen universiteit en bedrijfsleven: een wereld van verschil *ALV KiviNiria afdeling BMT*
[22] Prohaska, O J, Olcaytug, F, Pfunder, P, and Dragaun, H 1986 Thin-film multiple electrode probes: possibilities and limitations *IEEE Transactions on Biomedical Engineering* **BME-33** 223-229

[23] Ganesh, B, Ameel, T A, Normann, R A, Chinn, D A, Petelenz, D G, and Frazier, A B 1997 Packaging of neural stimulation/recording systems: review and new mechanism for interfacing passive electrodes and signal processing circuitry *Advances in Electronic Packaging 1997. Proceedings of the Pacific Rim/ASME International Intersociety Electronic and Photonic Packaging Conference. INTERpack '97* vol vol.1 Kohala Coast, HI, USA ASME pp 475-482

[24] Laser, D J and Santiago, J G 2004 A review of micropumps *Journal of Micromechanics and Microengineering* R35-R64

[25] Prodanov, D P, Marani, E, and Holsheimer, J 2004 Functional Electrical stimulation for sensory and motor functions: progress and problems. *Biomedical reviews (ISSN 1310-392X)* **14** 23-50

[26] Haga, Y and Esashi, M 2004 Biomedical microsystems for minimally invasive diagnosis and treatment *Proceedings of the IEEE* **92** 98-114

[27] Reed, M L and Lye, W K 2004 Microsystems for drug and gene delivery *Proceedings of the IEEE* **92** 56-75

[28] Weiland, J D, Liu, W, and Humayun, M S 2005 Retinal prosthesis *Annu.Rev.Biomed.Eng* **7** 361-401

[29] Zhang, H, Hutmacher, D W, Chollet, F, Poo, A N, and Burdet, E 2005 Microrobotics and MEMS-based fabrication techniques for scaffold-based tissue engineering *Macromolecular Bioscience* **5** 477-489

[30] Panescu, D 2006 MEMS in medicine and biology *IEEE Engineering in Medicine and Biology Magazine* **25** 19-28

[31] Gad-el-Hak, M 2002 *The MEMS Handbook* ed Gad-el-Hak, M London CRC Press 0-8493-0077-0

[32] Collins, C C 1967 Miniature passive pressure transensor for implanting in the eye *IEEE Trans.Biomed.Eng* **1967** 74-83

[33] Backlund, Y, Rosengren, L, Hok, B, and Svedbergh, B 1990 Passive silicone transensor intended for biomedical, remote pressure monitoring *Sensors and Actuators A* **21** 58-61

[34] Mokwa, W and Schnakenberg, U 2001 Micro-transponder systems for medical applications *IEEE Transactions on Instrumentation and Measurement* **50** 1551-1555

[35] Puers, R, Vandevoorde, G, and De Bruyker, D 2000 Electrodeposited copper inductors for intraocular pressure telemetry *Journal of Micromechanics and Microengineering* **10** 124-129

[36] Flick, B, Orglmeister, R, and Berger, J M 1997 Study and development of a portable telemetric intracranial pressure measurement unit *Annual International Conference of the IEEE Engineering in Medicine and Biology - Proceedings* **3** 977-980

[37] Hierold, C et al. 1998 Implantable low power integrated pressure sensor system for minimal invasive telemetric patient monitoring *Proceedings of the IEEE Micro Electro Mechanical Systems (MEMS)* Heidelberg, Ger IEEE, Piscataway, NJ, USA pp 568-573

[38] Chapman, P H, Cosman, E R, and Arnold, M A 1990 The relationship between ventricular fluid pressure and body position in normal subjects and subjects with shunts: a telemetric study *Neurosurgery* **26** 181-189

[39] Cosman, E R, Zervas, N T, Chapman, P H, Cosman, B J, and Arnold, M A 1979 A telemetric pressure sensor for ventricular shunt systems *Surg.Neurol.* **11** 287-294

[40] Brindley, G S, Polkey, C E, and Cooper, J D 1983 Technique for very long-term monitoring of intracranial pressure *Med.Biol.Eng Comput.* **21** 460-464

[41] Talamonti, L, Porrovecchio, G, and Marotta, G 1988 Contactless inductive-operation microcircuits for medical

applications *Proceedings of the Annual International Conference of the IEEE Engineering in Medicine and Biology Society (IEEE Cat. No.88CH2566-8)* New Orleans, LA, USA IEEE pp 818-819

[42] Zacheja, J, Clasbrummel, B, Binder, J, and Steinau, U 1995 Implantable Telemetric Endosystem for Minimal Invasive Pressure Measurements *Medtech 95, Berlin, Germany*

[43] Eggers, T, Marschner, C, Marschner, U, Clasbrummel, B, Laur, R, and Binder, J 2000 Advanced hybrid integrated low-power telemetric pressure monitoring system for biomedical applications *Proceedings of the IEEE Micro Electro Mechanical Systems (MEMS)* 329-334

[44] Marschner, C, Eggers, T, Drawger, J, Hille, K, Stegmaier, P, Laur, R, and Binder, J 2000 Wireless eye pressure monitoring system integrated into intra-ocular lens *Proceedings. MICRO.tec 2000. VDE World Microtechnologies Congress* vol vol.1 Hannover, Germany VDE Verlag pp 549-553

[45] Flick, B B and Orglmeister, R 2000 Portable microsystem-based telemetric pressure and temperature measurement unit *IEEE Transactions on Biomedical Engineering* **47** 12-16

[46] http://www.healthyaims.org/

[47] Wenzel, M 2004 Implantable Telemetric Pressure Sensor System for Long-Term Monitoring of Therapeutic Implants *Healthy Aims Dissemination Day* http://www.healthyaims.org

[48] http://www.codman.com/neuromonitor

[49] Signorini, D F, Shad, A, Piper, I R, and Statham, P F 1998 A clinical evaluation of the Codman MicroSensor for intracranial pressure monitoring *Br.J.Neurosurg.* **12** 223-227

[50] Pijls, N H J and De Bruyne, B 1994 *Practice and interpretationof intracoronary pressure recordings and calculation of flow reserve*

[51] Kalvesten, E, Smith, L, Stemme, G, and Tenerz, L 1998 The first surface micromachined pressure sensor for cardiovascular pressure *IEEE 11th International Workshop on Micro Electro Mechanical Systems* pp 574-579

[52] Aubert, A E, Vrolix, M, De Geest, H, and Van de, W F 1995 In vivo comparison between two tip pressure transducer systems *Int.J.Clin.Monit.Comput.* **12** 77-83

[53] 3,724,274 114,610 Millar, H. D 1973 *Physiological pressure transducers* Millar Instruments Inc

[54] 3,748,623 274,874 Millar, H. D 1973 *Pressure transducers* Millar Instruments Inc

[55] US 4,901,731 186,898 Millar, H. D 1990 *Single sensor pressure differential device* Millar Instruments Inc

[56] US 5,902,248 08/744,478 Millar, H. D and Smith, R. A. 1999 *Reduced catheter tip measurement device* Millar Instruments Inc

[57] Ji, J, Cho, S T, Zhang, Y, Najafi, K, and Wise, K D 1992 An Ultraminiature CMOS Pressure Sensor for a Multiplexed Cardiovascular Catheter *IEEE Transactions on Electron Devices* **39** 2260-2267

[58] Samaun, Wise, K D, and Angell, J B 1973 IC piezoresistive pressure sensor for biomedical instrumentation *IEEE Transactions on Biomedical Engineering* **BME-20** 101-109

[59] Sander, C S, Knutti, J W, and Meindl, J D 1980 A monolithic capacitive pressure sensor with pulse-period output *IEEE Transactions on Electron Devices* **ED-27** 927-930

[60] US 6,112,598 08/952,825 Tenerz, L., Hammarstrom, O., and Smith, L. 2000 *Pressure sensor and guide wire*

assembly for biological pressure measurements Radi Medical Systems AB
[61] WO 00/39550 PCT/SE99/02468 Stemme, G. and Kalvesten, E. 2000 *Resonant Sensor* Radi Medical Systems AB
[62] US 5,195,375 721,508 Tenerz, L. and Hok, B. 1993 *Miniaturized Pressure sensor* Radi Medical Systems AB
[63] WO 97/42478 PCT/SE97/00752 Engstrom, O. 2001 *Device for electro-optical pressure measurement* Samba Sensors AB
[64] WO 00/79233 A1 PCT/SE00/01296 Vidovic, N., Krantz, M., and Hojer, S. 2000 *A method and a device for bending compensation in intensity based fibre optical measuring systems* Samba Sensors AB
[65] WO 01/02824 A1 PCT/SE00/01404 Hojer, S., Josefsson, T., Krantz, M., and Vidovic, N. 2001 *Method and device for fibre-optical measuring systems* Samba Sensors AB
[66] Kandler, M and Mokwa, W 1990 Capacitive Silicon Pressure Sensor for Invasive Measurement of Blood Pressure *Micromechanics Europe*
[67] Manoli, Y, Eichholz, J, Kandler, M, Kordas, N, Langerbein, A, Mokwa, W, Fahnle, M, and Liebscher, F F 1991 Multisensor catheter for invasive measurement of blood parameters *Proceedings of the Annual Conference on Engineering in Medicine and Biology* vol 13 Orlando, FL, USA Publ by IEEE, Piscataway, NJ, USA pp 1599-1600
[68] Esashi, M, Shoji, S, Matsumoto, Y, and Furuta, K 1990 Catheter-tip capacitive pressure sensor *Electronics & Communications in Japan.Part II: Electronics* **73** 79-87
[69] Esashi, M, Komatsu, H, and Matsuo, T 1983 Biomedical pressure sensor using buried piezoresistors *Sensors and Actuators* **4** 537-544

[70] Esashi, M, Komatsu, H, Matsuo, T, Takahashi, M, Takishima, T, Imabayashi, K, and Ozawa, H 1982 Fabrication of catheter-tip and sidewall miniature pressure sensorsr *IEEE Transactions on Electron Devices* **ED-29** 57-63

[71] Totsu, K, Haga, Y, and Esashi, M 2005 Ultra-miniature fiber-optic pressure sensor using white light interferometry *Journal of Micromechanics and Microengineering* **15** 71-75

[72] US 5,392,117 45,680 Belleville, C. and Duplain, G. 1995 *Fabry-Perot optical sensing device for measuring a physical parameter* Institute Nationale D'Optique and Her Majesty the Queen in right of Canada

[73] US 5,202,939 915,645 Belleville, C. and Duplain, G. 1993 *Fabry-Perot optical sensing device for measuring a physical parameter* Institute Nationale D'Optique and Her Majesty the Queen in right of Canada

[74] Takahata, K, DeHennis, A, Wise, K D, and Gianchandani, Y B 2004 A wireless microsensor for monitoring flow and pressure in a blood vessel utilizing a dual-inductor antenna stent and two pressure sensors *International Conference on Micro Electro Mechanical Systems* vol 17 pp 216-219

[75] Ritzema-Carter, J L et al. 2006 Images in cardiovascular medicine. Dynamic myocardial ischemia caused by circumflex artery stenosis detected by a new implantable left atrial pressure monitoring device *Circulation* **113** e705-e706

[76] Walton, A S and Krum, H 2005 The heartpod implantable heart failure therapy system *Heart Lung Circ.* **14 Suppl 2** S31-S33

[77] Siess, T 2006 Blutpumpen *Festkolloquium 10 Jahre Mikrosystemtechnik and IWE 1 der RWTH Aachen*

[78] Parikh, K H et al. 2006 Effect of Metroprolol CR/XL on Pulmonary Artery Pressure in Patients With Heart Failure Measured Using First in Human Implantable Device Responding to Ultrasonic Signal *Journal of the American College of Cardiology* **47**

[79] Magalski, A et al. 2002 Continuous ambulatory right heart pressure measurements with an implantable hemodynamic monitor: a multicenter, 12-month follow-up study of patients with chronic heart failure *J.Card Fail.* **8** 63-70

[80] Bennett, T, Sharma, A, Sutton, R, Camm, A J, Erickson, M, and Beck, R 1992 Development of a rate adaptive pacemaker based on the maximum rate-of-rise of right ventricular pressure (RV dP/dtmax) *Pacing Clin.Electrophysiol.* **15** 219-234

[81] Ohlsson, A, Beck, R, Bennett, T, Nordlander, R, Ryden, J, Astrom, H, and Ryden, L 1995 Monitoring of mixed venous oxygen saturation and pressure from biosensors in the right ventricle. A 24 hour study in patients with heart failure *Eur.Heart J.* **16** 1215-1222

[82] Steinhaus, D M, Lemery, R, Bresnahan, D R, Jr., Handlin, L, Bennett, T, Moore, A, Cardinal, D, Foley, L, and Levine, R 1996 Initial experience with an implantable hemodynamic monitor *Circulation* **93** 745-752

[83] Braunschweig, F, Fahrleitner-Pammer, A, Mangiavacchi, M, Ghio, S, Fotuhi, P, Hoppe, U C, and Linde, C 2006 Correlation between serial measurements of N-terminal pro brain natriuretic peptide and ambulatory cardiac filling pressures in outpatients with chronic heart failure *Eur.J.Heart Fail.* **8** 797-803

[84] Ellozy, S H, Carroccio, A, Lookstein, R A, Jacobs, T S, Addis, M D, Teodorescu, V J, and Marin, M L 2006 Abdominal aortic aneurysm sac shrinkage after

endovascular aneurysm repair: correlation with chronic sac pressure measurement *J.Vasc.Surg.* **43** 2-7

[85] Milner, R, Verhagen, H J, Prinssen, M, and Blankensteijn, J D 2004 Noninvasive intrasac pressure measurement and the influence of type 2 and type 3 endoleaks in an animal model of abdominal aortic aneurysm *Vascular.* **12** 99-105

[86] Allen, M G 2005 Implantable micromachined wireless pressure sensors: approach and clinical demonstration *International Workshop on Wearable and Implantable Body Sensor Networks BSN-2005* London IEE pp 40-41

[87] Ellozy, S H et al. 2004 First experience in human beings with a permanently implantable intrasac pressure transducer for monitoring endovascular repair of abdominal aortic aneurysms *J.Vasc.Surg.* **40** 405-412

[88] Milner, R 2006 *Remote Pressure Sensing for Thoracic Endografts* Endovascular Today vol 2006, pp 75-77

[89] Puers, B, Van Den Bossche, A, Peeters, E, and Sansen, W 1990 Implantable pressure sensor for use in cardiology *Sensors and Actuators, A: Physical* **23** 944-947

[90] WO 00/74557 A1 Schmitz-Rode, T., Schnakenberg, U., Mokwa, W., Gunther, R. W., and Kruger, C. 2000 *Intravascularly implantable device*

[91] Schnakenberg, U, Kruger, C, Pfeffer, J G, Mokwa, W, Vom Bogel, G, Gunther, R, and Schmitz-Rode, T 2004 Intravascular pressure monitoring system *Sensors and Actuators, A: Physical* vol 110 Prague, Czech Republic Elsevier pp 61-67

[92] Sansen, W, Puers, B, and Vereecken, R 1984 Realization of a pressure telemetry capsule for cystometry *IEEE/Engineering in Medicine and Biology Society Annual Conference* Los Angeles, CA, USA IEEE, New York, NY, USA pp 711-714

[93] Siwapornsathain, E, Lal, A, and Binard, J 2002 A telemetry and sensor platform for ambulatory urodynamics *2nd Annual International IEEE-EMBS Special Topic Conference on Microtechnologies in Medicine and Biology. Proceedings (Cat. No.02EX578)* Madison, WI, USA IEEE pp 283-287

[94] Puers, B, Sansen, W, and Vereecken, R 1984 Development cconsiderations of a micropower control chip ans ultraminiature hybrid for bladder pressure telemetry *Biotelemetry* pp 328-332

[95] Puers, R 2005 Implantable sensor systems *Symposium of the Delft University Research Center of Intelligent Sensor Microsystems, DISens* Delft Delft University of Technology pp 66-79

[96] Sansen, W, Vereecken, R, Puers, B, Folens, G, and Van Nuland, T 1987 Closed loop system to control the bladder function *IEEE/Engineering in Medicine and Biology Society Annual Conference* Boston, MA, USA IEEE, New York, NY, USA pp 1149-1150

[97] Tooley, C 2004 Artificial Sphincter and Sphincter Sensor *Healthy Aims Dissemination Day* http://www.healthyaims.org

[98] Mundt, C, Ricks, B, Somps, C J, and Hines, J W 1998 Advanced sensor systems for improved labor and fetal monitoring *ISA EXPO 98. International Conference and Exposition for Advancing Measurement and Control Technologies, Products, and Services. Automation and Control Issues and Solutions* vol vol.2 Houston, TX, USA ISA pp 79-89

[99] Herber, S, Olthuis, W, Bergveld, P, and Van Den Berg, A 2004 Exploitation of a pH-sensitive hydrogel disk for CO_2 detection *Sensors and Actuators, B: Chemical* **103** 284-289

[100] Herber, S, Olthuis, W, and Bergveld, P 2003 A swelling hydrogel-based PCO_2 sensor *Sensors and Actuators, B: Chemical* **91** 378-382

[101] Rawer, R, Li, Q, Stork, W, and Muller-Glaser, K D 2004 Implantable osmotic-pressure based glucose sensor with non-invasive optical readout *Proceedings of SPIE - The International Society for Optical Engineering* vol 5275 Perth, WA, Australia The International Society for Optical Engineering pp 247-256

[102] Mariserla, S, Leseman, Z, and Mackin, T J 2005 A novel glucose sensor based on deflection of a thin membrane *Proceedings of the IEEE International Conference on Micro Electro Mechanical Systems (MEMS)* vol 7 MEMS Orlando, FL, United States Institute of Electrical and Electronics Engineers Inc., Piscataway, NJ 08855-1331, United States pp 479-480

[103] Lindemans, F W, Rankin, I R, Murtaugh, R, and Chevalier, P A 1986 Clinical experience with an activity sensing pacemaker *Pacing Clin.Electrophysiol.* **9** 978-986

[104] Langenfeld, H, Krein, A, Kirstein, M, and Binner, L 1998 Peak endocardial acceleration-based clinical testing of the "BEST" DDDR pacemaker. European PEA Clinical Investigation Group *Pacing Clin.Electrophysiol.* **21** 2187-2191

[105] Puers, R, Catrysse, M, Vandevoorde, G, Collier, R J, Louridas, E, Burny, F, Donkerwolcke, M, and Moulart, F 2000 Telemetry system for the detection of hip prosthesis loosening by vibration analysis *Sensors and Actuators, A: Physical* **85** 42-47

[106] Vergote, S, De Cooman, M, Wouters, P, and Puers, B 1993 Composite membrane movement detector with dedicated interface electronics for animal activity tracking *Sensors and Actuators, A: Physical* **37-38** 86-90

[107] Kim, Y T, Kim, Y Y, and Jun, C H 1999 Needle-shaped glucose sensor with multi-cell electrode fabricated by surface micromachining *Proceedings of SPIE - The International Society for Optical Engineering* **3680** 924-930

[108] Johnson, K W et al. 1992 In vivo evaluation of an electroenzymatic glucose sensor implanted in subcutaneous tissue *Biosens.Bioelectron.* **7** 709-714

[109] Mastrototaro, J J, Cooper, K, and Shah, R 2006 Early clinical experience with an integrated continuous glucose sensor/insulin pump platform *Diabetes Res.Clin.Pract.* **74 Suppl 2** S156-S159

[110] Hong, M K, Wong, S C, Mintz, G S, Popma, J J, Kent, K M, Pichard, A D, Satler, L F, and Leon, M B 1995 Can coronary flow parameters after stent placement predict restenosis? *Cathet.Cardiovasc.Diagn.* **36** 278-280

[111] http://www.verimetra.com

[112] Keoschkerjan, R 2003 Micro-Opto-Mechanical Flow Sensor for Medical Applications *International Conference & Exhibition on Micro Electro, Opto, Mechanical Systems and Components* pp 408-415

[113] US 4,175,566 679,066 Millar, H. D 1979 *Catheter Fluid Velocity Flow Probe* Millar Instruments Inc

[114] Tanase, D, Goosen, J F L, Trimp, P J, Reekers, J A, and French, P J 2003 3D position and orientation measurements with a magnetic sensor for use in vascular interventions *Asian Pacific Conference on Biomedical Engineering* vol 2003 IEEE EMBS pp 264-265

[115] Tanase, D, Goosen, J F L, Trimp, P J, and French, P J 2002 Multi-parameter sensor system with intravascular navigation for catheter/guide wire application *Sensors and Actuators, A: Physical* **97-98** 116-124

[116] Claes, W, Puers, R, Sansen, W, De Cooman, M, Duyck, J, and Naert, I 2002 A low power miniaturized

autonomous data logger for dental implants *Sensors and Actuators, A: Physical* vol 97-98 Munich Elsevier Science B.V. pp 548-556

[117] Canham, L 2003 *Biomedical MEMS: Clinical Applications of Silicon Technology* vol ISBN 0 7503 0921 0, QinetiQ and IoP Publishing

[118] Peirs, J, Clijnen, J, Reynaerts, D, Van Brussel, H, Herijgers, P, Corteville, B, and Boone, S 2004 A micro optical force sensor for force feedback during minimally invasive robotic surgery *Sensors and Actuators, A: Physical* **115** 447-455

[119] Rebello, K J, Lebouitz, K S, and Migliuolo, M 2003 MEMS tactile sensors for surgical instruments *Biomicroelectromechanical Systems (BioMEMS) Symposium. (Mater. Res. Soc. Symposium Proceedings Vol.773)* San Francisco, CA, USA Mater. Res. Soc pp 55-60

[120] Goosen, J F L, French, P J, and Sarro, P M 2000 Pressure, flow and oxygen saturation sensors on one chip for use in catheters *Proceedings IEEE Thirteenth Annual International Conference on Micro Electro Mechanical Systems (Cat. No.00CH36308)* Miyazaki, Japan IEEE pp 537-540

[121] WO 97/27802 PCT/SE97/00150 Smith, L. 2001 *Combined flow, pressure and temperature sensor* Radi Medical Systems AB

[122] Riistama, J and Lekkala, J 2004 Characteristic properties of implantable Ag/AgCl- and Pt-electrodes *Conference Proceedings. 26th Annual International Conference of the IEEE Engineering in Medicine and Biology Society (IEEE Cat. No.04CH37558)* vol Vol.4 San Francisco, CA, USA IEEE pp 2360-2363

[123] http://www.sensile-medical.com

[124] Heller, A 2005 Drug-delivering integrated therapeutic systems *2nd International Workshop on BSN 2005 Wearable and Implantable Body Sensor Networks* London, UK IEE pp 6-11

[125] Gelzer, A R and Ball, H A 1997 Validation of a telemetry system for measurement of blood pressure, electrocardiogram and locomotor activity in beagle dogs *Clin.Exp.Hypertens.* **19** 1135-1160

[126] Torres-Pereira, L, Ruivo, P, Torres-Pereira, C, and Couto, C 1997 A noninvasive telemetric heart rate monitoring system based on phonocardiography *ISIE '97. Proceedings of the IEEE International Symposium on Industrial Electronics (Cat. No.97TH8280)* vol vol.3 Guimaraes, Portugal IEEE pp 856-859

[127] http://www.destronfearing.com/elect/elect

[128] 2004 *Pistool met RFID* De Ingenieur vol 2004, pp 15-15

[129] Brindley, G S, Polkey, C E, and Rushton, D N 1982 Sacral anterior root stimulators for bladder control in paraplegia *Paraplegia* **20** 365-381

[130] Weil, E H J 2000 *Clinical and experimental aspects of sacral nerve neuromodulation in lower urinary tract dysfunction.* Faculteit der Geneeskunde, Universiteit Maastricht

[131] Schneider, A and Stieglitz, T 2004 *Implantable Flexible Electrodes for Functional Electrical Stimulation* Medical Device Technology vol 2004, pp 16-18

[132] Kewley, D T, Hills, M D, Borkholder, D A, Opris, I E, Maluf, N I, Storment, C W, Bower, J M, and Kovacs, G T A 1997 Plasma-etched neural probes *Sensors and Actuators, A: Physical* **58** 27-35

[133] Bell, T E, Wise, K D, and Anderson, D J 1997 Flexible micromachined electrode array for a cochlear prosthesis *International Conference on Solid-State Sensors and*

Actuators, Proceedings vol 2 Chicago, IL, USA IEEE, Piscataway, NJ, USA pp 1315-1318

[134] Madou, M 2005 A 3D Carbon World *Micro System Technologies* Poing (DE) Franzis Verlag GmbH pp 21-21

[135] Receveur, R A M, Marxer, C R, Woering, R, Larik, V C M H, and deRooij, N F 2005 Laterally Moving Bistable MEMS DC Switch for Biomedical Applications *Microelectromechanical Systems, Journal of* **14** 1089-1098

[136] Brindley, G S 1955 The site of electrical excitation of the human eye *J.Physiol* **127** 189-200

[137] Crapper, D R and Noell, W K 1963 Retinal excitation and inhibition from direct electrical stimulation *J.Neurophysiol.* **26** 924-947

[138] Brindley, G S and Lewin, W S 1968 The visual sensations produced by electrical stimulation of the medial occipital cortex *J.Physiol* **194** 54-5P

[139] Humayun, M, Propst, R, de Juan E Jr, McCormick, K, and Hickingbotham, D 1994 Bipolar surface electrical stimulation of the vertebrate retina *Arch.Ophthalmol.* **112** 110-116

[140] Weiland, J D, Fujii, G Y, Mahadevappa, M, Greenberg, R J, Tameesh, M, Guven, D, de Juan, E, Jr., and Humayun, M S 2002 Chronic electrical stimulation of the canine retina *Conference Proceedings. Second Joint EMBS-BMES Conference 2002. 24th Annual International Conference of the Engineering in Medicine and Biology Society. Annual Fall Meeting of the Biomedical Engineering Society (Cat. No.02CH37392)* vol vol.3 Houston, TX, USA IEEE pp 2051-2052

[141] Weiland, J D et al. 2003 Electrical stimulation of retina in blind humans *Proceedings of the 25th Annual International Conference of the IEEE Engineering in Medicine and Biology Society (IEEE Cat.*

No.03CH37439) vol Vol.3 Cancun, Mexico IEEE pp 2021-2022

[142] Schwarz, M, Ewe, L, Hauschild, R, Hosticka, B J, Huppertz, J, Kolnsberg, S, Mokwa, W, and Trieu, H K 2000 Single chip CMOS imagers and flexible microelectronic stimulators for a retina implant system *Sensors and Actuators A: Physical* **83** 40-46

[143] Eckmiller, R 1995 Towards retina implants for improvement of vision in humans with retinitis pigmentosa-challenges and first results *WCNN '95. World Congress on Neural Networks. 1995 International Neural Network Society Annual Meeting* vol vol.1 Washington, DC, USA Lawrence Erlbaum Associates pp 228-233

[144] Mokwa, Wilfried *Optimization of Stimulation Electrodes for Retinal Implants* International Microelectronics and Packaging Society Benelux Chapter IMAPS-Benelux Spring Event 2006

[145] Intelligent Implant Technologies Ltd. 2004 Epiretinal Electrical Stimulation *Healthy Aims Dissemination Day* http://www.healthyaims.org

[146] Hornig, R et al. 2005 A method and technical equipment for an acute human trial to evaluate retinal implant technology *J.Neural Eng* **2** S129-S134

[147] Grumet, A E, Wyatt, J L, Jr., and Rizzo, J F, III 2000 Multi-electrode stimulation and recording in the isolated retina *J.Neurosci.Methods* **101** 31-42

[148] Rizzo, J F, III, Wyatt, J, Loewenstein, J, Kelly, S, and Shire, D 2003 Methods and perceptual thresholds for short-term electrical stimulation of human retina with microelectrode arrays *Invest Ophthalmol.Vis.Sci.* **44** 5355-5361

[149] Chow, A Y and Chow, V Y 1997 Subretinal electrical stimulation of the rabbit retina *Neurosci.Lett.* **225** 13-16

[150] Chow, A Y 1993 Electrical stimulation of the rabbit retina with subretinal electrodes and high density microphotodiode array implants *Invest Ophthalmol.Vis.Sci.* **34** 835

[151] Chow, A Y et al. 2002 Subretinal implantation of semiconductor-based photodiodes: durability of novel implant designs *J.Rehabil.Res.Dev.* **39** 313-321

[152] Chow, A Y, Chow, V Y, Packo, K H, Pollack, J S, Peyman, G A, and Schuchard, R 2004 The artificial silicon retina microchip for the treatment of vision loss from retinitis pigmentosa *Arch.Ophthalmol.* **122** 460-469

[153] Zrenner, E, Stett, A, Weiss, S, Aramant, R B, Guenther, E, Kohler, K, Miliczek, K D, Seiler, M J, and Haemmerle, H 1999 Can subretinal microphotodiodes successfully replace degenerated photoreceptors? *Vision Res.* **39** 2555-2567

[154] Hammerle, H, Kobuch, K, Kohler, K, Nisch, W, Sachs, H, and Stelzle, M 2002 Biostability of micro-photodiode arrays for subretinal implantation *Biomaterials* **23** 797-804

[155] Sachs, H G, Schanze, T, Brunner, U, Sailer, H, and Wiesenack, C 2005 Transscleral implantation and neurophysiological testing of subretinal polyimide film electrodes in the domestic pig in visual prosthesis development *Journal of Neural Engineering* **2** S57-S64

[156] Schwahn, H N, Gekeler, F, Kohler, K, Kobuch, K, Sachs, H G, Schulmeyer, F, Jakob, W, Gabel, V P, and Zrenner, E 2001 Studies on the feasibility of a subretinal visual prosthesis: data from Yucatan micropig and rabbit *Graefes Arch.Clin.Exp.Ophthalmol.* **239** 961-967

[157] Bauerdick, S, Burkhardt, C, Kern, D P, and Nisch, W 2003 Substrate-Integrated Microelectrodes with Improved Charge Transfer Capacity by 3-Dimensional Micro-Fabrication *Biomedical Microdevices* **5** 93-99

[158] Zrenner, E et al. 1997 The development of subretinal microphotodiodes for replacement of degenerated photoreceptors *Ophthalmic Res.* **29** 269-280

[159] Sachs, H G and Gabel, V P 2004 Retinal replacement--the development of microelectronic retinal prostheses--experience with subretinal implants and new aspects *Graefes Arch.Clin.Exp.Ophthalmol.* **242** 717-723

[160] Veraart, C, Raftopoulos, C, Mortimer, J T, Delbeke, J, Pins, D, Michaux, G, Vanlierde, A, Parrini, S, and Wanet-Defalque, M C 1998 Visual sensations produced by optic nerve stimulation using an implanted self-sizing spiral cuff electrode *Brain Res.* **813** 181-186

[161] Delbeke, J. *Optic nerve implant: interface to the visual system* International Microelectronics and Packaging Society Benelux Chapter IMAPS-Benelux Spring Event 2006

[162] Dobelle, W H and Mladejovsky, M G 1974 Phosphenes produced by electrical stimulation of human occipital cortex, and their application to the development of a prosthesis for the blind *J.Physiol* **243** 553-576

[163] Dobelle, W H 2000 Artificial vision for the blind by connecting a television camera to the visual cortex *ASAIO J.* **46** 3-9

[164] Campbell, P K, Normann, R A, and Horch, K W 1988 Noble metal penetrating cortical stimulating electrode array: preliminary results *Proceedings of the Annual International Conference of the IEEE Engineering in Medicine and Biology Society (IEEE Cat. No.88CH2566-8)* New Orleans, LA, USA IEEE pp 716-717

[165] Normann, R A, Campbell, P K, and Jones, K E 1991 Micromachined, silicon based electrode arrays for electrical stimulation of or recording from cerebral cortex *Proceedings. IEEE Micro Electro Mechanical Systems. An Investigation of Micro Structures, Sensors, Actuators,*

Machines and Robots (Cat. No.91CH2957-9) Nara, Japan IEEE pp 247-252

[166] Normann, R A 2003 Microfabricated electrode arrays for restoring lost sensory and motor functions *TRANSDUCERS '03. 12th International Conference on Solid-State Sensors, Actuators and Microsystems. Digest of Technical Papers (Cat. No.03TH8664)* vol vol.2 Boston, MA, USA IEEE pp 959-962

[167] Nordhausen, C T, Rousche, P, and Normann, R A 1993 Chronic recordings of visually evoked responses using the Utah intracortical electrode array *Proceedings of the Annual Conference on Engineering in Medicine and Biology* vol 15 San Diego, CA, USA Publ by IEEE, Piscataway, NJ, USA pp 1391-1392

[168] Normann, R A, Warren, D J, Ammermuller, J, Fernandez, E, and Guillory, S 2001 High-resolution spatio-temporal mapping of visual pathways using multi-electrode arrays *Vision Research* **41** 1261-1275

[169] Normann, R A, Campbell, P K, and Jones, K E 1989 A silicon based electrode array for intracortical stimulation: structural and electrical properties *Images of the Twenty-First Century. Proceedings of the Annual International Conference of the IEEE Engineering in Medicine and Biology Society (Cat. No.89CH2770-6)* Seattle, WA, USA IEEE pp 939-940

[170] Jones, K E, Campbell, P K, and Normann, R A 1992 A glass/silicon composite intracortical electrode array *Annals of Biomedical Engineering* **20** 423-437

[171] Patterson, W R et al. 2004 A microelectrode/microelectronic hybrid device for brain implantable neuroprosthesis applications *IEEE Trans.Biomed.Eng* **51** 1845-1853

[172] Schmidt, E M, Bak, M J, Hambrecht, F T, Kufta, C V, O'Rourke, D K, and Vallabhanath, P 1996 Feasibility of a

visual prosthesis for the blind based on intracortical microstimulation of the visual cortex *Brain* **119 (Pt 2)** 507-522

[173] Harvey, J F and Sawan, M 1996 Image acquisition and reduction dedicated to a visual implant *Annual International Conference of the IEEE Engineering in Medicine and Biology - Proceedings* Amsterdam, Neth IEEE, Piscataway, NJ, USA pp 403-404

[174] Trepanier, A, Trepanier, J L, Sawan, M, and Audet, Y 2004 A multiple operation mode CMOS digital pixel sensor dedicated to a visual cortical implant *The 2004 47th Midwest Symposium on Circuits and Systems (IEEE Cat. No.04CH37540)* vol 1 Hiroshima, Japan IEEE pp 369-372

[175] Gosselin, B, Simard, V, and Sawan, M 2004 Low-power implant able microsystem intended to multichannel cortical recording *Proceedings - IEEE International Symposium on Circuits and Systems* vol 4 Vancouver, BC, Canada Institute of Electrical and Electronics Engineers Inc., Piscataway, NJ 08855-1331, United States pp 5

[176] van Humbeeck, C. *The bionic ear: the engineering challenges of delivering electrical signals to the auditory nerve* International Microelectronics and Packaging Society Benelux Chapter IMAPS-Benelux Spring Event 2006

[177] Peeters, S. *Electrode-Neural interface* International Microelectronics and Packaging Society Benelux Chapter IMAPS-Benelux Spring Event 2006

[178] Kloeck, B 2004 Cochlear Implant *Healthy Aims Dissemination Day* vol 2004 http://www.healthyaims.org

[179] Corless, T 2004 Electrodes *Healthy Aims Dissemination Day* vol 2004 http://www.healthyaims.org

[180] Branner, A, Stein, R B, Fernandez, E, Aoyagi, Y, and Normann, R A 2004 Long-term stimulation and recording with a penetrating microelectrode array in cat sciatic nerve *IEEE Transactions on Biomedical Engineering* **51** 146-157

[181] Brindley, G S, Polkey, C E, and Rushton, D N 1979 Electrical splinting of the knee in paraplegia *Paraplegia* **16** 428-437

[182] Donaldson, P E 1987 Twenty years of neurological prosthesis-making *J.Biomed.Eng* **9** 291-298

[183] van der Aa, H E, Bultstra, G, Verloop, A J, Kenney, L, Holsheimer, J, Nene, A, Hermens, H J, Zilvold, G, and Buschman, H P 2002 Application of a dual channel peroneal nerve stimulator in a patient with a "central" drop foot *Acta Neurochir.Suppl* **79** 105-107

[184] Spensley, J 2004 Electrical stimulation (FES) *Healthy Aims Dissemination Day* vol 2004 http://www.healthyaims.org

[185] Scott, T R, Peckham, P H, and Keith, M W 1995 Upper extremity neuroprostheses using functional electrical stimulation *Baillieres Clin.Neurol.* **4** 57-75

[186] Thorsen, R, Spadone, R, and Ferrarin, M 2001 A pilot study of myoelectrically controlled FES of upper extremity *IEEE Trans.Neural Syst.Rehabil.Eng* **9** 161-168

[187] Loeb, G E, Zamin, C J, Schulman, J H, and Troyk, P R 1991 Injectable microstimulator for functional electrical stimulation *Med. Biol. Eng. Comput. (UK)* vol 29 Antwerp, Belgium pp 13-19

[188] Loeb, G E, Peck, R A, Moore, W H, and Hood, K 2001 BION system for distributed neural prosthetic interfaces *Med.Eng Phys.* **23** 9-18

[189] Baker, L L, Waters, R L, Winstein, C, Kaplan, H, Tran, W, Richmond, F J R, and Loeb, G E 2005 Clinical applications of BION^{tm} microstimulators *2005 First*

International Conference on Neural Interface and Control Proceedings (IEEE Cat. No. 05EX999) Wuhan, China IEEE pp 185-188

[190] Rutten, W L C, van Wier, H J, and Put, J H M 1991 Sensitivity and selectivity of intraneural stimulation using a silicon electrode array *IEEE Transactions on Biomedical Engineering* **38** 192-198

[191] Rutten, W L C, Frieswijk, T A, Smit, J P A, Rozijn, T H, and Meier, J H 1995 3D neuro-electronic interface devices for neuromuscular control: design studies and realisation steps *Biosensors & Bioelectronics* **10** 141-153

[192] Smit, J P A, Rutten, W L C, and Boom, H B K 1999 Endoneural selective stimulating using wire-microelectrode arrays *IEEE Transactions on Rehabilitation Engineering* **7** 399-412

[193] Dokmeci, M R, von Arx, J A, and Najafi, K 1997 Accelerated testing of anodically bonded glass-silicon packages in salt water *Tranducers 97. 1997 International Conference on Solid-State Sensors and Actuators. Digest of Technical Papers (Cat. No.97TH8267)* vol vol.1 Chicago, IL, USA IEEE pp 283-286

[194] Harpster, T and Najafi, K 2002 Long-term testing of hermetic anodically bonded glass-silicon *Proceedings of the IEEE Micro Electro Mechanical Systems* 423-426

[195] Stark, B H, Dokmeci, M R, Harpster, T J, and Najafi, K 2001 Improving corrosion-resistance of silicon-glass micropackages using boron doping and/or self-induced galvanic bias *2001 IEEE International Reliability Physics Symposium Proceedings. 39th Annual (Cat. No.00CH37167)* Orlando, FL, USA IEEE pp 112-119

[196] Ziaie, B, Von Arx, A, Dokmeci, M R, and Najafi, K 1996 A hermetic glass-silicon micropackage with high-density on-chip feedthroughs for sensors and actuators *IEEE Journal of Solid-State Circuits* **5** 166-179

[197] Rousche, P J and Normann, R A 1998 Chronic recording capability of the Utah intracortical electrode array in cat sensory cortex *Journal of Neuroscience Methods* **82** 1-15

[198] Rodriguez, F J, Ceballos, D, Schuttler, M, Valero, A, Valderrama, E, Stieglitz, T, and Navarro, X 2000 Polyimide cuff electrodes for peripheral nerve stimulation *J.Neurosci.Methods* **98** 105-118

[199] Hoffman, K P, Koch, K-P, and Doerge, Th 2005 *Schnittstelle zwischen Biologie und Technik: Implantierbare Mikroelektroden* INNO IVAM Fachverband fuer Mikrotechnik pp 8-9

[200] Koch, K.-P. *Implantable electrodes based on flexible substrates* International Microelectronics and Packaging Society Benelux Chapter IMAPS-Benelux Spring Event 2006

[201] Feili, D, Schuettler, M, Doerge, T, Kammer, S, Hoffmann, K P, and Stieglitz, T 2006 Flexible organic field effect transistors for biomedical microimplants using polyimide and parylene C as substrate and insulator layers *Journal of Micromechanics and Microengineering* **16** 1555-1561

[202] Arabi, K and Sawan, M 1997 A monolithic miniaturized programmable implant for neuromuscular stimulation *1995 IEEE Engineering in Medicine and Biology 17th Annual Conference and 21 Canadian Medical and Biological Engineering Conference (Cat. No.95CH35746)* vol vol.2 Montreal, Que., Canada IEEE pp 1131-1132

[203] Arabi, K and Sawan, M A 1999 Electronic design of a multichannel programmable implant for neuromuscular electrical stimulation *IEEE Transactions on Rehabilitation Engineering* **7** 204-214

[204] Callewaert, L, Puers, B, Sansen, W, and Salmons, S 1987 Programmable implantable stimulator with percutaneous

optical control *IEEE/Engineering in Medicine and Biology Society Annual Conference* Boston, MA, USA IEEE, New York, NY, USA pp 1370-1371

[205] Callewaert, L, Puers, B, Sansen, W, Jarvis, J C, and Salmons, S 1991 Programmable implantable device for investigating the adaptive response of skeletal muscle to chronic electrical stimulation *Medical & Biological Engineering & Computing* **29** 548-553

[206] Wise, K D and Angell, J B 1975 A low-capacitance multielectrode probe for use in extracellular neurophysiology *IEEE Transactions on Biomedical Engineering* **BME-22** 212-219

[207] Peeters, E, Puers, B, Sansen, W, Gybels, J, and De Sutter, P 1991 Two-wire, digital output multichannel microprobe for recording single-unit neural activity *Sensors and Actuators, B: Chemical* **B4** 217-223

[208] Najafi, K, Wise, K D, and Mochizuki, T 1985 High-yield IC-compatible multichannel recording array *IEEE Transactions on Electron Devices* **ED-32** 1206-1211

[209] Lisby, T, Nikles, S A, Najafi, K, Hansen, O, Bouwstra, S, and Branebjerg, J A 2004 Mechanical characterization and design of flexible silicon microstructures *Microelectromechanical Systems, Journal of* **13** 452-464

[210] Lee, K K, He, J, Singh, A, Massia, S, Ehteshami, G, Kim, B, and Raupp, G 2004 Polyimide-based intracortical neural implant with improved structural stiffness *Journal of Micromechanics and Microengineering* **14** 32-37

[211] Lee, K, Singh, A, He, J, Massia, S, Kim, B, and Raupp, G 2004 Polyimide based neural implants with stiffness improvement *Sensors and Actuators, B: Chemical* **102** 67-72

[212] Neves, H. *Probe arrays for in vivo studies of the central nervous systems* International Microelectronics and

Packaging Society Benelux Chapter IMAPS-Benelux Spring Event 2006

[213] Griss, P, Enoksson, P, Tolvanen-Laakso, H K, Merilainen, P, Ollmar, S, and Stemme, G 2001 Micromachined electrodes for biopotential measurements *Journal of microelectromechanical systems* **10** 10-16

[214] Capaldi, J., Naud, P., and Ioudina, N. New Canadian Technology set to revolutionize treatment of neurological disorders 11-8-2004 http://www.lhrionhealth.ca/news/News_Articles_2004/news_11_08_04.htm

[215] Maillefer, D, Gamper, S, Frehner, B, Balmer, P, Van Lintel, H, and Renaud, P 2001 A high-performance silicon micropump for disposable drug delivery systems *Proceedings of the IEEE Micro Electro Mechanical Systems (MEMS)* Interlaken Institute of Electrical and Electronics Engineers Inc. pp 413-417

[216] Maillefer, D 2003 Development of novel drug delivery products based on Micro System Technologies *International Conference & Exhibition on Micro Electro, Opto, Mechanical Systems and Components* pp 387-394

[217] Leung Ki, Y s, Maillefer, D, Rey-Mermet, G, Monkewitz, P A, Renaud, P, and van Lintel, H T G 1998 Microfluidics of a planar microfabricated fluid filter *American Society of Mechanical Engineers, Dynamic Systems and Control Division (Publication) DSC* vol 66 Anaheim, CA, USA ASME, Fairfield, NJ, USA pp 165-170

[218] 2005 *ISSYS achieves ISO 9001:2000 certification* MicroNews vol 2005, pp 15-15

[219] Deo, S K, Moschou, E A, Peteu, S F, Bachas, L G, Daunert, S, Eisenhardt, P, and Madou, M 2003 *Responsive drug delivery systems* Analytical Chemistry vol 75, American Chemical Society pp 206-213

[220] US 5,279,6071994 *Telemetry capsule and process* Gastrotarget Corp
[221] Clewlow, P 2005 Tiny trials can give nead start *Chemistry and Industry (London)* 23-25
[222] Clewlow, P 2004 Drugs in transit *Chemistry and Industry (London)* **2004** 22-24
[223] Prescott, J H, Lipka, S, Baldwin, S, Sheppard, J, Maloney, J M, Coppeta, J, Yomtov, B, Staples, M A, and Santini, J 2006 Chronic, programmed polypeptide delivery from an implanted, multireservoir microchip device *Nature Biotechnology* **24** 437-438
[224] Gardeniers, H J G E, Luttge, R, Berenschot, E J W, De Boer, M J, Yeshurun, S Y, Hefetz, M, van't Oever, R, and Van Den Berg, A 2003 Silicon micromachined hollow microneedles for transdermal liquid transport *Journal of microelectromechanical systems* **12** 855-862
[225] Gardeniers, J G E, Berenschot, J W, De Boer, M J, Yeshurun, Y, Hefetz, M, van't Oever, R, and Van Den Berg, A 2002 Silicon micromachined hollow microneedles for transdermal liquid transfer *Technical Digest. MEMS 2002 IEEE International Conference. Fifteenth IEEE International Conference on Micro Electro Mechanical Systems (Cat. No.02CH37266)* Las Vegas, NV, USA IEEE pp 141-144
[226] Griss, P and Stemme, G 2003 Side-opened out-of-plane microneedles for microfluidic transdermal liquid transfer *Microelectromechanical Systems, Journal of* **12** 296-301
[227] Roxhed, N, Griss, P, and Stemme, G 2005 Generic leak-free drug storage and delivery for microneedle-based systems *Proceedings of the IEEE International Conference on Micro Electro Mechanical Systems (MEMS)* Miami Beach, FL, United States Institute of Electrical and Electronics Engineers Inc., Piscataway, NJ 08855-1331, United States pp 742-745

[228] Roxhed, N, Griss, P, and Stemme, G 2005 Reliable in-vivo penetration and transdermal injection using ultra-sharp hollow microneedles *International Conference on Solid-State Sensors, Actuators and Microsystems* vol 1 pp 213-216

[229] Eriksson, E et al. 1998 In vivo gene transfer to skin and wound by microseeding *J.Surg.Res.* **78** 85-91

[230] Mikszta, J A, Alarcon, J B, Brittingham, J M, Sutter, D E, Pettis, R J, and Harvey, N G 2002 Improved genetic immunization via micromechanical disruption of skin-barrier function and targeted epidermal delivery *Nat.Med.* **8** 415-419

[231] Knight, J G and Degertekin, F L 2003 Fabrication and characterization of cMUTs for forward looking intravascular ultrasound imaging *Proceedings of the IEEE Ultrasonics Symposium* vol 2 Honolulu, HI, United States Institute of Electrical and Electronics Engineers Inc., Piscataway, United States pp 1175-1178

[232] Degertekin, F L, Guldiken, R O, and Karaman, M 2005 Micromachined capacitive transducer arrays for intravascular ultrasound *Progress in Biomedical Optics and Imaging - Proceedings of SPIE* vol 5721 San Jose, CA, United States International Society for Optical Engineering, Bellingham, WA 98227-0010, United States pp 104-114

[233] Dickinson, R J and Kitney, R I 2004 Miniature ultrasonic probe construction for minimal access surgery *Physics in Medicine and Biology* **49** 3527-3538

[234] Johnson, J, Oralkan, O, Demirci, U, Ergun, S, Karaman, M, and Khuri-Yakub, P 2002 Medical imaging using capacitive micromachined ultrasonic transducer arrays *Ultrasonics* **40** 471-476

[235] Wong, K A, Panda, S, and Ladabaum, I 2003 Curved micromachined ultrasonic transducers *Proceedings of the*

IEEE Ultrasonics Symposium vol 1 Honolulu, HI, United States Institute of Electrical and Electronics Engineers Inc., Piscataway, United States pp 572-576

[236] Knight, J G and Degertekin, F L 2002 Capacitive micromachined ultrasonic transducers for forward looking intravascular imaging arrays *Proceedings of the IEEE Ultrasonics Symposium* vol 2 Munich, Germany Institute of Electrical and Electronics Engineers Inc. pp 1079-1082

[237] Knight, J, McLean, J, and Degertekin, F L 2004 Low temperature fabrication of immersion capacitive micromachined ultrasonic transducers on silicon and dielectric substrates *IEEE transactions on ultrasonics, ferroelectrics and frequency control* **51** 1324-1333

[238] Schulze-Clewing, J, Eberle, M J, and Stephens, D N 2000 Miniaturized circular array *Proceedings of the IEEE Ultrasonics Symposium* vol 2 San Juan Institute of Electrical and Electronics Engineers Inc. pp 1253-1254

[239] Lee, W, Idriss, S F, Wolf, P D, and Smith, S W 2004 A miniaturized catheter 2-D array for real-time, 3-D intracardiac echocardiography *IEEE Transactions on Ultrasonics, Ferroelectrics, and Frequency Control* **51** 1334-1346

[240] Light, E D, Hultman, P A, Idriss, S F, Lee, W, Wolf, P D, and Smith, S W 2000 Two dimensional arrays for real time volumetric and intracardiac imaging with simultaneous electrocardiogram *Proceedings of the IEEE Ultrasonics Symposium* vol 2 San Juan Institute of Electrical and Electronics Engineers Inc. pp 1195-1198

[241] Panescu, D 2005 An imaging pill for gastrointestinal endoscopy *IEEE Engineering in Medicine and Biology Magazine* **24** 12-14

[242] Schutz, R, Dorschel, K, and Muller, G J 1997 Confocal microscanner technique for endoscopic vision

Proceedings of SPIE - The International Society for Optical Engineering vol 3197 San Remo, Italy The International Society for Optical Engineering pp 223-233

[243] Murakami, K 2005 A miniature confocal optical scanning microscope for endoscope *Progress in Biomedical Optics and Imaging - Proceedings of SPIE* vol 5721 San Jose, CA, United States International Society for Optical Engineering, Bellingham, WA 98227-0010, United States pp 119-131

[244] Pan, Y, Xie, H, and Fedder, G K 2001 Endoscopic optical coherence tomography based on a microelectromechanical mirror *Optics Letters* **26** 1966-1968

[245] Neidlinger, T, Harendt, C, Gloeckner, J, and Schubert, M B 2000 Novel device concept for voltage-bias controlled color detection in amorphous silicon sensitized CMOS cameras *Materials Research Society Symposium - Proceedings* vol 558 San Francisco, CA, USA Materials Research Society, Warrendale, PA, USA pp 285-290

[246] Sell, C 2005 Improving the image *Engineer* **293** 33

[247] Arena, A et al. 2005 Intracorporeal Video Probe (IVP) *ICMCC, The International Council on Medical and Care Compunetics* IOS Press pp 167

[248] Kanukurthy, K, Viswanathan, U, Andersen, D R, Olesberg, J, Arnold, M A, and Coretsopoulos, C 2006 Controller for a continuous near infrared glucose sensor *Proceedings of the ISA/IEEE 2005 Sensors for Industry Conference (IEEE Cat. No.05EX995)* Houston, TX, USA ISA pp 59-65

[249] Lane, S S, Kuppermann, B D, Fine, I H, Hamill, M B, Gordon, J F, Chuck, R S, Hoffman, R S, Packer, M, and Koch, D D 2004 A prospective multicenter clinical trial to evaluate the safety and effectiveness of the implantable miniature telescope *Am.J.Ophthalmol.* **137** 993-1001

[250] Peli, E 2002 The optical functional advantages of an intraocular low-vision telescope *Optometry and Vision Science* **79** 225-233
[251] http://www.sarcos.com/medicalproj
[252] Mineta, T, Mitsui, T, Watanabe, Y, Kobayashi, S, HAGA, Y, and Esashi, M 2001 Batch fabricated flat meandering shape memory alloy actuator for active catheter *Sensors and Actuators A (Physical)* **88** 112-120
[253] Langelaar, M 2005 *DIMES Whitepapers 2005 Designing Memory Metal Devices Design optimization of shape memory alloy structures - targeted at medical and microsystem applications* Delft, The Netherlands TU Delft, DIMES pp 42-51
[254] Lal, A and White, R M 1995 Micromachined silicon needle for ultrasonic surgery *IEEE Ultrasonics Symposium* vol 2 pp 1593-1596
[255] Chen, X and Lal, A 2001 Integrated pressure and flow sensor in silicon-based ultrasonic surgical actuator *Proceedings of the IEEE Ultrasonics Symposium* vol 2 Atlanta, GA Institute of Electrical and Electronics Engineers Inc. pp 1373-1376
[256] Son, I S, Lal, A, Hubbard, B, and Olsen, T 2001 A multifunctional silicon-based microscale surgical system *Sensors and Actuators, A: Physical* **90** 351-356
[257] Thapa, A, Webster, T J, and Haberstroh, K M 2003 Polymers with nano-dimensional surface features enhance bladder smooth muscle cell adhesion *Journal of Biomedical Materials Research - Part A* **67** 1374-1383
[258] Miller, D C, Haberstroh, K M, and Webster, T J 2004 Mechanisms controlling increased vascular cell adhesion to nano-structured polymer films *Transactions - 7th World Biomaterials Congress* Sydney, Australia Biomaterials 2004 Congress Managers, Sydney, NSW 2001, Australia pp 730

[259] Palin, E, Liu, H, and Webster, T J 2005 Mimicking the nanofeatures of bone increases bone-forming cell adhesion and proliferation *Nanotechnology* **16** 1828-1835

[260] Webster, T J, Waid, M C, McKenzie, J L, Price, R L, and Ejiofor, J U 2004 Nano-biotechnology: Carbon nanofibres as improved neural and orthopaedic implants *Nanotechnology* **15** 48-54

[261] King, K R, Chiaochun, W, Vacanti, J P, and Borenstein, J T 2002 Biodegradable polymer microfluidics for tissue engineering microvasculature *BioMEMS and Bionanotechnology. Symposium (Materials Research Society Proceedings Vol.729)* San Francisco, CA, USA Mater. Res. Soc pp 3-8

[262] Leclerc, E, Furukawa, K S, Miyata, F, Sakai, Y, Ushida, T, and Fujii, T 2004 Fabrication of microstructures in photosensitive biodegradable polymers for tissue engineering applications *Biomaterials* **25** 4683-4690

[263] Bettinger, C J, Weinberg, E J, Kulig, K M, Vacanti, J P, Wang, Y, Borenstein, J T, and Langer, R 2006 Three-dimensional microfluidic tissue-engineering scaffolds using a flexible biodegradable polymer *Advanced Materials* **18** 165-169

[264] http://www.psivida.com.au/application/other

[265] Zimmermann, S, Fienbork, D, Flounders, A W, and Liepmann, D 2004 In-device enzyme immobilization: Wafer-level fabrication of an integrated glucose sensor *Sensors and Actuators, B: Chemical* **99** 163-173

[266] Madou, M 1997 *Fundamentals of microfabrication* New York, United States CRC Press LLC 0-8493-9451-1

[267] Maluf, N 2000 *An introduction to microelectromechanical systems engineering* Boston, United States Artech House Inc. 0-89006-581-0

[268] Mayr, W, Bijak, M, Rafolt, D, Sauermann, S, Unger, E, and Lanmuller, H 2001 Basic design and construction of

the Vienna FES implants: existing solutions and prospects for new generations of implants *Medical Engineering & Physics* **2001** 53-60

[269] Klein, M, Oppermann, H, and Reichl, H 2005 Gold-Gold Flip Chip Bonding Processes for RF, Optoelectronic, High Temperature and Power Devices *Micro System Technologies* Poing (DE) Franzis Verlag GmbH pp 345-352

[270] Herber, S, Eijkel, J, Olthuis, W, Bergveld, P, and Van Den Berg, A 2004 Study of chemically induced pressure generation of hydrogels under isochoric conditions using a microfabricated device *Journal of Chemical Physics* **121** 2746-2751

[271] Schuettler, M and Stieglitz, T 2000 18polar Hybrid Cuff Electrodes for Stimulation of Peripheral Nerves *Annual Conference of the International Functional Electrical Stimulation Society* Aalborg, Denmark International Functional Electrical Stimulation Society pp 265-268

[272] Bohlmann, H, Gotzen, R, and Reinhardt, A 2001 3D-CSP, an innovative packaging methods based on RMPD *Proceedings of the SPIE - The International Society for Optical Engineering* **4407** 180-184

[273] Farrel, B et al. 2005 A polymer-based, chronic nerve electrode technology *Micro System Technologies* Poing (DE) Franzis Verlag GmbH pp 148-155

[274] Albers, T 2004 Inert biomaterials and antifouling strategies *Healthy Aims Dissemination Day* vol 2004 http://www.healthyaims.org

[275] US 6,167,763 B1 09/547,733 Tenerz, L., Hammarstrom, O., and Smith, L. 2001 *Pressure sensor and guide wire assembly for biolgical pressure measurements* Radi Medical Systems AB

[276] Kim, S 2003 Evaluation and Optimization of Planar Micro-Coils Fabricated by Polyimide based

Electroplating for the Application of Implantable Telemetry Systems *International Conference & Exhibition on Micro Electro, Opto, Mechanical Systems and Components* pp 379-386

[277] Sawan, M, Duval, F, Jin-Sheng, L, Hassouna, M, and Elhilali, M M 1993 A new bladder stimulator-hand-held controller and miniaturized implant: preliminary results in dogs *Biomedical Instrumentation & Technology* **27** 143-149

[278] http://www.alchimer.com

[279] http://www.gfe.com

[280] Xiao, X, Birrell, J, Gerbi, J E, Auciello, O, and Carlisle, J A 2004 Low temperature growth of ultrananocrystalline diamond *Journal of Applied Physics* **96** 2232-2239

[281] Antonov, E N et al. 1998 Biocompatibility of laser-deposited hydroxyapatite coatings on titanium and polymer implant materials *Journal of Biomedical Optics* **3** 423-428

[282] Lee, S H, Kim, H W, Lee, E J, Li, L H, and Kim, H E 2006 Hydroxyapatite-TiO2 hybrid coating on Ti implants *Journal of Biomaterials Applications* **20** 195-208

[283] Desai, T A, Hansford, D J, Leoni, L, Essenpreis, M, and Ferrari, M 2000 Nanoporous anti-fouling silicon membranes for biosensor applications *Biosensors & Bioelectronics* **15** 453-462

[284] US 6,553,263 B1 09/627,803 Meadows, P. M., Mann, C. M., Tsukamoto, H., and Chen, J. 4-22-2003 *Implantable pulse generators using rechargeable zero-volt technology lithium-ion batteries* Advanced Bionics and Quallion, LLC

[285] US 6,850,803 B1 09/596,402 Jimenez, O., Echarri, G., Kast, J. E., Riekels, J. E., and Schommer, M. E. 2-1-2005 *Implantable medical device with a recharging coil magnetic shield* Medtronic

[286] Van Schuylenbergh, K and Puers, R 1996 Self-tuning inductive powering for implantable telemetric monitoring systems *Sensors and Actuators, A: Physical* **52** 1-7

[287] Van Schuylenbergh, K and Puers, R 1995 Self tuning inductive powering for implantable telemetric monitoring systems *International Conference on Solid-State Sensors and Actuators, Proceedings* vol 1 Stockholm, Sweden IEEE, Piscataway, NJ, USA pp 55-58

[288] Imec 2005 *First prototype of a MEMS vibration scavenger* Imec news

[289] 2004 *Lichaam voedt pacemaker* De Ingenieur vol 2004, pp 15-15

[290] Arra, S, Heinusuo, S, and Vanhala, J 2005 Acoustic power transmission into an implantable device *2nd International Workshop On Wearable and Implantable Body Sensor Networks BSN 2005* London IEE

[291] von Stetten, F, Kerzenmacher, S, Sumbharaju, R, Zengerle, R, and Ducree, J 2006 Biofuel cells as power generator for implantable devices *Eurosensors XX* vol 1 pp 222-225

[292] Hammond, K et al. 2005 An integrated node for energy-scavenging, sensing, and data transmission: applications in medical diagnostics *2nd International Workshop On Wearable and Implantable Body Sensor Networks BSN 2005* London IEE

[293] Arnold, D P, Cros, F, Zana, I, Veazie, D R, and Allen, M G 2004 Electroplated metal microstructures embedded in fusion-bonded silicon: conductors and magnetic materials *Microelectromechanical Systems, Journal of* **13** 791-798

[294] Pakula, L S, Yang, H, Pham, H T M, French, P J, and Sarro, P M 2004 Fabrication of a CMOS compatible pressure sensor for harsh environments *J.Micromech.Microeng.* **14** 1478-1483

[295] Elmqvist, R and Senning, A 1960 An implantable pacemaker for the heart *International Conference on Medical Electronics* London Illife & Sons

[296] Rickards, A F and Norman, J 1981 Relation between QT interval and heart rate. New design of physiologically adaptive cardiac pacemaker *Br.Heart J.* **45** 56-61

[297] Cammilli, L, Alcidi, L, Papeschi, G, Padeletti, L, and Grassi, G 1978 Clinical and biological aspects in patient with pH-triggered implanted pacemaker (author's transl) *G.Ital.Cardiol.* **8 Suppl 1** 252-258

[298] Wirtzfeld, A, Goedel-Meinen, L, Bock, T, Heinze, R, Liss, H D, and Munteanu, J 1982 Central venous oxygen saturation for the control of automatic rate-responsive pacing *Pacing Clin.Electrophysiol.* **5** 829-835

[299] Faerestrand, S, Ohm, O J, Stangeland, L, Heynen, H, and Moore, A 1994 Long-term clinical performance of a central venous oxygen saturation sensor for rate adaptive cardiac pacing *Pacing Clin.Electrophysiol.* **17** 1355-1372

[300] Chevalier, P A, Lindemans, F, Murthaugh, R, and Rankin, I 1985 Improved heart rate and exercise performance with an activity sensing pacemaker: a multicenter study *Pacing Clin.Electrophysiol.* **8** 775

[301] Rossi, P, Plicchi, G, Canducci, G, Rognoni, G, and Aina, F 1983 Respiratory rate as a determinant of optimal pacing rate *Pacing Clin.Electrophysiol.* **6** 502-510

[302] Alt, E, Hirgstetter, C, Heinz, M, Theres, H, and Blomer, H 1988 Central venous blood temperature for rate control of physiological pacemakers *J.Cardiovasc.Surg.(Torino)* **29** 80-88

[303] Hegbom, F, Hoff, P I, Oie, B, Folling, M, Zeijlemaker, V, Lindemans, F, and Ohm, O J 2001 RV function in stable and unstable VT: is there a need for hemodynamic monitoring in future defibrillators? *Pacing Clin.Electrophysiol.* **24** 172-182

[304] Receveur, R A M, Lindemans, F W, de Rooij, N F, 2007 Micro System Technologies for Implantable Applications *Journal of Micromechanics and Microengineering* **17** 50-80

3 Laterally Moving Bi-Stable MEMS DC-Switch

This chapter will describe the design of a bi-stable micro electro-mechanical switch for an implantable lead electrode multiplexer application. Fabrication is based on a single mask process. State changes require an 18V pulse to the actuators consuming only 0.2nJ energy. The switch does not consume any energy in either the ON or the OFF state. Total chip size including bond pads is approximately 1.5mm x 1.5mm. The initial contact resistance is below 5Ω with a contact force in the order of 10μN. The contact resistance stays consistently below 30Ω for the first 40000 cycles. Breakdown voltage between the two contact members in OFF state is 300V.

3.1 Introduction

In many fields of medicine, delivering electrical pulses to the body via a chronically implanted electrode connected to an implantable pulse generator (IPG) via a lead can restore a patient's health. The ability to select electrodes from a plurality of possibilities non-invasively enhances the patient's therapy since the stimulation site can be adapted to changes that may occur during his/her lifetime. In addition the implanting procedure is facilitated because the lead position is less critical, which is advantageous for both the patient and the physician. A dedicated connection from each electrode to the IPG requires bulky connector blocks on the IPG, thick leads and adaptations of the circuitry in the IPG itself.

This chapter has been published for the most part in the Journal of Microelectromechanical Systems authored by R.A.M. Receveur, C.R. Marxer, R. Woering, V.C.M.H. Larik and N.F. de Rooij [23]

The lead proposed here has a bi-polar Industry Standard (IS-1) connector on the proximal side that plugs in to any IPG and multiplexer functionality to allow addressing of multiple electrodes on the distal side (Figure 3.1). Apart from control logic, interconnects and possibly power, some form of switching is needed to enable the multiplexing functionality. The focus will be on the switches only in this chapter.

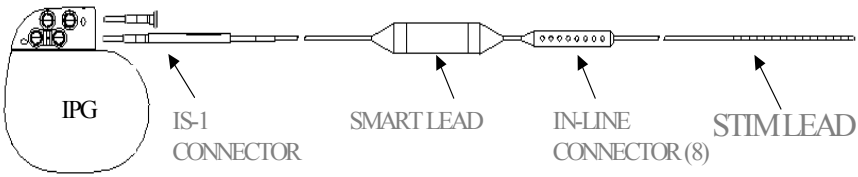

Figure 3.1 Implantable Pulse Generator (IPG) with two bi-polar Industry Standard (IS-1) connectors. One lead is shown having a bi-polar IS-1 connector on the proximal side and 8 electrodes on the distal side (labeled STIMLEAD) connected via an IN-LINE connector. The SMARTLEAD contains switches and communication- and control logic that allow selection of any (combination of) electrode(s) on the stimlead to deliver optimal therapy.

A single pole single throw (SPST) switch has one signal input and one signal output terminal. It either transfers the signal from the input to the output (ON state) or it does not transfer it (OFF state). The switch state is controlled via a control terminal. Bi-stable switches do not consume any energy in either the ON or the OFF state. Mono-stable switches are either OFF or ON in the absence of a control signal (normally open or normally closed respectively). They constantly consume energy to stay in the 'abnormal' state (ON or OFF respectively). The main advantages of mono-stable Micro Electro Mechanical System (MEMS) switches over conventional solid state switches are low power [1,2], low contact resistance, small size and high breakdown voltage [2]. The additional advantage of bi-stable over mono-stable switches is the zero energy consumption in either state,

Table 3.1 Target specifications for bi-stable MEMS switch. FET switch specifications are given to illustrate advantages of MEMS switch.

	Bi-stable MEMS	FET
Size (μmxμm)	<500x500	550x275
Operating power (μW)	0	2
Switching energy (nJ)	<1	25
Breakdown voltage (V)	>300	20
Contact resistance (Ω)	<5	20

providing even lower power and state retention in case of power failure (Table 3.1). The MEMS switch should be able to transfer 4 ms pulse width electrical pulses coming from the IPG.

There are numerous mono stable micro electro mechanical DC-switches [3,4,5,6,7,8,9,10]. Bi-stable switches with out of plane movement of contact members use either a current pulse to change the preferential magnetization of a permalloy cantilever in a permanent external magnetic field [11] or a mechanical latch caused by a thermally actuated two segment multimorph cantilever [12]. Laterally moving bi-stable switches use a compliant structure consisting out of a central slider supported by double pinned arms on both sides [2] or two double pinned arms pushed in two possible directions by actuators on both sides [1]. An overview of the reported properties of these devices is given in Table 3.2 and Table 3.3.

Table 3.2 Overview of mono stable switch properties as reported in literature (continued on next page). *two numbers indicate area LxB

Institute	Unit↓	Cronos	Nrth.East Analog Devices	TU Berlin	IMT
People		E.A.Hill	Zavracky	Schimkat	Gretillat
Principle		Rotating	Beam	Beam under internal stress	Bridge
Actuation		Thermal	E-stat	E-stat	E-stat
Reference		[10]	[7]	[6]	[3]
ON-resistance	Ω	<0.4	0.5-20		20-300
Contact material		Au, Rh, Ni		Ro	Au-Ni
Contact force	μN			1000	
Airgap	μm			8	1.2
OFF-resistance	Ω	$>10^{13}$	$>10^{12}$		
DC-breakdown	V	>300	>100		
Operating Voltage	V	5,6,9 or 12	>30	12	40
Operating Current	mA	30			
Operating Power	mW	150		0.002	
Switching Energy	nJ				
Life #switching	#		$>10^{9}$	$>20x10^{6}$	
Turn on time	μs	8000			2-18
Turn off time	μs	8000			2-18
Switching speed	Hz	30	$3\ x10^{5}$	1000	$2\ x10^{4}$
Size (LxBxH)*	mm^3	1.5x3x.5	.07x.03x.002	1.2 mm^2	.4x.4
Operating temp.	°C	40			
Transp. temp.	°C	250			
Shock sensitivity	g			>1000	
Signal current	mA				

Table 3.2 (continued from previous page) Overview of mono stable switch properties as reported in literature. *two numbers indicate area LxB

Institute	Unit↓	ASULAB	Rockwell	FhG-SST	Imec-3 CP Clare CSEM
People		F.Gueissaz	R.L.Borwick	Schiele	Tilmans
Principle		Microreed		Beam	Armature is pulled down
Actuation		Magnetic	Magnetic E-stat	E-stat	Magnetic
Reference		[9]	[8]	[4]	[5]
ON-resistance	Ω	2-100	2-8	10-80	0.4
Contact material		Ro	Au	Au	Au
Contact force	µN	30	50-300		1000
Airgap	µm	4		10-60	
OFF-resistance	Ω		>100M		$>10^{13}$
DC-breakdown	V	75			200
Operating Voltage	V	n.a	0.9-10 (hold)	20-100	1.9
Operating Current	mA	n.a	0.9-20 (actuate)	$50x10^{-6}$	8.4
Operating Power	mW	n.a.		0.004	16
Switching Energy	nJ	n.a.	11.3-480		
Life #switching	#	$>100x10^{6}$	$>30x10^{6}$	$>10^{6}$	$>10^{6}$
Turn on time	µs		700-120	2.6-20	1000
Turn off time	µs		20	2.6-20	200
Switching speed	Hz	100	4000		>500
Size (LxBxH)*	mm^3	1x.1x.02 ($2mm^3$ packaged)	.8-1.6	.3x.3	5x4
Operating temp.	°C				
Transp. temp.	°C				
Shock sensitivity	g	15000		$>10^{5}$	
Signal current	mA	5 (1 switched)	10	1	

Table 3.3 Overview of bi-stable switch properties as reported in literature. *two numbers indicate area LxB

Institute	Unit↓	ASU	Berkely	NJIT	Ford	Medtronic
People		Ruan	Kruglick	Sun	Gomm	Receveur
Principle		Beam in perm. magn. field	Lateral movement with leverage	Bimorph latching beam	Pin joints	Mechanical springs system has two stable positions
Actuation		Magn.	E-stat	Thermal	Thermal	E-stat
Reference		[11]	[1]	[12]	[2]	This work
ON-resistance	Ω	<50m	9	2-35	49.2	5
Contact material			Au	Au		Au-Ni
Contact force	μN		10	21	23.4	25
Airgap	μm			12	33	8
OFF-resistance	Ω	?		$>10^{12}$		$>10^{13}$
DC-breakdown	V			>400	350-360	>200
Operating Voltage	V		7-12	2.2	11	16
Operating Current	mA			5	85	$2x10^{-4}$
Operating Power	mW			12		0.003
Switching Energy	nJ			6200		0.2
Life #switching	#			$>10^{5}$		$4x10^{4}$
Turn on time	μs			600	340	500
Turn off time	μs			600	340	200
Switching speed	Hz			300		1000
Size (LxBxH)*	mm^3		.2x.2	1x.2		1.5x1.5
Operating temp.	°C					
Transp. temp.	°C					
Shock sensitivity	g					$>10^{7}$
Signal current	mA		1			250

In this chapter a novel design for a laterally moving bi-stable DC-switch is presented. The bi-stable part of the design was proposed by Hichwa et al to build an optical switch [13]. It has a central moving contact member with two stable positions. This is achieved by a dual spring suspension system with hinges and

double clamped beams as qualitatively explained in Fig. 3.2. An opposing contact member is contacted in the second stable position that closes the electrical contact. Electrostatic comb actuators can change the switch position. The contact is designed to meet the target specifications given in Table 3.1.

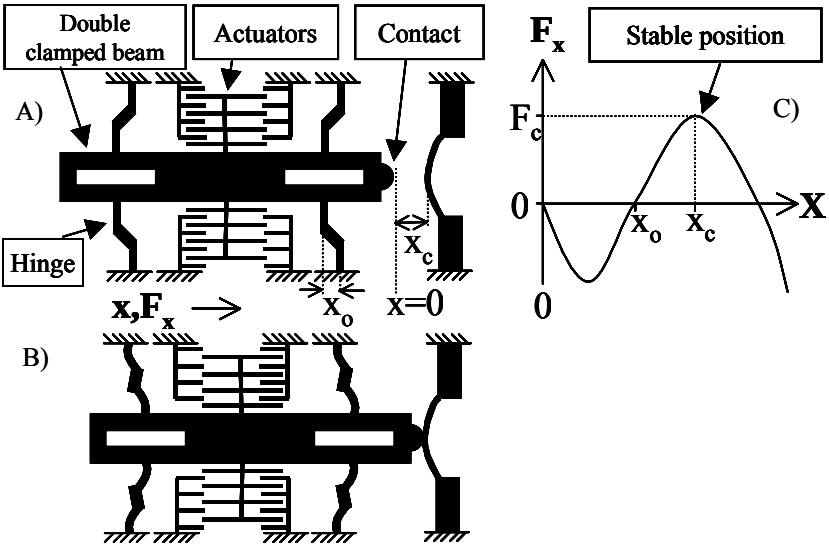

Fig. 3.2. Schematic of the bi-stable switch, not on scale, shown in open position (OFF, A)) and closed position (ON, B)). x is the displacement of the moving parts, were x=0 is defined at the initial position of the central beam (as fabricated). F_x is the mechanical force exerted on the central beam by the double clamped beam and the hinges (C). x_0 is an offset distance and x_c is the contact distance. The central beam can be moved in positive and negative x-direction by the electrostatic comb actuators. When the structure is moved to the right the double clamped beam is deflected and generates a force in lateral (y) direction. For displacements smaller/larger then x_0 this results in an opposing/supporting force in longitudinal (x) direction. A quantitative description is given in paragraph 3.3.2. The fixed contact member is placed at position x_c. for maximum contact force (F_c) (stable ON state).

In this chapter the focus is on the design and characterization of the electrical switch and its long-term contact properties. In section 3.2 the fabrication process, switch layout including definitions of switch parameters and experimental setup are given. Theoretical expressions describing switch properties in terms of the parameters are provided in section 3.3. Design choices are made in section 3.4 resulting in actual parameter values given in Table 3.4. The remainder of section 3.4 presents measurement results and a comparison with theory by applying the expressions to the parameter values. Finally the measured characteristics of the switch are summarized, it is discussed how well this demonstrator meets the specs and an overview of possible actions to improve performance is provided.

Table 3.4 Typical Parameter Values

Parameter	Description	Value	Unit
Bi-stable switch			
l	Overlap of comb finger	20	μm
w	Width of comb finger	3	μm
g	Gap between comb fingers	2	μm
d	Tip-base distance combs	15	μm
h	Height of combs	50	μm
L_h	Total arm length of hinges	500	μm
l_h	Length of hinges	100	μm
t_h	Thickness of hinges	3	μm
t_l	Thickness double clamped beam	10	μm
L_l	Length double clamped beam	180	μm
x_0	Offset	8	μm
x_c	Contact position	12	μm
N	Number of moving fingers	240	#
Mono-stable switch (all comb actuator parameters identical to bi-stable case)			
l_h	Length of hinges	800	μm
t_h	Thickness of hinges	7	μm
N	Number of moving fingers	300	#

3.2 Materials and methods

3.2.1 Fabrication Process

The switch is fabricated out of a Silicon On Insulator (SOI) wafer (350µm thick carrier layer, 1µm silicon dioxide, 50µm device layer, SICO) using a single mask step. This wafer is dehydrated, treated to enhance adhesion and a 2.3µm photo resist layer (AZ1518) is spun on and prebaked. The mask pattern (Cr on glass) is transferred to the wafer using a mask aligner (Electronic Visions, Fig. 3.3a). The device layer is Deep Reactive Ion Etched (DRIE, Surface Technology Systems, Fig. 3.3b). Settings are carefully chosen to prevent notching and create slightly overhanging structures restricting the contact area to the upper side of the device layer where maximum metal coverage is expected. Structures are released in 50%HF and dried with a sublimation technique (Fig. 3.3c). An annealed Ni/Au alloy with a Cr adhesion layer is used as contact material for minimum -contact resistance and -sticking. It was evaporated in a special setup, also covering the vertical sidewalls of the silicon structure (Fig. 3.3d). The complete wafer is dipped in photo resist before dicing to protect the released structures and individual dies are stripped afterwards. Fig. 3.4 shows a SEM picture of the completed switch and a detailed image of the contact members.

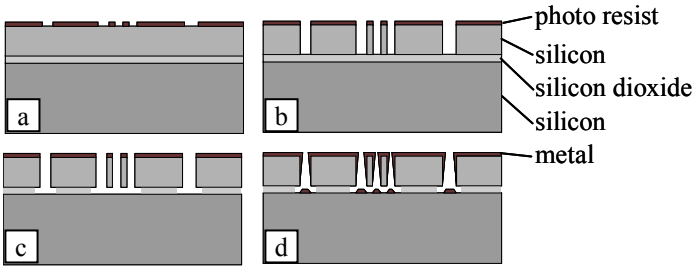

Fig. 3.3. Cross section of a Silicon On Insulator (SOI) wafer during various stages of the fabrication process. a)after patterning of the photo resist with lithography b)after Deep Reactive Ion Etching of the silicon of the SOI device layer c) after removal of the sacrificial silicon dioxide layer d)after removal of the photo resists and deposition of metal.

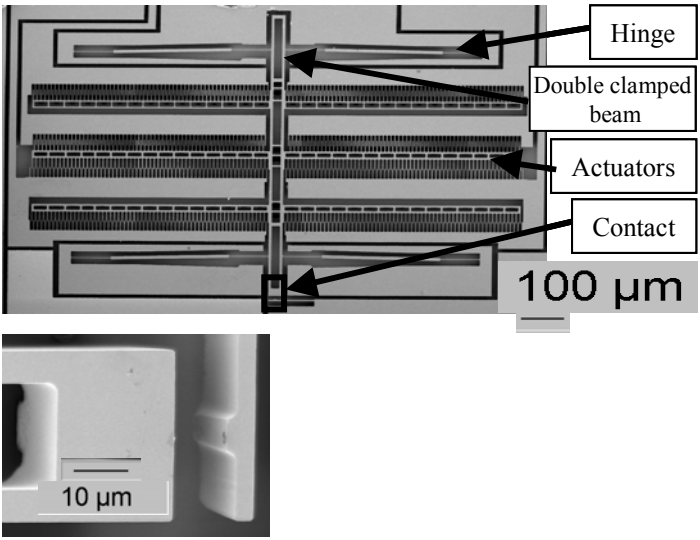

Fig. 3.4. Top: SEM picture of the bi-stable switch. The structure in the middle in vertical direction is the central moving beam. There are three arms of comb actuators on either side of the beam. The micro contact area is marked in the little black box. Bottom: Detailed picture of the micro contact rotated 90 degrees counter clockwise with respect to the top picture. In the detailed orientation the left part is the central moving beam that moves to the right to contact the fixed (but flexible) opposing contact member to close the contact.

3.2.2 Design

The etch mask is drawn using the Expert system (Silvaco.com). The electrostatic comb actuators are shown in Fig. 3.5 and the mechanical spring system is shown in Fig. 3.6. A mono-stable test structure was also designed to better be able to study contact properties (Fig. 3.7). In this case the movable beam is supported by a linear spring. Note that two different contact-shapes, shown

in Fig. 3.6 and Fig. 3.7, were tried on both the bi-stable and mono-stable switches. The springs on the fixed contact members are meant to create a “soft” landing. The difference between the symmetric and asymmetric shape is that the latter creates a ‘scrubbing’ motion which is expected to influence contact cleaning. These figures define parameters that will be used in the theory and results section to quantitatively describe switch behavior and design choices respectively. Typical values are given in table (Table 3.4).

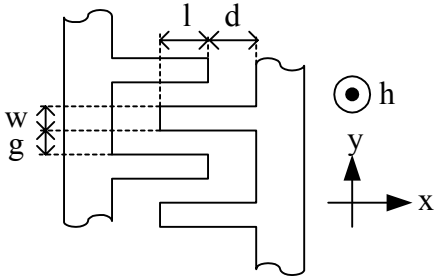

Fig. 3.5. Top view of electrostatic comb fingers. w is the width of the fingers, g is the gap between the fingers, l is the overlap of the fingers, d is the tip to comb base distance and h is the height of the structure (l and d as fabricated). The left part moves towards the mechanically fixed right part.

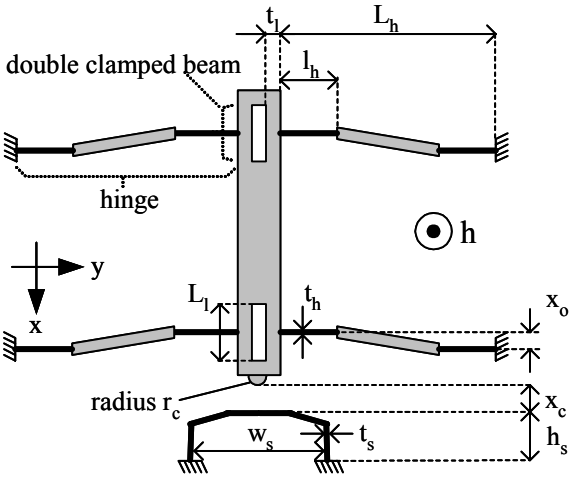

Fig. 3.6. Mechanical spring system in initial position (as fabricated). t_l is the thickness and L_l is the length of the double clamped beam. t_h is the thickness, l_h is the length and L_h is the arm length of the hinges. x_o is the offset and x_c is the contact position. t_s is the thickness, w_s is the width and h_s the length of the contact spring. The moving contact member contains a bump with radius r_c. The complete structure has a height h. Actuators (not shown) are positioned as shown in Fig. 3.2 and designed as shown in Fig. 3.5.

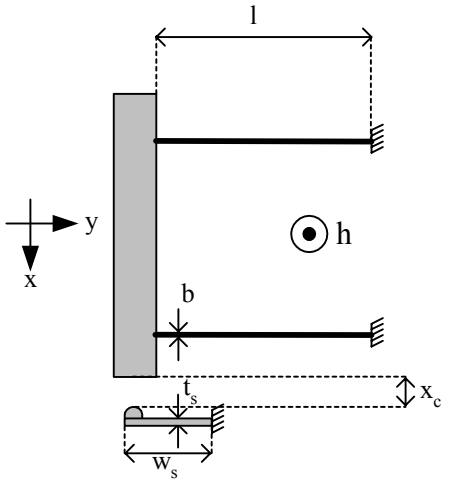

Fig. 3.7. Mono stable mechanical system in initial position (as fabricated). The central moving beam can move down to close the contact. Actuators (not shown) are positioned in a similar way as for the bi-stable switch and designed as shown in Fig. 3.5. The hinges with length l and thickness b function as springs, pulling the switch back to its initial position as soon as actuation force is removed. The fixed contact member is designed as a flexible beam and has a contact bump.

3.2.3 Experimental setup

Unpackaged MEMS chips (bare dies) are contacted using an Alessi Industries needle prober with microscope (Mitutuyo) positioned in a class 10000-controlled environment. Standard power supplies in combination with EMCO High Voltage amplifiers were used to create actuation voltage and standard voltage meter to measure contact voltage.

Switches were wire bonded in ceramic packages (Kyocera, 8 lead side brazed package) and hermetically sealed in an N_2 environment by an outside vendor (Hymec, the Netherlands) to allow easy operation outside the cleanroom in a controlled

atmosphere. On some packages glass lids were glued non-hermetically to allow for visual inspection.

Switch dynamics were investigated by providing periodic pulses of controlled duration and magnitude to the actuators while monitoring contact voltage on an oscilloscope (Tektronix TDS3014B). The voltage on the actuator was switched on and off using FET switches (BSS100) with the gate being controlled by a programmable one shot (Tektronix) triggered by a function generator (Yokogawa FG120, see Fig. 3.8 middle). For duration testing a data acquisition card with both digital and analog I/O capability (NI 6024E) was used to control the voltage on the actuators and record the contact voltage using a computer with Labview (Fig. 3.8 upper and lower). Contact resistance as a function of actuator voltage and contact current was measured under computer control (Labview) using the mono-stable test structures. The voltage on the actuators could be increased in small steps using a programmable high voltage source (Agilent 6030A, via GPIB, see Fig. 3.8 upper). The current through the contact was also controlled via GPIB while the voltages were recorded as described above.

Displacements were measured as a fraction of the contact gap from the monitor of the needle probe station with the microscope on maximum magnification. The contact gap distance was then replaced with the value as measured using the SEM. Structural dimensions were also taken from SEM measurement. EDX analysis is used to show material presence. Destructive tests were used to better assess the vertical dimensions and side wall properties.

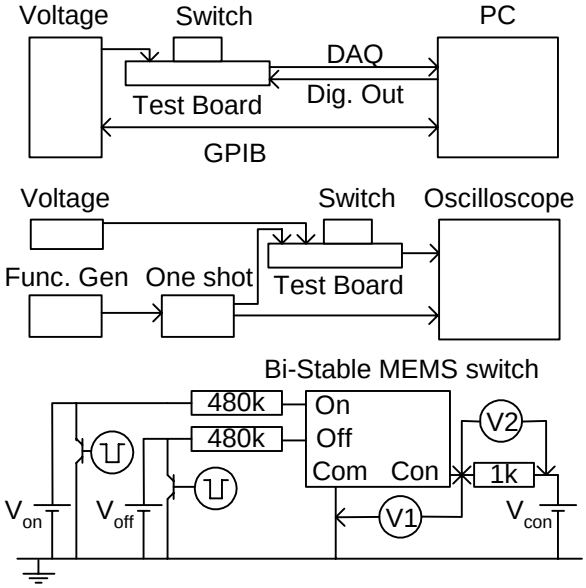

Fig. 3.8. Schematic drawing of the experimental set-up. Upper: Duration testing and contact characterization. The hermetically sealed switches are placed on a test board and tested under complete computer control (labview). The voltage is programmable via GPIB; voltage measurement and digital control is done via a NI-DAQ card in the PC. Middle: Dynamic behavior is monitored on the oscilloscope. The function generator and one shot provide the control pulses of the actuators, while the voltage is set by a separate source. Lower: Electrical schematic for duration test of a bi-stable switch. Voltage on the On and Off actuators is controlled by pulses on the corresponding FET switches. After each state change the voltage V1 (over the contact) and V2 (over a known series resistor) is measured.

3.3 Theory

3.3.1 Electrostatic actuators

By approximating the comb fingers (Fig. 3.5) as parallel plate capacitors, the capacitance C between the two parts of the actuator as a function of displacement *x* is given by [14]

$$C = 2N\varepsilon\left(\frac{wh}{d-x} + \frac{(l+x)h}{g}\right) \tag{3.1}$$

with N the number of moving comb fingers and ε the permittivity of the medium between the combs. The first term is the tip to base contribution (C_t) and the second term is the side-to-side contribution (C_s).

The *x*-derivative of the energy stored in the capacitor when a voltage *V* is applied over it (equation 3.14) gives an expression for the attractive force F_x between the two parts of the actuator in *x* direction [14]

$$F_x = N\varepsilon V^2\left(\frac{wh}{(d-x)^2} + \frac{h}{g}\right). \tag{3.2}$$

3.3.2 Mechanical system

Total force exerted by the hinges and double clamped beams on the central movable beam (Fig. 3.6) as a function of displacement is given by [15,16]

$$F_{springs} = -k_h x + \frac{x - x_o}{L_h} k_l \left(\sqrt{x_o^2 + L_h^2} - \sqrt{(x_o - x)^2 + L_h^2}\right) \tag{3.3}$$

with k_h, k_l respectively the spring constant of the four hinges and the four double clamped beams given by

$$k_h = 2\frac{Eht_h^{\,3}}{4l_h^{\,3} - 6l_h^{\,2}L_h + 3l_hL_h^{\,2}} \tag{3.4}$$

$$k_l = 4\frac{16Eht_l^{\,3}}{L_l^{\,3}} \tag{3.5}$$

with E the Youngs modulus of the material. The first term in equation 3.3 is associated with linear spring behavior of the hinges, resulting in a negative force (opposing the displacement). The second term in equation 3.3 is a reaction force in x direction due to compression of the double clamped beam in y direction related to equilibrium of momentum. Note that this term is initially also negative but changes sign when the beam is displaced further then the offset distance x_0 (the $(x\text{-}x_{0)}$ term). This term is responsible for the bi-stable behavior as shown schematically in Fig. 3.2.

The force required to close the switch is given by the local minimum in the force-displacement curve (Fig. 3.2). The required force to open it is given by the contact force. Any sticking force will add to this. An upper limit on the parasitic non-electric force the switch can sustain and avoid unintended switching to the alternative state can be found by taking Newton's law of inertia of mass

$$F = ma \tag{3.6}$$

with a the acceleration, F equal to the minimal required switching force and m the mass of the movable part given by

$$m = Ah\rho \tag{3.7}$$

with A the total area of the moving parts and ρ the density of the material. The mass of the gold layer on top of the silicon should also be taken into account.

For the mono-stable test structures (Fig. 3.7) the spring force F_{mono} is described by

$$F_{mono} = -k_m x \tag{3.8}$$

$$k_m = \frac{12EI}{l^3} \tag{3.9}$$

$$I = \frac{hb^3}{12} \tag{3.10}$$

with k_m the spring constant, I the moment of inertia and l, h and b the length, height and width of the beam respectively.

3.3.3 Dynamics

Newton's law of inertia gives the differential equation for the displacement as a function of time [15]

$$m\frac{d^2x}{dt^2} = F_x(V,t) - c\frac{dx}{dt} + F_s(x) + F_{cs}(x) \tag{3.11}$$

with m the mass of the structure and c a friction coefficient given by [15]

$$c = \mu\frac{A_c}{d_c} \tag{3.12}$$

in which μ is the absolute viscosity of the medium between the combs, A_c is the total sliding surface area and d_c is the gap between the sliding surfaces.

Resonance for the mono-stable structures is expected at

$$\omega_0 = \sqrt{\frac{k_m}{m}} \qquad (3.13)$$

with k_m and m given by equation 3.9 and 3.7 respectively.

The energy E needed to change the state of the switch equals the energy stored in the charged actuator given by

$$E = \frac{1}{2} CV^2 \qquad (3.14)$$

with C the capacitance of the actuators and V the switching voltage.

The average current I needed to charge the actuator in a time t is

$$I = CV / t \qquad (3.15)$$

3.3.4 Micro contact

Contact properties of micro contacts are described in [17,18,9,19,20,21,1,22].The contact resistance R_c depends on the contact force F_c as [20]

$$R_c \propto F_c^{-\frac{1}{\alpha}} \qquad (3.16)$$

with α=3 for elastic deformations and α=2 for plastic deformations.

Since the hinges are long and thin, they significantly contribute to the measured contact resistance (see section 3.2.3). The

measured resistance values are corrected with a value R_{cor} given by

$$R_{cor} = \frac{\rho l}{hw} = \rho_s n_s \qquad (3.17)$$

with $\rho_s=\rho/h$ the resistance per square of the gold layer and $n_s=l/w$ the number of squares.

Under adiabatic conditions and using the Wiedemann-Franz law a relation between the voltage over the contact U_c and the contact temperature T_c independent of material properties or contact shape can be found [20]

$$T_c = \sqrt{T_0^{\,2} + \frac{U_c^{\,2}}{4L_0}} \qquad (3.18).$$

with T_0 the ambient temperature and $L_0=2.4\cdot10^{-8}V^2K^{-2}$ (Lorentz number). This contact voltage U_c is not to be confused with the contact voltage V_c on the electrostatic actuators needed to make contact. When the contact temperature T_c reaches the melting temperature of the contact metal the switch will be damaged. Equation 3.18 can be used to calculate the corresponding voltage U_c over the contact. This in turn can be related to the maximum current I_c when the contact resistance R_c is known using Ohm's law

$$I_c = U_c / R_c \qquad (3.19)$$

An example calculation is presented in the results section (section 3.4.4)

3.4 Results and discussion

3.4.1 Design choices

The requirements that should be met by the switch are given in Table 3.1. The design intention is a switch that has a consistent and low contact resistance, with a minimum size and maximum breakdown voltage.

A great deal of work has been performed and published to provide design input for micro contacts [19]. However, contact properties depend to a large extend on surface topology and contact material properties that are hard to determine in advance [17,18,9,19,20,21,1,22]. Required minimum contact force for a reliable contact ranges from 10μN [9] to 100μN [19]. The contact force is determined by the magnitude of the (local) maximum in the force versus displacement curve (Fig. 3.2). This is mainly influenced by the spring constant of the double clamped beam k_l (equation 3.5). The (local) minimum in this curve has the same order of magnitude. This is the minimum force that needs to be provided by the electrostatic actuators to overcome the opposing behavior of the spring system and change the state from OFF to ON. The electrostatic force is mainly controlled by the number of comb fingers N (of influence on the size) and the actuation voltage V (equation 3.2). The design is a balance between maximal contact force, minimal structure size and minimal actuation voltage. A matlab program was made to optimize the design. The dimensions of the bi stable mechanical spring system (equation 3.3-5) and the comb actuators (equation 3.2) as well as material properties and the actuation voltage are used as input parameters to calculate the force displacement curve. The maximum- and minimum-force, the electrostatic force, the maximum stresses and an estimate of the switch area are calculated as output parameters. It is checked if the assumptions for the validity of the model hold (Lh>lh and Lc>dc,wc,hc) and if the structure will be working (stress lower

then maximum stress, contact force larger then required minimum, electrostatic force sufficient to overcome barrier). A sensitivity analysis of selectable output variables on input parameters is carried out to identify the critical dimensions. As a contact material AuNi was choose since it has been reported that this gives low contact resistance and small sticking force [19].

The height h of the structure is chosen to have maximum actuator force per unit area. The bigger the height, the larger the electrostatic force (equation 3.2). However the size of the details that can be etched using DRIE also increases with increasing height, meaning less comb fingers per unit area. Optimum structures have an estimated height between 50 and 80μm. The comb finger overlap l and tip to base distance d are chosen so edge effects may be neglected in the capacitance for all allowed values of the displacement x (equation 3.1, see also 3.4.2).

An N_2 atmosphere and a distance of 12μm between the two contact members was chosen. The N_2 has a positive effect on the long term contact properties [19].

Typical values for the parameters are given in Table 3.4. Comparison of theoretically expected behavior with experiment on various aspects will be given throughout the following sub sections. First an inspection of basic properties is given (3.4.2), followed by bi-stable switch characterization (3.4.3) and micro contact characterization (3.4.4).

3.4.2 Verification of basic properties

The mono-stable test structures were used to verify basic properties of the fabricated structures. The displacement was measured as a function of voltage on the actuators. The electrostatic force is calculated from the voltage over the actuators using equation 3.2. In equilibrium the spring force F_{mono} equals the electrostatic force F_x

$$F_{mono} = F_x \tag{3.20}$$

Using this equation the spring force versus displacement can be plotted (Fig. 3.9). Fitted value is 4.6N/m for the spring constant. When calculating the spring constant directly (equation 3.9) using SEM measured values for the dimensions a value of 4.2N/m is found.

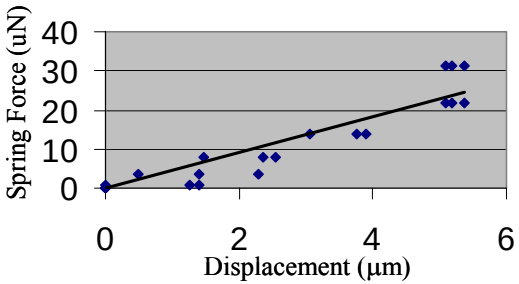

Fig. 3.9. Spring force as a function of displacement. The force is calculated from the voltage on the actuators while the displacement is measured. Fitted value is 4.6N/m for the spring constant, while theoretical expectation was 4.2N/m.

The capacitance was calculated as a function of displacement using a finite element analysis method (Maxwell) and the analytical formula given by equation 3.1 (Fig. 3.10). Note that the tip-to-base contribution to the capacitance is almost negligible. Note that the combs are operated in a range of displacements were the simulations show a linear behavior, this means that equation 3.1 may be used. Also note that the roughly constant offset between analytical and numerical capacitance values is of no influence on the electrostatic force since that is proportional to the derivative with respect to displacement (equation 3.2).

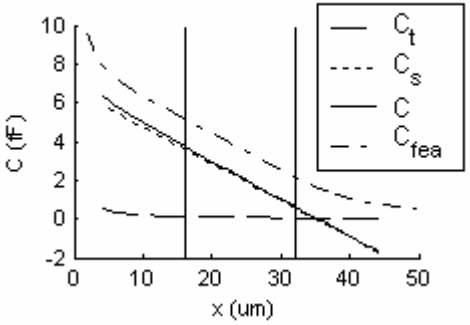

Fig. 3.10. The analytically (C) and numerically (C_{fea}) calculated capacitance in fF (vertical axis) as a function of displacement x in μm (horizontal axis) for one comb finger. C_t and C_s represent the contributions from tip to base and side to side respectively (see equation 3.2). The vertical lines denote the range in which the comb fingers are operated. These two curves (C and C_{fea}) are used to calculate the two theoretical curves in Fig. 3.11 (labeled Analytical and FEA respectively) as explained in the text.

The relative capacitance change as a function of voltage was measured using a setup from Delft University of Technology. To compare this with the theoretical values the following iterative approach is used. First calculate the electrostatic force F_x (either using equation 3.2 or the derivative of the simulated capacitance versus displacement) for a specific voltage V and the spring force F_{mono} (equation 3.8) as a function of displacement. Then use equation 3.20 to find an equilibrium value for the displacement. Calculation of the capacitance at this displacement (equation 3.1) yields one point on the theoretical capacitance versus voltage curve. When the desired range of voltages is calculated the capacitance values are changed to relative units (see Fig. 3.11). The three curves compare very well (differences <<10%).

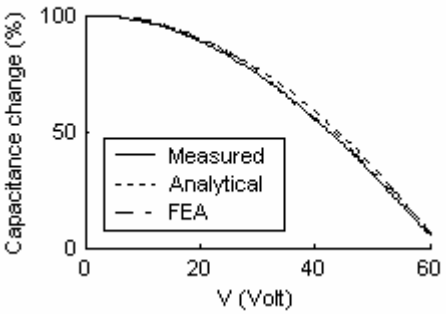

Fig. 3.11. The relative capacitance change as a function of voltage V (Volt) as measured, calculated analytically and calculated using FEA (see text 3.4.2).

Resonance frequency of mono-stable structures was visually determined under the microscope with an AC voltage on the actuators and found at 3.6±0.1kHz. For the theoretical value equation 3.13 is used. The spring constant k_m is calculated using equation 3.9 (see above). The mass is estimated using the dimensions of the movable part of the structure as determined under the SEM and the density of silicon ($2.3 \cdot 10^3 kg/m^3$) in equation 3.7. The mass of the gold layer is taken into account. The calculated resonance frequency is 3.4kHz.

The theoretical value for the contact voltage V_c is 50V by using equation 3.20 at the contact displacement x_c. Experimentally V_c is defined as the first voltage at which the measured contact resistance R_c drops below 10Ω while slowly increasing the voltage on the actuators and find 54V. When the voltage is decreased again in small steps a release voltage V_r is found (defined as the first voltage the measured contact resistance rises above 10Ω) that is lower then the contact voltage. This difference is explained by contact sticking. The sticking force is

easily calculated from the difference in V_c and V_r using equation 3.2. This results in a sticking force in the order of 10 to 15μN.

All measured values are within 10% of theoretical expectation, giving confidence to proceed with inspecting the bi-stable switches and characterization of the contact properties.

3.4.3 Bi-stable switch properties

The force that is needed to overcome the mechanical barrier (equation 3.3) is 5.7μN. This corresponds to a theoretically expected actuation voltage of 16V (equation 3.2), corresponding well with the observed 17V (see Fig. 3.12). The contact position x_c of 12μm is exactly at the local maximum of the mechanical force versus displacement curve, yielding a contact force of 2μN. The theoretical required voltage required to overcome this contact force in order to open the switch is 10V. The observed value is 24V (see Fig. 3.12). The difference corresponds to an excess in required opening force in amount of 10μN. This can be explained by sticking of the Ni-Au contact members. In this bi-stable design the opening comb actuators overcome this sticking force.

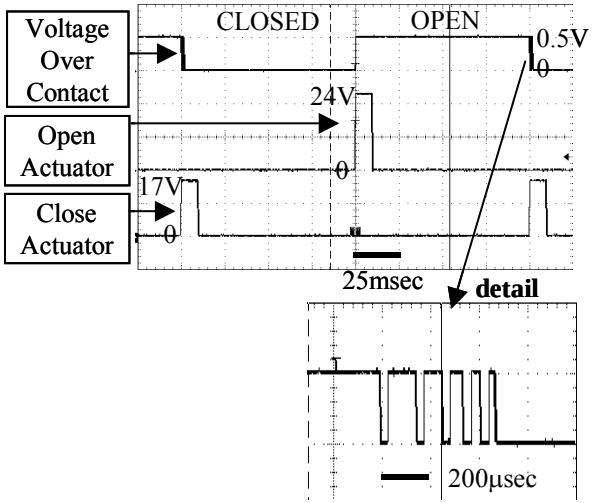

Fig. 3.12. Voltage over the contact and on the actuators as a function of time during operation of a bi-stable switch. The contact voltage is ca. zero in closed position and 0.5 V in open position. A short pulse on the appropriate actuator causes the switch to change state. Bi-stability is shown by the fact that the switch holds its position after removal of the actuator voltage. The detail shows that the switch bounces when closing. (see text for further explanation)

The energy needed to change the state of the switch (equation 3.14) is only 0.2nJ using an approximate value of 1pF for the capacitance of the actuators. The structures show underdamped response. Bouncing could be observed when closing the contact (Fig. 3.12). An upper limit of the actuator charging time (not visible on the actuator pulses shown in Fig. 3.12 on that scale) is 80µsec, which means an approximate current drain during switching of 200nA (equation 3.15). The mass m of the movable structure (equation 3.7) is approximately $m \sim 10^{-14}$kg. If the contact force F_c (discarding sticking) and this mass are used in equation 6 the resulting acceleration is approximately $2 \cdot 10^8 m/s^2$.

Despite the small contact force, the external acceleration needed to accidentally change the switch state is very large due to the small mass. The size of one bi-stable switch including actuators is 1374μmx927μm, or 1374μmx1320μm including bondpads.

The initial measured contact resistance is below 5Ω. Life cycle testing was performed in which the switch was continuously opened and closed while measuring the contact resistance after each actuation pulse. The test results show that the contact resistance starts increasing after approximately $4 \cdot 10^4$ times (Fig. 3.13). SEM-EDX analysis shows damage in gold coverage at the contact spots compared to untouched areas (Fig. 3.14). Although the electrical contact was damaged, the correct mechanical operation of the switch could still be verified by measuring a high resistance (ON) or an infinite resistance (OFF). This showed that mechanically speaking the bi-stable switches reliably open and close for over 10^6 times.

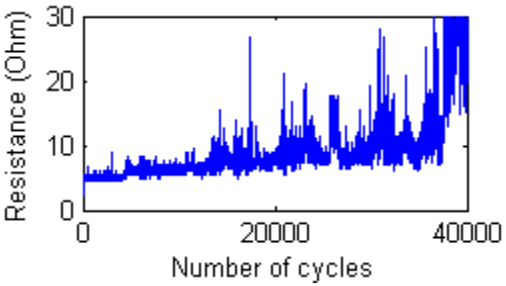

Fig. 3.13. Contact resistance vs. number of cycles for bi-stable switch actuated at 18V, hot switched at 0.5mA. The resistance is measured as shown in Fig. 3.8 Lower)

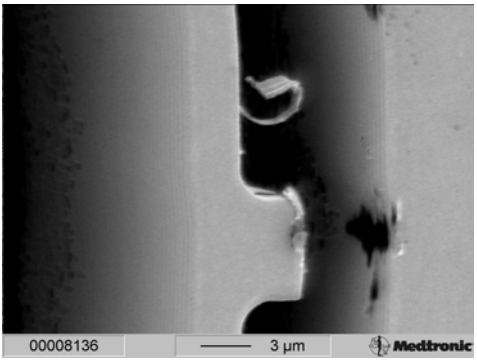

Fig. 3.14. SEM picture of micro contact showing metalization damage after 10 million cycles at 0.5mA. The right part is the movable contact member and the left part is the opposing fixed contact member. The metal peels off and is damaged at the point of contact.

DC breakdown of the central moving beam to the opposing fixed contact member with open contact gap (12µm) was found to be 305V for switches sealed in an N_2 environment (theoretically expected value is 250V). Breakdown from the actuators to the carrier layer occurred at 150V.

3.4.4 Micro contact properties

Life cycle testing of both the beam (Fig. 3.7) and arc (Fig. 3.6) contact shapes on mono-stable test structures showed an increase in contact resistance after $1 \cdot 10^5$ to $3 \cdot 10^5$ cycles similar to that observed for the bi-stable switch as described above. SEM inspection showed a damaged contact metal similar to that of the bi-stable switch shown in Fig. 3.14. These observations do not reveal a difference in duration behavior between the two contact shapes. The limited robustness of the contact metal is more important then the (small) difference in contact design.

In further investigations the contact resistance as a function of contact force was measured using the mono-stable test structures. The measured contact resistance is corrected for the contribution

from the hinges R_{cor}~3Ω (equation 3.17 with n_s=114 squares with a resistance per square ρ_s of 24mΩ). Values compare well with other publications as shown in Fig. 3.15 (adapted from [9]).

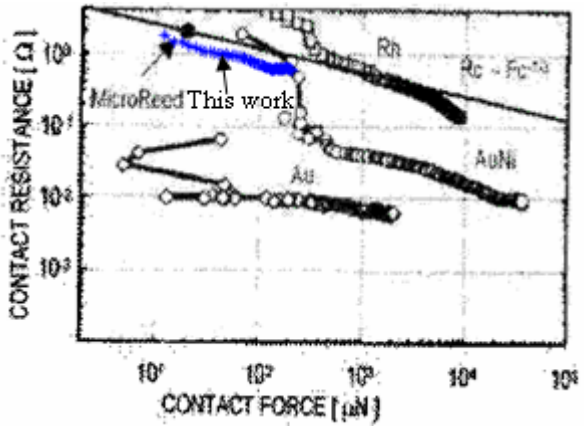

Fig. 3.15. Contact resistance versus contact force (adapted from [9]). Values obtained in this work are indicated by the arrow, measured on mono-stable test structure with 0.5mA current and corrected for series resistance from the hinges.

With the contact temperature T_c equal to the melting temperature of gold (1336K) the contact voltage U_c over the contact is 0.4V (equation 3.18). A closed mono-stable contact actuated at 100V has a measured contact resistance of approximately 1.6Ω (corrected for the contribution from the hinges). Using equation 3.19 with these values a maximum current of 258mA is expected. The measured maximum current on mono stable test structures is 257mA (see Fig. 3.16). Section 5.1.4 provides and overview of possible micro contact failure mechanisms as described in literature.

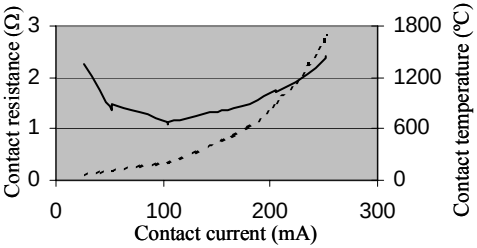

Fig. 3.16. The contact-resistance (solid line, left axis) and –temperature (dashed line, right axis) as a function of contact current. Contact resistance is corrected for resistance of the hinges and used to calculate the voltage over the contact U_c. This is used to calculate the corresponding contact temperature T_c (equation 3.18). Breakdown occurs at 258mA or around 1300ºC (melting point of gold is 1063ºC).

3.5 Conclusion and outlook

Working prototypes of a bi-stable micro electro mechanical switch have been produced. The initial contact resistance is approximately 5Ω. Breakdown voltage between the two contact members in OFF state is 300V, while breakdown between actuators and contact member occurs at 150V. The energy needed to change state is estimated to be 0.2nJ. The switch is bi-stable, meaning that it consumes no energy in either the ON or the OFF state. The total size of the structure including bondpads and actuators is 1374µmx1320µm. Advantages over FET switches are achieved in terms of power consumption; ON resistance and breakdown voltage (see Table 3.1). The size target is not met by these prototypes. However, size can be interchanged with actuation voltage rather effectively. Actuation force is proportional to the square of the actuation voltage and linear with the number of comb fingers that are also linear proportional to the size. Therefore a factor of 10 in actuation

voltage means a factor of 100 decrease in size. These prototype switches operate at 24 V. This is higher then the voltages normally available in implantable devices. An arrangement has to be made in the smartlead to provide the actuation pulses. The step to allow an even higher actuation voltage is possible, decreasing the size to a level that can meet the target.

With measurements on both mono-stable and bi-stable test structures it has been demonstrated that the experiment compares well with the theory. All measurements were within 10% of the calculated values assuming simple models. Furthermore it has been shown that it is possible to create an initial contact resistance below 5Ω with a contact force in the order of 10μN.

The focal areas for further investigations of this switch for biomedical applications will be the contact metalization and the reliability of the switch. Further fundamental investigations into the dynamics, the sticking force and a theoretical treatment of the contact resistance to be expected are also considered.

3.6 References

[1] Kruglick, E J J and Pister, K S J 1999 Lateral MEMS microcontact considerations *Microelectromechanical Systems, Journal of* **8** 264-271

[2] Gomm, T, Howell, L L, and Selfridge, R H 2002 In-plane linear displacement bistable microrelay *J.Micromech.Microeng.* **2002** 257-264

[3] Gretillat, M A, Gretillat, F, and Rooij, N F d 1999 Micromechanical relay with electrostatic actuation and metallic contacts *J.Micromech.Microeng.* 324-331

[4] Schiele, I, Huber, J, Hillerich, B, and Kozlowski, F 1998 Surface micromachined electrostatic microrelay *Sensors and Actuators A* **66** 345-354

[5] Tilmans, H A C et al. 1999 A fully packaged electromagnetic microrelay *MEMS 99* pp 1-6

[6] Schimkat, J 1999 Silicon Microrelays with optimized electrostatic actuator *MEMS* vol 1 pp 175-180
[7] McGruer, N E, Zavracky, P M, and Majumder, S 1997 Microswitches and Microrelays *Proceedings Snesors Expo.* USA Helmers Publishing & Expocon pp 215-218
[8] Borwick, R L, Stupar, P A, and DeNatale, J 2003 A hybrid approach to low voltage MEMS switches *International Conference on Solid State Actuators and Microsystems* Piscataway, NJ, United States IEEE pp 859-862
[9] Gueissaz, F and Piguet, D 2001 The MicroReed, an ultrasmall passive MEMS magnetic proximity sensor designed for portable applications *Fourteenth IEEE International Conference on Micro Electro Mechanical Systems*
[10] US6137206 Hill, E. A. 2000 *Microelectromechanical rotary structures*
[11] Ruan, M, Shen, J, and Wheeler, C B 2000 Latching Micro Electromagnetic Relays *Solid State Sensor and Actuator Workshop* pp 146-149
[12] Sun, X Q, Farmer, K R, and Carr, W N 1998 A bistable microrelay based on two segment multimorph cantilever actuators *11th anual workshop on micro electrical mechnical systems* pp 154-159
[13] Hichwa, B, Duelli, M, Friedrich, D, Iaconis, C, Marxer, C, Mao, M, and Olson, C 2000 A unique latching 2x2 MEMS fiber optics switch *Optical MEMS conference (post deadline paper)*
[14] Marxer, C 1997 *Silicon Micromechanics for Applications in Fiber Optic Communication* University of Neuchatel
[15] Marxer, C and Roth, S 2000 *Design Summary Latching Mechanism* Neuchatel Institute of Microtechnology, University of Neuchatel

[16] US 6,303,885 B1 09/517,649 Hichwa, Bryant P., Marxer, Cornel, and Gale, Michael 10-16-2001 *Bi-Stable Micro Switch* Optical Coating Laboratory Inc.

[17] Majumder, S, McGruer, N E, Zavracky, P M, Morrison, R H, Adams, G G, and Krim, J 1998 Contact Resistance modeling and measurement of an electrostatically actuated micromechanical switch *Micro Electro Mechanical Systems (MEMS)* vol 66 New York ASME pp 341-346

[18] Majumder, S, McGruer, N E, Zavracky, P M, Adams, G G, Morrison, R H, and Krim, J 1997 Measurement and modeling of surface micromachined, electrostatically actuated microswitches *1997 International Conference on Solid State sensors and actuators* vol 2 New York IEEE pp 1145-1148

[19] Schimkat, J 1996 *Grundlagen und Modell zur Entwicklung und Optimierung von Silizium-Mikrorelais* Technical University Berlin

[20] Holm, R 1967 *Electric Contacts, Theory and Applications* Springer Verlag Berlin 3-540-03875-2

[21] Hyman, D and Mehregany, M 1999 Contact physics of gold microcontacts for MEMS switches *IEEE Transactions on Components, Packaging and Manufacturing Technology* **22** 357-364

[22] Tringe, J, Wilson, W, and Houston, J 2001 Conduction properties of microscopic gold contact surfaces *Reliability Testing and Characterization of MEMS/MOEMS* vol 4558 SPIE pp 151-158

[23] Receveur, R A M, Marxer, C R, Woering, R, Larik, V C M H, de Rooij, N F, 2005, Latterally Moving Bistable MEMS DC Switch for Biomedical Applications, *Journal of Microelectromechanical Systems*, **14** (5) 1089-1098

4 Wafer level hermetic package and device testing of the bi-stable MEMS switch

In this chapter a design of a wafer level chip scale package for a bi-stable SOI-MEMS DC switch using a silicon-glass hermetic seal with through the lid feedthroughs is presented. Bonded at 365 ˚C, 230 V and 250 kg they pass fine/gross leak test after thermal cycling and mechanical shock/vibration according to MIL-STD-833 fulfilling the requirements for biomedical applications. Measured shear strength is 114±26 N in correspondence with the theoretically expected 100 N. Ruthenium micro contacts are a factor 100 more robust then gold micro contacts, being stable over 10^6 cycles measured in an N_2 atmosphere inside the package presented here.

4.1 Introduction

Packaging of Micro Electro Mechanical System (MEMS) devices is one of the most difficult parts of the product development process due to the many requirements and functions[1]. It is more complex then conventional integrated circuit (IC) packaging due to difference in nature between MEMS and IC[2]. In many cases a special environment needs to be created in cavities in the package to improve the function of the packaged MEMS device [3,4,5,6,7,8,9,10,1].

This chapter has been published for the most part in the Journal of Micromechanics and Microengineering authored by Receveur, R A M, Zickar, M, Marxer, C R, Larik, V C M H and de Rooij N F [30]

The package serves as an electrical interconnect platform, is a mechanical support, needs to be able to handle the power and takes care of thermal management. It needs to be compatible with other mounting techniques[11] and solves the temperature coefficient of expansion (TCE) mismatch between device and substrate[4,12].

Conventional packaging techniques take up between 75-90% of device costs [13,7,2] and are responsible for as much as 99% of the size[7]. As a consequence, wafer level packaging is increasing in importance[1] and still largely under development[7,2]. Wafer level packaging is low cost due to the batch character of the process[4,5,13,12], and small size[11,13,12,10]. Structures are already protected early in the process[5,7] and testing can be done on the wafer[12]. Smaller packages could enable entirely new applications[13]; lead to better reproducibility[4] and reliability[5,13] and to better electrical properties[4].

A bi-stable silicon on insulator (SOI)-MEMS direct current (DC)-switch for biomedical applications has been designed [14]. A schematic drawing of the working principle of the bi-stable MEMS switch is shown in Figure 4.1. This switch will be used to select electrical stimulation electrodes located on leads implanted in the human body.

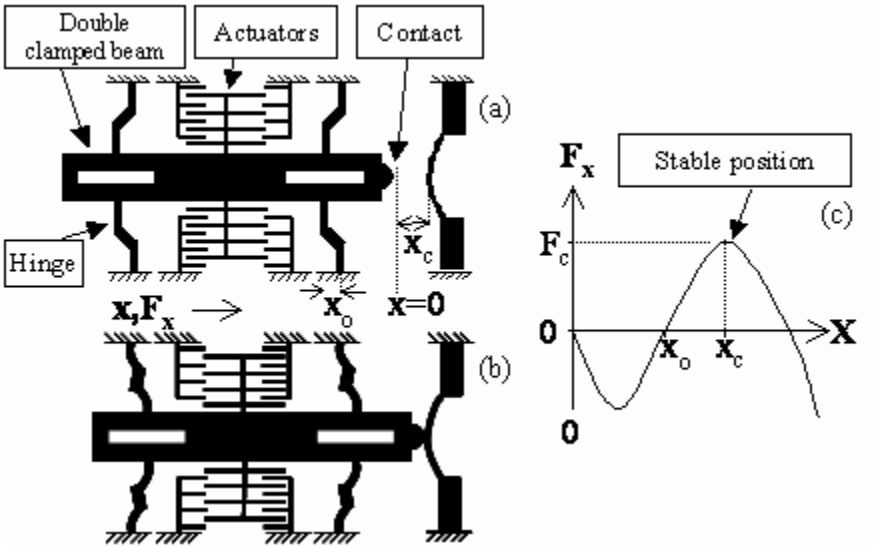

Figure 4.1 Schematic of the bi-stable switch, not on scale, shown in OFF position (a) and ON position (b). x is the displacement of the moving parts, were x=0 is defined at the initial position of the central beam (as fabricated). F_x is the mechanical force exerted on the central beam by the double clamped beam and the hinges, which is plotted as a function of displacement in (c). Bi-stable behavior is generated by the double clamped beam and hinges. x_0 is an offset distance and x_c is the contact distance. The central beam can be moved in positive and negative x-direction by the electrostatic comb actuators. In the ON state the central beam is moved to the right to contact the opposing contact member. When the beam is displaced from its initial stable position (OFF state) in the positive x-direction the force becomes negative, meaning it is opposing the motion. At the offset position x_0 the force changes direction and is now promoting further motion. The fixed contact member is placed at position x_c. for maximum contact force (F_c) (stable ON state).

The wafer level hermetic package protects the fragile movable microstructures of the switch against dust. In addition it provides a cavity in which a controlled environment can be maintained, improving the long-term micro contact reliability. It allows for batch processing of multiple packages in parallel leading to low cost per package. A hermetic feedthrough technique using a

through the lid approach that allows contact to the two control pads and two signal pads needed to operate the bi-stable switch is also presented. The requirements on the package are presented in Table 4.1. These are part of the requirements that a component inside an implantable medical device must fulfill. This chapter will not address the requirements that have to be fulfilled when exposing this package to the body.

Table 4.1 Sealing requirements

Item	MIL-STD-883 Method	Description
Fine leak	1014 Fine	He BOM
Gross leak	1014 Gross	Bubble test
Shear strength	2019	Destructive
Thermal cycling	1010 Cond B	-55ºC/+125ºC 10 cycl.
Mechanical shock	1010 Cond B	5 shocks, x6 directions 1500g 0.5 ms half sine
Mechanical vibration	2007 Cond A	var. frequency 150 - 2000 Hz 20g

This chapter starts with a short review of hermetic wafer level packages and feedthroughs as reported in literature. The design, experimental and theoretical methods are described. Chapter 4 contains the results and discussion, including the results of device testing performed inside the wafer level package. In the last section the measured characteristics are compared with the requirements for use in biomedical application.

4.2 Packaging and interconnect

A short overview of ways to hermetically seal MEMS devices and how to electrically interconnect to them from the outside is presented in this section to place the design presented in this chapter in the proper context.

4.2.1 Hermetic seal

Direct bonding creates a bond between two silicon wafers that are pressed together at high temperature (1000 ºC). A very low surface roughness and no particles between the wafers are required. With a special surface activation method a low temperature (200-400 ºC) variant was developed, creating bond strengths up to 2 J/m^2[15]. This technique makes it possible to make very small gaps between the two wafers, has no TCE mismatch and is compatible with complementary metal oxide semiconductor (CMOS).

The anodic (or electrostatic) bond between glass and silicon is one of the most applied techniques in MEMS for example in pressure sensors and accelerometers[16]. It is believed that a covalent bond is formed between the surface atoms of the glass and the silicon when both wafers are pressed together under application of a voltage at elevated temperatures[7] creating a hermetic seal[6]. The surfaces need to be clean[1] and planar, with a surface roughness of ~100 Å[17]. A glass with a TCE close to that of silicon (like Pyrex) should be used[16], while the silicon can also be a fine grain poly silicon layer[17] or an SOI wafer[12,1]. Applied temperatures are in the range of 300-450 ºC[12,1,17,18] with optimum bond quality achieved at uniform distribution and slow cooling down. Voltages can range from 200-2000 V[12,1,17,18] with an importance for the uniformity. The required bond width is 250 μm[17]. The processing time is in the range of 10-20 min[12,1] and can be done in an arbitrary environment. The resulting bond strength can be >20 MPa[1]. Outgassing of oxygen from the glass during bonding[3,16] can be limited by prebaking prior to bonding[17]. The mobile alkali ions in the glass (required for anodic bonding) can diffuse to other parts of the microstructure and/or electronics and cause failures[16]. The process can be performed locally using a Nd:YAG laser with 300 μm beam and 10-30 MPa applied pressure at temperatures of <250 ºC[16].

For bonding using an intermediate glass layer a paste filled with glass particles is screen printed on the lid width a thickness of 20 μm and a width of 500-600 μm. Both wafers are pressed together and bonded at a temperature of ~450 ºC[12,9]. Alternatively a metal intermediate layer can be used. SnPb/NiAu[5,19] SnAgCu/Pd[5] material combinations have been demonstrated. The metal system is deposited, patterned, plated and or printed on both wafers and reflowed at temperatures in the range of 180-320 ºC. Minimum frame width is in the range of 80 μm[5]. Polymer intermediate layers are classified as non-hermetic seal[4,9]. BenzoCycloButene (BCB) is spin coated and patterned on one of the two wafers and cured at temperatures <250 ºC[20,21].

An entirely different class of protection is to provide a thin film encapsulation. In general a seal layer is deposited over a sacrificial layer and released through etch holes that are then hermetically sealed. It can be a poly silicon layer over an oxide layer, HF vapor released and hermetically sealed by a passivation layer [11] or a 40 μm electroplated Ni layer over photoresist sealed with a solder using a mold and transfer technique[10]. A variation on this process is presented in [8] using a thick epipoly layer with DRIE etched release holes.

4.2.2 Hermiticity.

When fabricating wafer level packaged devices one would like to know the hermiticity level or more in general the quality of the bond to assess compliance with the requirements. Often MIL STD 883 is used to objectively define various hermeticity levels[5]. General bond quality test methods employed include gross leak test, fine leak test, mechanical shear test and fracture[5,1]. Stressing the pacakage is done by temperature cycling, high T high RH storing, drop test and thermal shock, autoclave or saline soaking[4,10,17]. In situ test structures used to determine changes occurring inside the sealed cavity include

pressure sensors, moisture sensors, dew point sensors, tensiometric bridge and pirani gauges[12,22,10,17]. Packages can be inspected using SEM, Scanning Acoustic Microscopy or ultrasound[1,18].

4.2.3 Hermetic feedthrough

In most cases it should be possible to electrically connect structures inside the package without disturbing the long-term stability of the environment created inside the cavity. A development decreasing the need for feedthroughs is 3D system design and CMOS-MEMS integration but a review of those possibilities is beyond the scope of this chapter.

"Under the lid" interconnects extend out of the pacakage in lateral direction, in the plane of the substrate and lid. Filling the trenches in the SOI device layer would allow an under the lid approach. A sealing ring can then be constructed over these areas without causing a leakage path to the inside of the cavity. A silicon nitride[23,24] or silicon dioxide[25] layer can be used to form a mechanical connection but an electrical isolation. LPCVD deposited low stress silicon nitride has good conformal step coverage (completely filling the trenches) and a smooth and flat surface remains after removal of the top layer with CMP[24]. Buried conductor traces in the substrate are another possibility to electrically get out of the hermetic cavity in a lateral way[17,6,26]. The addition of electrical interconnect between lid and MEMS wafer can decrease the need for feedthroughs[19]. This has been demonstrated using the same metal as is used for the sealing [19] and with the use of mechanical press contacts between metallization on the lid and substrate[6,26].

"Through the lid" interconnects extend out of the package in vertical direction, perpendicular to the plane of the substrate and lid. A silicon cap wafer with wet etched through holes eutectic bonded to a silicon substrate is described in [1]. A small remaining gap between metallization on the substrate wafer

(deposited prior to the eutectic bonding) and the cap wafer is closed by sputtering a thick (1 μm)aluminum layer. Deep reactive ion etched through holes of 40-60 μm in 130 μm Pyrex glass filled with Ni by pulsed electroplating are described in [27]. Through the lid wet etched holes in glass have been shown in [26] but are used as a pressure inlet only.

4.3 Materials and methods

4.3.1 Design and fabrication process

Anodic bonding is selected since it is a well known process capable of forming a hermetic seal. It can be performed at the wafer level which has a positive effect on the packaging costs. A new process for creating hermetic feedthroughs through the lid is presented. Each contact is electrically isolated in the SOI device layer.

Structures and lid are designed using the Expert system. A 200 μm sealing ring surrounds the complete structure and each individual bond pad. The switch is fabricated out of a SOI wafer using a single mask step[14]. The DRIE process is tuned to create a slight negative angle, causing the contact position to be at the top side of the device layer where most metal is expected. A shadow mask technique is used to selectively deposit metal on the contact members and bond pads while keeping the glass silicon bond area clean (Figure 4.2). A silicon wafer with KOH etched through holes is manually attached to MEMS wafer. A chromium-gold-nickel-gold layer (Cr/Au/Ni/Au, 10/250/30/200 nm) is deposited using a special rotating evaporation setup and the shadow mask is removed. As a comparison, ruthenium (Ti/Ru 10/1000 nm) was also deposited using a conventional sputtering setup with no special measures to deposit on the vertical side walls. Ruthenium has a higher Vickers Hardness then gold (220 vs. 25) so a longer lifetime for switches coated with this metal is expected. This difference also leads to an

expected lower sticking level and higher required contact force for Ruthenium in comparison to Gold. In addition, Ruthenium is not as good a conductor as gold. Glass lids (Pyrex, 500 μm) are pre etched in 50%HF from both sides through a 0.5 μm polysilicon etch mask deposited by LPCVD (temperature is 570°C and the deposition rate is 2.7 nm/min). After removal of the polysilicon, glass lid and MEMS wafer are aligned (Electronic Visions) and moved to the wafer bonder (EVG). Anodic bonding is done at two different conditions, group I 365ºC, 350V, 200kg and Au metalization and group II 365ºC, 230V, 250kg and no metalization both in an N_2 atmosphere. Bond areas and scribe lines in the glass lid are opened by a final 50%HF etch of the complete wafer stack. The wafer can then be diced into individual capped switches (Figure 4.2).

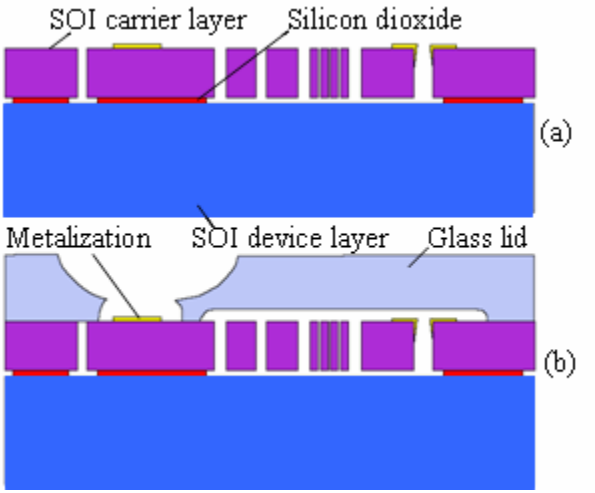

Figure 4.2 Schematic cross section of the packaged micro switch. SOI carrier layer, silicon dioxide, SOI device layer, metalization and glass lid are indicated. (a) After removal of the temporary shadow mask used for selective metal deposition on the contact members and bondpads. (b) Final packaged switch.

4.3.2 Experiment, theory and simulation

The packaged switches are inspected under the scanning electron microscope (SEM). Cross sections of the feedthroughs are made by encapsulating the complete die in epoxy, dicing and inspection under an optical microscope. Bond quality and environmental stress tests are carried out by Zarlink (Caldicot, South Whales) according to the standards as described in table 1. Finite element analysis is done by Infinite (The Netherlands) using ANSYS. Wafer level packaged individually diced switches are placed inside a 8 pin Dual Inline Package (DIL-8) and electrically contacted by wirebonding to the metal pads inside the through the lid holes. Switch contact properties are then measured as reported earlier [14] with the exception that the current through the contact is switched off before opening and closing the switch (cold switching).

4.4 Results and discussion

A SEM picture of a sealed chip is shown in Figure 4.3 and a cross section in Figure 4.4. Details of the lid are shown in Figure 4.5.

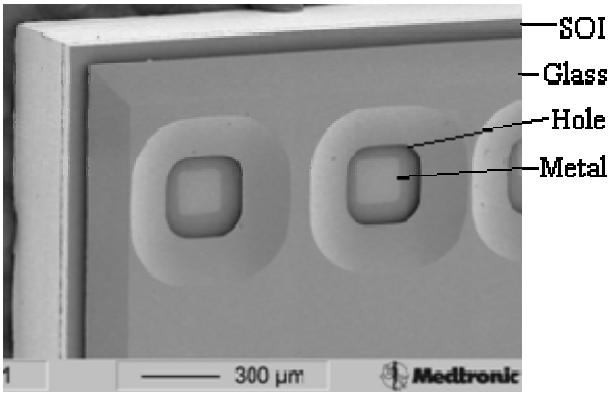

Figure 4.3 SEM picture of packaged switch with feedthroughs. The etched holes in the glass lid open the way to contact the metal on the pads (visible as the light square areas). On the side the SOI carrier layer, silicon dioxide and device layer are visible.

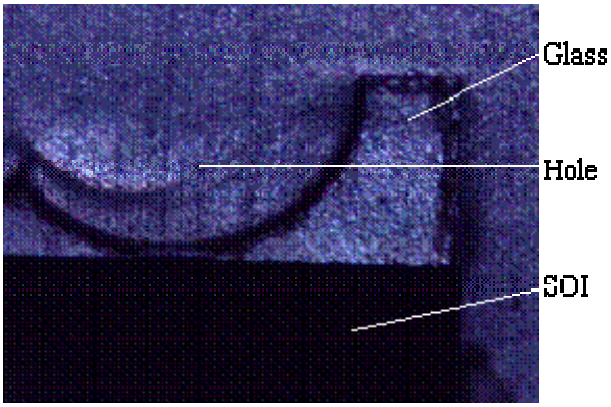

Figure 4.4 Cross section through a feedthrough encapsulated in epoxy.

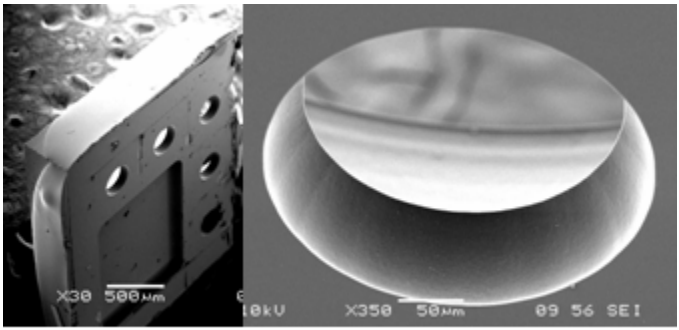

Figure 4.5 SEM photographs of the glass lid. (a) Bottom view showing the recessed area that is positioned above the moving structures and the feedthroughs. (b) Detail of the feedthrough seen from the bottom side.

4.4.1 Bond quality

With the small cavity volumes of typical MEMS packages special care has to be taken with the interpretation of leakrate results[20]. In this design the cavity volume is approximately 150nL. Following the same approach as in [20], this leads to an upper limit for the fine leak rate (Rfu) of 1.5e-6 mbar.l/sec and a lower limit for the gross leak rate (Rgl) of 1e-4 mbar.l/sec. The lower limit fine leak rate Rfl is 0.4e-9 mbar.l/sec. The hermiticity of anodic bond as reported in the literature is limited by the diffusion of gass through the glass. This leads to an expected leakrate of 10e-15 mbar.l/sec. With this in mind the samples with zero leak rate have been interpreted as having a leak rate below the detection limit, and they have been classified as pass. In order to be able to formulate a required leakrate for the package a quantitative expression for the reliability as a function of gas content in the micro contact environment needs to be known. Qualitatively it can be stated that for example water content should be prevented because of possible formation of non conducting layers on the contact material under the influence of water. For simplicity assuming a pressure gradient across the package sealing of 1000mbar the required leakrate for a desired

lifetime of 10 years is 5e-13 mbar.l/s which is below the lower detection limit of 4e-10 mbar.l/s. This means that care has to be taken with the interpretation of the fine leak test results. The required leakrate is however more then two orders of magnitude higher then the expected leakrate of 1e-15 mbar.l/s. Measurements on the MEMS devices itself inside the cavity to detect leakrates in the undefined regime are under investigation. From the 37 as fabricated dies 33 and 31 pass both seal tests (group I and II respectively). The overall bond quality and stress test results are given in Table 4.2 and Table 4.3 and will be described in more detail in the following sections.

Table 4.2 Test results for group I 200N, 350V, 365ºC, Au. The table is to be read from left to right, an each column from top to bottom. The number in the first column indicates the initial sample quantity. These all proceed to the next column titled Bond Quality. The three samples that are entered into the shear test are lost for further testing since it is a destructive test. The number between brackets () are the failed samples. All remaining functional samples pass to the next test towards the bottom of the column. Finally all passed samples proceed to the test in the next column. Note that the group is split in two at the third column.

Initial Quantity	Bond Quality	Stress	Bond Quality	Stress	Bond Quality
40	Shear 3(0)	Thermal 18	Fine 18(0)		
	Fine 33(4)		Gross 18(0)		
	Gross 33(0)		Shear 3(0)		
		Mech. Shock 15	Fine 14(1)	Mech. Vibr. 14	Fine 14(0)
			Gross 14(0)		Gross 14(0)
					Shear 3(0)

Table 4.3 Test results for group II 250N, 230V, 365ºC, no metal (* operator error). (more explanation see table 4.2)

Initial Quantity	Bond Quality	Stress	Bond Quality	Stress	Bond Quality
40	Shear 3(0)	Thermal 16	Fine 14(2)		
	Fine 32(5)		Gross 14(0)		
	Gross 31(1*)		Shear 3(0)		
		Mech. Shock 15	Fine 14(2)	Mech. Vibr. 14	Fine 13(1)
			Gross 14(0)		Gross 13(0)
					Shear 3(0)

For the shear test a custom holder was made to fix a single packaged chip on the SOI side and pressing the glass lid sideways with a automated tool while measuring the force according to MIL-STD-883 method 2019 (destructive test). All shear strength tests (before and after thermal/mechanical stress tests) are passed. The actual value was 137±37 N (group I) and 114±26 N (group II). Reported bond strengths are larger then 20 MPa[1]. The bond area for the devices as estimated from the mask sets is $5x10^{-6}m^2$, giving an expected bond force of 100 N. An estimate of the total bond area of all the devices on the wafer plus the additional bond area around the periphery leads to an anodic bonding pressure of approximately 0.5MPa for the 250kg bonding force.

The test samples are fixated to a holder using glue for mechanical stress tests. The glue is carefully removed afterwards in order to prevent negative side effects in the leakage tests.

Mechanical shock is carried out according to MIL-STD-883 method 1010 condition B. The package is subjected to five 1500 g shocks in 6 directions. Mechanical vibration is carried out according to MIL-STD-883 method 2007 condition A. The package is subjected to a varying frequency between 150 and 2000 Hz with an acceleration of 20 g. Both mechanical tests are survived by 14 out of 15 and 13 out of 15 respectively (group I and II).

For thermal stress tests the samples are placed in a chip carrier that is placed inside an oven. This oven can provide the thermal profile as prescribed by MIL-STD-833 method 1010 condition B. The temperature is cycled 10 times between -55 ˚C and +125 ˚C with a rise and fall time of less then 1 minute and a stable time of 10 minutes. Thermal cycling is survived by 18 out of 18 respectively 14 out of 16 samples (group I and II). In order to assess the thermally induced stresses caused by the difference in TCE between glass and silicon, numerical calculations were carried out. Table 4.4 gives the material properties that were used to numerically calculate the thermally induced stresses. Figure 4.6 gives a picture of the induced stresses at the glass silicon interface. The maximum stress is in the order of 0.12-1Mpa and occurs at the edges and around the holes in the lid. Dynamic calculations do not pose any significant additional stress.

Table 4.4 Material properties used for finite element analysis[28,7,29]
*Depends on temperature

Property	Unit	Symbol	Si	SiO2	Pyrex
Coefficient of thermal expansion	10^{-6}/°C	α	2.6*	0.55	3.2
Thermal conductivity at 300K	W/cmK	λ	1.57	0.014	0.011
Young's Modulus	Gpa	Y	160	73	0.65
Poisson's ratio	#	ν	0.22	0.17	0.2
Yield strength	Gpa	σ	7	8.4	?
Specific Heat	J/gK	c_p	0.7	1.0	0.75
Density	g/cm^3	ρ	2.4	2.3	2.23

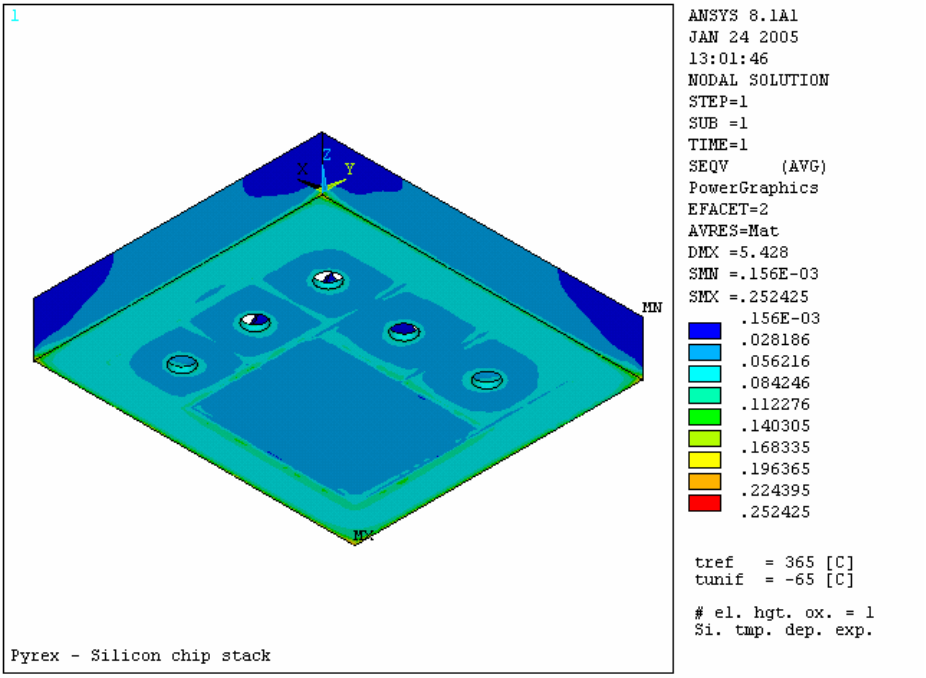

Figure 4.6 Equivalent stress in the pyrex lid (looking at the surface that interfaces with the SOI device layer) at a temperature of –65ºC calculated using Finite Element Analysis. Maximum stress in the order of 0.252 Mpa occurs at the edges and around the holes.

All failed samples were visually inspected under a microscope (see Figure 4.7). Sometimes defects could be observed, but not on all samples. In addition, similar types of defects could also be observed on passed samples. Other inspection methods as described in [18,1] are not available for this research. Therefore it cannot be more specifically stated why the samples failed. Possible failure mechanisms are related to surface contamination, surface finish (flatness, roughness) and capability of the bonding process at the current values of bonding force, voltage and temperature. The anodic bonding process parameters that have been used are at the low side of the spectrum reported in

literature and not at the optimum[18]. However, the measured bonding strength is close to the expected value and the largest part of the samples passes the leakage tests after thermal and mechanical stress. It is concluded that the process described above creates an acceptable bond quality for the intended purpose.

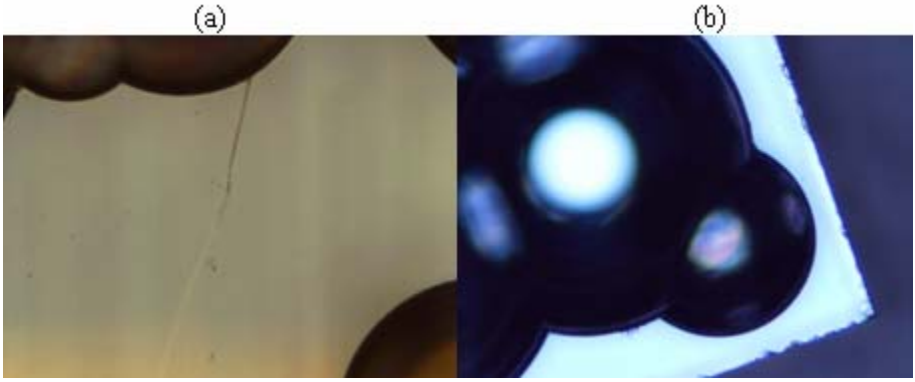

Figure 4.7 Top view of glass lid of failed samples inspected under an optical microscope (scale approximately 500μm). (a) visible crack in the top of the glass lid. (b) pit in the top of the glass lid, due to a hole in the etch mask. The pit clearly does not penetrate all the way through the glass. Similar defects could be observed on passed samples. These observations do not explain the failures.

4.4.2 Micro contact properties.

As an alternative to the gold metallization as described above, samples with a titanium (Ti)-ruthenium (Ru) layer (1000 Å/8000 Å) deposited using a conventional sputtering setup have also been fabricated. The main advantage of Ru over Au is that it is much harder and can withstand higher temperatures. The latter means that there are fewer constraints on the temperatures that can be used during the anodic bonding. Since this metal is much harder it is expected that less contact damage will occur in comparison to Au[14].

Ruthenium coverage on top of the SOI device layer as measured with the alpha stepper is 1μm. EDX measurements were performed at the top of the structures and on the vertical sidewalls of the device layer close to the top and the bottom. Since the same angle of incidence was used at all positions relative comparisons between Ru coverage at different locations can be made. From these measurements it is estimated that there is approximately 0.39μm Ru at the top of the side wall. Figure 4.8 shows a SEM picture with a close up of the two contact members. Inspection of the contacts before the duration tests shows contact damage (see Figure 4.10). This is attributed to electrical effects on the released structures during the anodic bonding process. Unfortunately high resistive silicon was used for these samples so the influence on the initial contact resistance cannot be determined. Therefore only relative changes in contact resistance over time will be investigated in the remainder of this chapter.

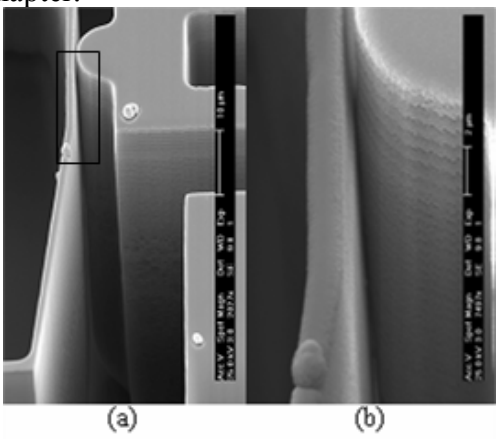

Figure 4.8 SEM pictures showing the contact position and the gaps between the contact members. (b) is an enlarged view of the part indicated by the rectangle in (a). The right part with the semispherical bump on it is the movable part, touching the thin opposing contact member that is fixed.Note that there is a small gap at the top of the contacts that can be influenced by the deep reactive ion etching.

To assess the difference in contact properties between Ru and Au metalized switches the open and closed resistance while repeatedly cold switching the contact (see Figure 4.9) was measured for both metallization systems. Switches were packaged as described above. The ruthenium covered switches show a marked change in behavior after roughly 10^6 cycles, compared to 10^4 for the gold covered switches. Switches will only have to change state at the time of implant and in exceptional cases during the lifetime of the device so it is expected that both of these switches can be applied in this case. A SEM picture of the contact surface before and after the test for both metalizations is shown in Figure 4.10. From these pictures a clear difference in the type of damage between Ru and Au can be seen as well. The contact damage in the ruthenium coated switches is much more localized then the gold coated switches. Both these results correspond with what was expected because of the higher hardness of ruthenium compared to gold. In summary, given the difference between the two metals described above, ruthenium would be the preferred choice.

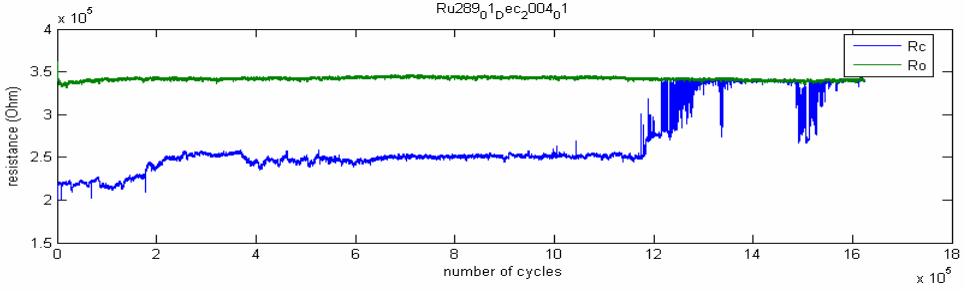

Figure 4.9 Resistance as a function of number of cycles for a ruthenium covered switch in closed and open position (cold cycled). The absolute resistance is very high since undoped silicon was used for these tests. However, the difference between closed and open resistance, and in particular the change of this difference over time is attributed to the microcontact properties. It is clear that at approximately $12x10^5$ the contact is damaged and the difference between open and closed disappears. The required number of times a switch has to change state depends on the specific biomedical application.

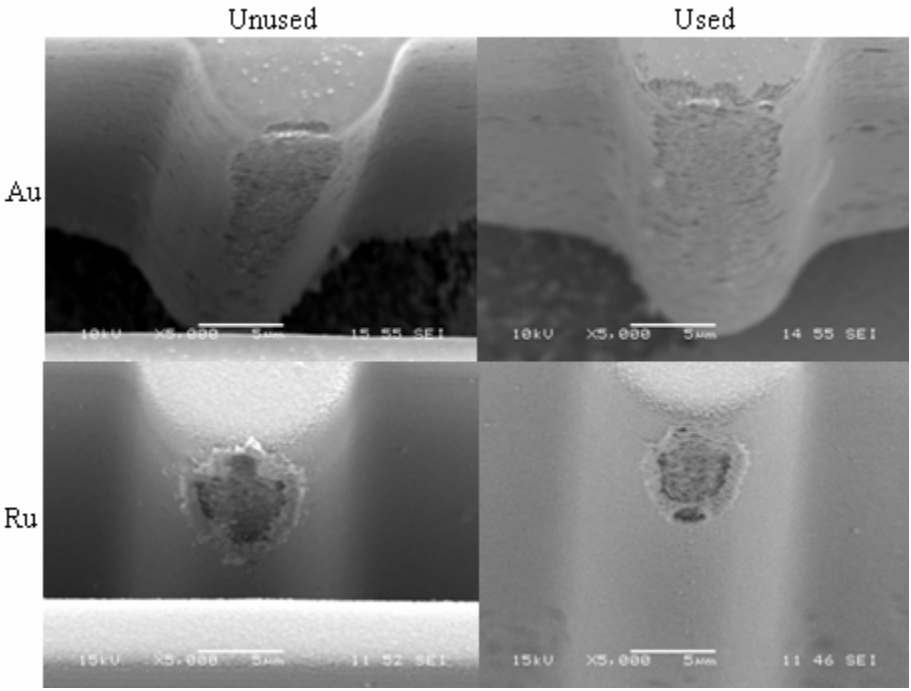

Figure 4.10 SEM pictures of the movable contact part all at same magnification. Au and Ru coated switches (top and bottom row respectively) and unused and used switches (left and right column respectively). Note that the unused switches already show contact damage attributed to electrical effects on the released structures during anodic bonding. The used switches have gone through duration testing. Only relative changes in micro contact properties as a function of duration test cycles are investigated. Note the difference in morphology of the contact damage between gold and ruthenium coated switches due to the differences in material properties.

4.5 Conclusion

A short review of the available packaging and feedthrough techniques has been presented. Anodic bonding is selected since it is a well known process capable of forming a hermetic seal that will fulfill the requirements for the targeted biomedical application of the MEMS switch as given in the introduction. It can be performed at the wafer level of which has a positive effect on the packaging costs.

A process for creating hermetic feedthroughs through the lid has been presented. Each contact is electrically isolated in the SOI device layer and individually surrounded by a sealing ring. Structures bonded at 250 kg, 230 V, 365 ºC pass thermal and mechanical stress tests according to MIL-STD-883 and meet the requirements for biomedical applications for these aspects. Numerical analysis shows that the thermal stresses in the glass silicon stack are a factor of 20 lower then the bond strength, which is confirmed by shear strength measurements to be in the order of 20 MPa.

It has been demonstrated that ruthenium covered contacts are robust for 10^6 cycles, which is a factor of 100 more then gold coated contacts. These measurements were carried out in an N_2 atmosphere inside the wafer level package.

In summary, the anodic bonding of a glass lid with through the lid feedthroughs to the MEMS device passes the initial requirements for biomedical application. Ruthenium metalized switches tested inside the wafer level hermetic cavities show longer lifetime then gold coated switches. These results form the basis for further advancements towards application in medical devices. Future work will include a more extensive bond quality assessment and continued micro contact reliability measurements.

4.6 References

[1] Wong, C K, Wei, J, Qi, G J, Wang, Z F, Jin, Y F, and Lim, P C 2003 A Wafer Level Packaging for Pressure Sensors MEMS *Micro System Technologies 2003* (Poing, Germany: Franzis Verlag GmbH) pp 123-130

[2] Najafi, K 2003 Micropackaging technologies for integrated microsystems: Applications to MEMS and MOEMS *Proceedings of SPIE - The International Society for Optical Engineering* vol 4982 (San Jose, CA, United States: The International Society for Optical Engineering) pp ix-xxvii

[3] Caplet, S, Sillon, N, Delaye, M T, and Berruyer, P 2003 Vacuum wafer-level packaging for MEMS applications *Proceedings of SPIE - The International Society for Optical Engineering* vol 4979 (San Jose, CA, United States: The International Society for Optical Engineering) pp 271-278

[4] Feiertag, G, Kruger, H, and Selmeier, P 2003 Advanced Packages for Surface Acoustic Wave Components *Micro System Technologies* (Poing, Germany: Franzis Verlag GmbH) pp 44-51

[5] Harder, T, Schimanski, H, Bertels, L, and Zoberbier, M 2003 Wafer-level encapsulation of MEMS using solder sealing *Micro System Technologies* (Poing, Germany: Franzis Verlag GmbH) pp 52-59

[6] Hedenstierna, N, Habibi, S, Nilsen, S M, and Kvisteroy, T 2003 Bulk Micromachined Angular Rate Sensor Based on the 'Butterfly'-Gyro Structure *Micro Mechanics Europe Workshop* (Delft, The Netherlands: Delft University of Technology) pp 175

[7] Madou, M 1997 *Fundamentals of microfabrication* (New York, United States: CRC Press LLC)

[8] Partridge, A 2003 A lateral Piezoresistive Accelerometer with Epipoly Encapsulation Stanford University, CA, United States)

[9] Reimann, M, Ulm, M, Buck, T, Schobel, J, and Dechow, J 2003 RF MEMS Glass Frit Packaging *Micro System Technologies* (Poing, Germany: Franzis Verlag GmbH) pp 60-67

[10] Stark, B H and Najafi, K 2004 A mold and transfer technique for lead-free fluxless soldering and applications to wafer-level low-temperature thin film packages *International Conference on Micro Electro Mechanical Systems* vol 17 (Piscataway, NJ, United States: IEEE) pp 13-16

[11] Aigner, R, Opperman, K-G, Kapels, H, and Kolb, S 2001 "Cavity-Micromachining" Technology: Zero-Package Solution for Inertial Sensors *The 11th International Conference on Solid-State Sensors and Actuators* vol 11 (Piscataway, NJ, United States: IEEE) pp 186-189

[12] Iliescu, C, Miao, J, and Tay, F E H 2003 Chip Scale Packaging in Glass of Pressure Sensors *Micro System Technologies* (Poing, Germany: Franzis Verlag GmbH) pp 110-116

[13] Hierold, C 2003 Micro- and Nanosystems: Review and Outlook *MicroMechanics Europe Workshop* (Delft, The Netherlands: Delft University of Technology) pp 101-104

[14] Receveur, R, Marxer, C, Duport, F, Woering, R, Larik, V, and De Rooij, N F 2004 A laterally moving bi-stable MEMS DC switch for biomedical applications *International Conference on Micro Electro Mechanical Systems* (Piscataway, NJ, United States: IEEE) pp 854-856

[15] Hiller, K, Kurth, S, Neumann, N, Hahn, R, and Kaufmann, C 2003 Application of low temperature direct bonding in optical devices and integrated systems *Micro System Technologies* (Poing, Germany: Franzis Verlag GmbH) pp 102-109

[16] Wild, M J, Gillner, A, and Poprawe, R 2001 Locally selective bonding of silicon and glass with laser *Sensors and Actuators A* **93** 63-69
[17] Ziaie, B, Von Arx, A, Dokmeci, M R, and Najafi, K 1996 A hermetic glass-silicon micropackage with high-density on-chip feedthroughs for sensors and actuators *IEEE Journal of Solid-State Circuits* **5** 166-179
[18] Cao, Z, Chen, H, Xue, J, and Wang, Y 2005 Evaluation of mechanical quality of field-assisted diffusion bonding by ultrasonic nondestructive method *Sensors and Actuators A: Physical* **118** 44-48
[19] Tilmans, H A C, Van De Peer, M, and Beyne, E 2000 The indent reflow sealing (IRS) technique - A method for the fabrication of sealed cavities for MEMS devices. *Journal of microelectromechanical systems* **9** 206-217
[20] Jourdain, A, De Moor, P, Pamidighantam, S, and Tilmans, H A C 2002 Investigation of the hermeticity of BCB-sealed cavities for housing (RF-) MEMS devices *International Conference on Micro Electro Mechanical Systems* (Piscataway, NJ, United States: IEEE) pp 677-680
[21] Jourdain, A, Ziad, H, De Moor, P, and Tilmans, H A C 2003 Wafer-scale 0-level packagin of (RF-) MEMS devices using BCB *Design, Test, Integration and Packaging of MEMS/MOEMS* (Grenoble, France: CNRS, TIMA Laboratory) pp 239-244
[22] Information Society Technologies Programme 2004 *Long-term stability of vacuum-encapsulated MEMS devices using eutectic wafer bonding (VABOND)* http://www.cordis.lu/ist/ Information Society Technologies
[23] MEMSCAP 2002 *MetalMUMP: Plated Metal Multi User MEMS Processes* www.memscap.com)
[24] Sarajlic, E, De Boer, M J, Jansen, H V, Arnal, N, Puech, M, Krijnen, G, and Elwenspoek, M 2003 Integration of trench isolation technology and plasma release for advanced

MEMS design on standard silicon wafers *MicroMechanics Europe Workshop* (Delft, The Netherlands: Delft University of Technology) pp 123-126

[25] Borwick, R L, Stupar, P A, and DeNatale, J 2003 A hybrid approach to low voltage MEMS switches *International Conference on Solid State Actuators and Microsystems* (Piscataway, NJ, United States: IEEE) pp 859-862

[26] Jakobsen, H, Lapadatu, A, and Kittilsland, G 2001 Anodic Bonding for MEMS *Symposium on Semiconductor Wafer Bonding* (Pennington, NJ, United States: The Electrochemical Society

[27] Li, X, Abe, T, Liu, Y, and Esashi, M 2002 Fabrication of high-density electrical feed-throughs by deep-reactive-ion etching of Pyrex glass *Journal of microelectromechanical systems* **11** 625-630

[28] Corning 2004 *Glass Silicon Constraint Substrates* www.slam.corning.com

[29] Maluf, N 2000 *An introduction to microelectromechanical systems engineering* (Boston, United States: Artech House Inc.)

[30] Receveur, R A M, Zickar, M, Marxer, C R, Larik, V C M H, de Rooij, N F, 2006 Wafer level hermetic package and device testing of a SOI-MEMS switch for biomedical applications, *Journal of Mircomechanics and Microengineering* **16** (2006) 676-683

5 Analysis of the dynamics of the bi-stable MEMS switch

Besides low power and small size, reliability is a major requirement for medical devices, especially for life saving applications. The first section of this chapter provides a theoretical basis for a quantitative approach towards reliability in general and a more specific treatment of MEMS switch reliability aspects for implantable applications. The second part of this chapter contains a treatment of the switch dynamics and its relation to switch reliability.

5.1 Reliability

This section first provides an introduction to reliability in general. Then more specific issues that play a role in reliability of Active Implantable Medical Devices (AIMD) and reliability of MEMS are described including a focused review of possible failure mechanisms for the particular MEMS device under investigation in this thesis.

5.1.1 Reliability Theory

Almost every discussion about reliability benefits from a quantitative and preferably objective approach. A reliability theory approach enables experimental planning, accelerated testing, lifetime predictions including confidence intervals, risk assessments when accepting lots bought from third party manufacturers and design for reliability too name just a few examples. Since this chapter deals with reliability, a description of the basic concepts is appropriate.

A generally accepted definition of reliability is: Reliability is the probability that an item will perform a required function under stated conditions for a stated period of time [1,2]. This definition implies that further treatment of reliability requires knowledge of probability theory. The improvement of reliability is done by identification-, studying- and elimination of failure mechanisms [1,2,3]. A failure is defined as the termination of the ability to perform a required function. A failure mode is the effect by which the failure is observed. A failure mechanism is a physical, chemical or other process that results in failure. Product requirements and specifications are needed to be able to state the required function, conditions and period of time.

A practical mathematical approach towards reliability is given in [3]. The remainder of this section is a summary of that text. The life distribution F(t) (or "unreliability function") is the probability that a random unit drawn from a population fails by t hours. It can also be interpreted as the fraction of all units in a population that fail by t hours. The reliability function $R(t) = 1-F(t)$, the Probability Distribution Function (PDF) $f(t)=dF(t)/dt$, the hazard function $h(t)=f(t)/R(t)$ and the cumulative hazard function $H(t)=\int h(t)$ can all be mathematically transformed into each other. The hazard function is also called failure rate, instantaneous failure rate or hazard rate. It is the conditional rate of failure for survivors at time t and it is expressed in failures per unit time (failures expressed as a fraction).

Reliability data are generated by putting a certain number of test samples on test and monitoring the functionality. Examples of types of test data are fixed test time T with exact failure times, predetermined number of failures with exact failure times, predetermined inspection times or a mix of all of the above.

Mathematical expressions of the functions introduced above can describe observed data. Examples regularly encountered in reliability work are the exponential distribution, the Weibull distribution, the normal and lognormal distribution which can be

applied to a variety of failure mechanisms. If the failure mechanism is known, the applicable model may be determined on the basis of theory or from existing literature.

Parameters that describe the distribution functions can be estimated with use of the collected data. How well the chosen distribution function fits the data can be determined with for example the Chi-Square Goodness of Fit test. In short this method is based on a comparison between the observed number of failures and the calculated number of failures (from parameter estimates). This method also results in confidence bounds on the parameters. Graphical plotting of the data should always be done to reveal reasons for rejecting a model that can be obscured by looking at the numbers only. The best way to estimate the parameters is the Method of Maximum Likelihood (Maximum Likelihood Estimates MLE). The technique is equivalent to maximizing an equation of several variables.

Collecting failure data for high reliability products takes a long time, too long to be of any use in a development phase. If a component operating under the right levels of increased stress has the same failure mechanisms as seen when used at normal stress accelerated testing can be used to reduce testing times. In case of linear acceleration the mathematical form of each accelerated distribution function can be easily derived. An acceleration model is an equation that calculates a distribution scale parameter as a function of the operating stress. Each mode of failure typically follows a completely different acceleration model. Examples of acceleration stresses are temperature, voltage, humidity or frequency. The Arrhenius- and Eyring-models are well known examples.

5.1.2 Essential Requirements Active Implantable Medical Devices

Besides fulfilling functional requirements aimed at providing patient benefits, every AIMD released on the European market

needs to conform to the applicable general requirements. These so called Essential Requirements and their applicability are described at high level in the European AIMD Directive (AIMD 90/385/EEC Annex I). Essential Requirements cover a variety of product- and design- aspects ranging from the application of risk management to labeling, from sterilization to biocompatibility and from traceability to user interface. An important requirement is that the device must remain functional under normal use conditions for the device life time. These normal use conditions include foreseeable stresses from the outside. Most important, the device must be safe for both the patient and the persons working with it under all circumstances. There are several ways to show compliance to the Essential Requirements. One such way is the use of standards. The list with applicable standards is long. A particularly interesting example in the context of this chapter is EN 45502-1:1997 Active Implantable Medical Devices – Part 1: General Requirements for Safety. A device that survives the applicable test performed according to the description in this standard fulfills this part of the requirements for safety. Tests described in this standard that are typical for implantable medical applications are protection against defibrillation and Magnetic Resonance Imaging (MRI) and electrical surgery compatibility.

5.1.3 MEMS reliability

In the previous sections reliability aspects typical for active implantable medical applications were described both in general and specifically for the MEMS switch. Likewise, reliability aspects that are typical for MEMS will be treated in general in this section and specific for the MEMS switch in the next section.

MEMS reliability has a number of peculiarities. Not all MEMS failure modes are well understood [4,5]. This is related to the fact that the mechanisms that cause failure of MEMS devices vary significantly from one type to another because of the wide

variety of functions that MEMS perform. [5,4]. The failure modes depend on materials used, fabrication approach, packaging and design [4,6] which are also diverse (see for example [7,8,9,10]). In addition not all available data are published and most of the time the parts are not mature and are not available in large numbers [4]. Even though MEMS are manufactured using IC like fabrication techniques, there are differences with IC's. This means: the knowledge from IC reliability cannot be used [5]. Packaging fails to provide the required reliability There is a lack of knowledge in packaging of MEMS again due to the highly diversified functions and materials the lack if information flow in the industry and a focus on the MEMS device and process itself[5]. Some MEMS devices are not being commercialized because of reliability concerns.

Nevertheless, carefully designed MEMS can be more reliable then conventional solutions. Many ways have been reported to mitigate MEMS failure modes. [4] provides a summary of good design practices. Computer Assisted Design Tools become more and more powerful. Design for test is being recognized as a good way to improve reliability in a structured way [4,5]. Similarity in basic design requirements can be used to provide a general procedure for developing high reliability MEMS parts [6]. This guideline also describes the use of technology characterization vehicle (TCV). This is a structure that is used to evaluate the effects of specific failure mechanisms on a technology. The use of these devices is a critical part of the qualification process, as they provide a wealth of knowledge about the reliability of structures. A standard evaluation device, or SED, is similar to a TCV except that a SED is not constructed out of typical design elements, but is instead constructed out of actual sensor and actuator structures. As in TCVs, SEDs should be treated in the same fashion as a fully functional device. Other controls described in [6] are parametric monitors used to measure properties of materials, beam stubs for layer thickness control,

several structures for elastic measurements, resonance beam structures to measure dynamical properties, several structures to measure stress, undercut squares to check the amount of under etching and fracture specimens. The guideline also contains a complete Qualification Testing Protocols for MEMS.

5.1.4 Micro contact failure mechanisms

The micro contact is the main reliability issue. In this section possible micro contact failure mechanisms will be briefly described. System level failure mechanisms are not included in this overview; MEMS switch level failure mechanisms (other then having to do with the micro contact) are included. This section serves as a brief overview of the possible mechanisms, a more detailed treatment of the dynamics of the switch forms the second major section of this chapter. Note that the reliability literature for metal contact RF MEMS switches contains failure mechanisms that may play a role in DC switches [11,12].

5.1.4.1 Materials

The silicon dioxide and silicon of the Silicon On Insulator (SOI) wafer could have build in defects. A weakness in the oxide could influence the break down voltage from device to handle layer.

5.1.4.2 Process variations

The roughness of the sidewalls is a result of the Deep Reactive Ion Etching (DRIE) and post processing. Surface roughness may also induce local stress concentration that may result in fracture at other values then expected [5]. Geometric tolerances [5] of critical parts due to process variations influence the magnitude of mechanical- and electrostatic forces. Material properties depend on process conditions [6]. Material properties of a given material made on a given process need to be characterized.

5.1.4.3 Mechanical failure mechanisms

The mechanical impact of contact members upon closure could have an influence on contact reliability. Repetitive impact of contact members can lead to contact pitting and hardening. External mechanical vibrations may influence the movable parts of the MEMS switch. Vibrations may induce fatigue type of process [5] or wear [4] that may lead to failure. Material might be removed from a solid surface as the result of mechanical action [6]. The electrostatic comb drives might move in the wrong direction [6]. Touching surfaces might stick [4]. Fatigue, creep and structural deformation can cause gradual change in the properties of materials [4,6]. Stress concentrators (sharp edges) influence the mechanical fracture strength [4] and edges of metal layers are vulnerable for micro cracks [2]. Mechanical stress changes the mechanical properties of the micro system. This can be temperature induced mechanical stress between materials with different CTE [5] or intrinsic stress in deposited layers [6]. Material transport due to mechanical stress relaxation can lead to whiskers, hillocks or voids [2]. Mechanical contact force influences the micro contact properties.

5.1.4.4 Electrical failure mechanisms

The design should incorporate the effects of parasitic elements between for example device and substrate [6]. Electrical fields can lead to material deterioration [2]. Charges trapped in dielectric layers influence the actuation voltage [4,2,6]. Arcing across small gaps as described by a modified Paschen curve creates damage [4]. Electro Static Discharge (ESD) can damage gate oxides, cause micro cracks or complete meltdown [2,6]. Dendrites and whiskers formed under the influence of an electric field can short- and open circuits [4]. Electrical potentials can accelerate electro chemical reactions or cause electro migration [4,2].

5.1.4.5 Other failure mechanism

Delamination [4,5,6], dust particles[5,2] and material interdifffusion [2] can have its impact on the switch. Contamination on-or oxidation of the contact members influences the contact resistance. The quality of the hermetic package (amongst others) determines the magnitude of these effects [2,5]. Low contact force makes the contact resistance extra sensitive to thin films [13].

5.2 Switch dynamics

The switch must open and close in a predictable manner. In this sense it is interesting to know how the switch' response to an actuation pulse depends on the dynamical characteristics of the switch. In addition, the bouncing of the contact members upon closure of the switch (which is also determined by the switch dynamics) might have an influence on the micro contact reliability as well. A good understanding of the dynamical behavior of the switch may lead to design- or operational improvements that yield a more reliable switch. First the bi-stable MEMS switch is explained and parameters are defined. A numerical method to model the dynamics is described. The resonance- and bouncing- measurement setup and theoretical expectation are given. Results of simulations and measurements are presented followed by the conclusions.

5.2.1 Bi-stable MEMS switch

Design and packaging of the bi-stable MEMS switch has been described in chapter 3 and 4 respectively. Those parts that are needed to explain the measurement results in the next section are repeated here, complemented with additional new theory. The principle of operation is shown in Figure 5.1. Parameters are defined in Figure 5.2.

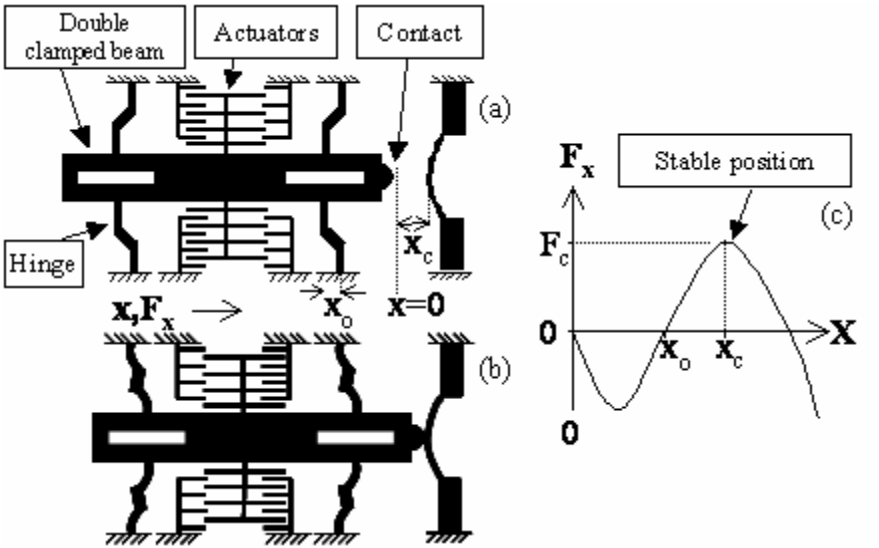

Figure 5.1. Schematic of the bi-stable switch, not on scale, shown in OFF position (a) and ON position (b). x is the displacement of the moving parts, were x=0 is defined at the initial position of the central beam (as fabricated). Fx is the mechanical force exerted on the central beam by the double clamped beam and the hinges, which is plotted as a function of displacement in (c). Bi-stable behavior is generated by the double clamped beam and hinges. x0 is an offset distance and xc is the contact distance. The central beam can be moved in positive and negative x-direction by the electrostatic comb actuators. In the ON state the central beam is moved to the right to contact the opposing contact member. When the beam is displaced from its initial stable position (OFF state) in the positive x-direction the force becomes negative, meaning it is opposing the motion. At the offset position x0 the force changes direction and is now promoting further motion. The fixed contact member is placed at position xc. for maximum contact force (Fc) (stable ON state).

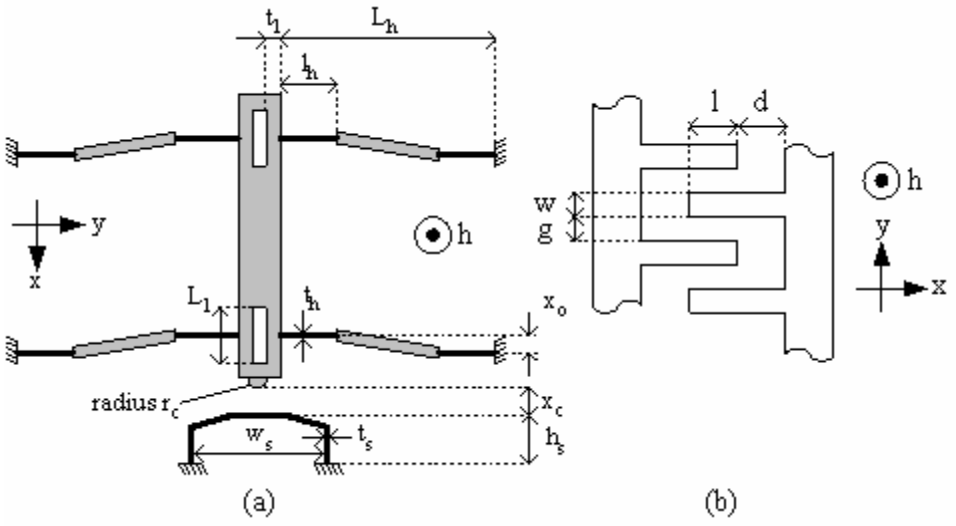

Figure 5.2. (a) Mechanical spring system in initial position (as fabricated). tl is the thickness and Ll is the length of the double clamped beam. th is the thickness, lh is the length and Lh is the arm length of the hinges. xo is the offset and xc is the contact position. ts is the thickness, ws is the width and hs the length of the contact spring. The moving contact member contains a bump with radius rc. The complete structure has a height h. Actuators (not shown) are positioned as shown in figure 1. (b). Top view of electrostatic comb fingers. w is the width of the fingers, g is the gap between the fingers, l is the overlap of the fingers, d is the tip to comb base distance and h is the height of the structure (l and d as fabricated). The left part moves towards the mechanically fixed right part.

The capacitance C between the two parts of the actuator as a function of displacement *x* is given by [14]

$$C = 2N\varepsilon\left(\frac{wh}{d-x} + \frac{(l+x)h}{g}\right) \quad (5.1)$$

with N the number of moving comb fingers and ε the permittivity of the medium between the combs. The first term is

the tip to base contribution (C_t) and the second term is the side-to-side contribution (C_s).

The attractive force F_x between the two parts of the actuator in x direction is given by [14]

$$F_x = N\varepsilon V^2 \left(\frac{wh}{(d-x)^2} + \frac{h}{g}\right). \quad (5.2)$$

Total force exerted by the hinges and double clamped beams on the central movable beam (figure 5.2 (a)) as a function of displacement is given by [15]

$$F_{springs} = -k_h x + \frac{x - x_o}{L_h} k_l \left(\sqrt{x_o^2 + L_h^2} - \sqrt{(x_o - x)^2 + L_h^2}\right) \quad (5.3)$$

with k_h, k_l respectively the spring constant of the four hinges and the four double clamped beams given by

$$k_h = 2\frac{Eht_h^3}{4l_h^3 - 6l_h^2 L_h + 3l_h L_h^2} \quad (5.4)$$

$$k_l = 4\frac{16Eht_l^3}{L_l^3} \quad (5.5)$$

with E the Youngs modulus of the material.

Newton's law of inertia gives the differential equation for the displacement as a function of time

$$m\frac{d^2x}{dt^2} = F_x(V,t) - c\frac{dx}{dt} + F_s(x) + F_{cs}(x) \quad (5.6)$$

with m the mass of the structure given by

$$m = Ah\rho \qquad (5.7)$$

with A the total area of the moving parts and ρ the density of the material. The mass of the metal layer on top of the silicon should also be taken into account. c is a friction coefficient given by [15]

$$c = \mu \frac{A_c}{d_c} \qquad (5.8)$$

in which μ is the absolute viscosity of the medium between the combs, A_c is the total sliding surface area and d_c is the gap between the sliding surfaces.

$F_{cs}(x)$ is the contact and sticking force.

5.2.2 Resonance

When an ac voltage is applied to the electrostatic actuators we expect to excite the movable portion of the structure and a corresponding change in capacitance. The current through a capacitor is given by

$$I = \frac{dQ}{dt} = \frac{d(CV)}{dt} \qquad (5.9)$$

therefore we expect a dC/dt.V component in the current, which gives information about the movement of the structure. The current is transformed into a voltage by a resistor and measured with a Lock In amplifier [16]. The power of the Lock In is that it demodulates the signal and only looks at the DC component with the use of a narrow bandwidth low pass filter. The demodulation

can be set to any desired harmonic of the reference frequency. The measurement setup is described in Figure 5.3. Parasitic effects will be discussed in the results section.

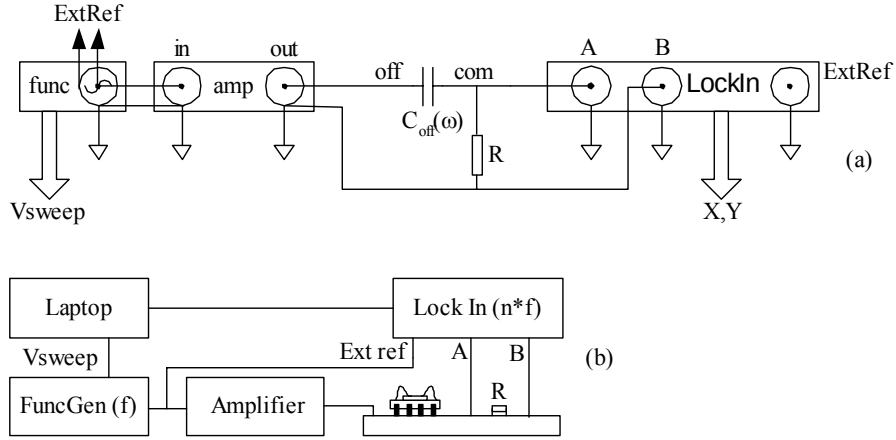

Figure 5.3. (a) Ideal electrical equivalent of the measurement setup used for resonance measurements. The function generator sweeps the frequency of an ac voltage which is supplied to the electrostatic actuator ($C_{off}(\omega)$) after amplification. The current is transformed to a voltage by the resistor R and measured differentially by the Lock In amplifier. The Lock In is set to measure the in- and out of phase component of the current (X and Y) at a specific multiple of the reference frequency supplied by the function generator (ExtRef). A laptop equipped with data acquisition card (NI-DAQ) records X, Y and Vsweep which is proportional to the frequency. (b) Schematic representation of the actual physical setup.

The ac voltage (after amplification) imposed on the off actuator is defined as

$$\mathbf{V} = Ve^{i\omega t} \qquad (5.10)$$

The resulting current after some rearrangement is

$$\mathbf{I} = \frac{\mathbf{V}}{\mathbf{Z}} = \frac{i\omega C_{off}(\omega)\mathbf{V}}{1 + i\omega R C_{off}(\omega)} \qquad (5.11)$$

with

$$C_{off}(\omega) = C_{off,0} + \mathbf{C}_{\omega} \qquad (5.12)$$

and

$$\mathbf{C}_{\omega} = \frac{2N\varepsilon h}{g}\mathbf{X}_{\omega} = c_x \mathbf{X}_{\omega} \qquad (5.13)$$

where $\mathbf{X}_{\omega}$ is the solution of (5.6) and $C_{off,0}$ is the initial as fabricated capacitance of the OFF actuator. Further calculations involving the influence of the parasitics is done in the results section.

5.2.3 Bouncing

The measurement setup for observing contact bouncing has been described in chapter 3. Another setup that was used is shown in Figure 5.4 Measurement setup for contact dynamics. The function generator provides a pulse on a manual trigger. The oscilloscope captures this in single shot mode. The resistors on the actuation side are optional..

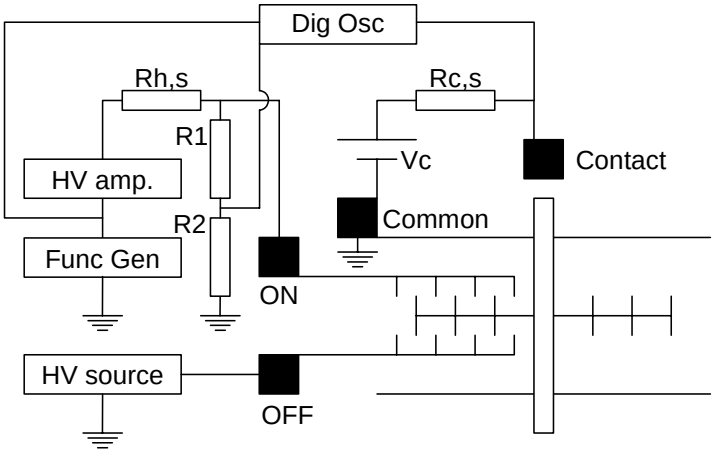

Figure 5.4 Measurement setup for contact dynamics. The function generator provides a pulse on a manual trigger. The oscilloscope captures this in single shot mode. The resistors on the actuation side are optional.

5.2.4 Numerical Simulation

For comparison with theory the dynamics equation (5.6) is numerically solved using a variable time- and displacement step. The contact is modeled as a linear spring with spring constant k_c resulting in a contact force

$$F_c = -k_c(x_t - x_c) \qquad (5.14)$$

with x_t the displacement at time t. Each time the movable part makes first contact with the fixed contact member the total energy of the system (kinetic and spring) is reduced with an amount that is a factor e of the total. When the contact members are in contact and x_t becomes smaller then x_c a sticking force is added to the equation. This sticking force is equal an opposed to the contact force until a certain maximum sticking force, after

which the contact members are released and the fixed contact member is reset to the initial position.

The structure of the program is as follows.

1)Initial Conditions

Time window, nominal time step, maximum displacement, start position of switch, variables to store, mass of moving part, constant multiplier to arrive at electrical force as function of voltage, mechanical spring force as function of displacement, contact position and contact spring constant

2)Calculate forces on moving structure at time t

The electrostatic force Fe is provided by defining a voltage as a function of time (various scenarios). The contact force Fc and related contact phenomena are calculated. The maximum sticking force Fstick is defined. Energy loss due to non elastic collision is defined (e). The voltage over the contact is calculated to be able to simulate an observable property. Four different regimes of switch movement are distinguished. 1)first time the contact is closing, 2)the contact is opening and might be sticking, 3)the contact is closing and has not touched yet, 4)the contact is closing while sticking. The damping force Fd is calculated with the damping coefficient c and the mechanical force Fm is taken from the (bi-stable) force displacement relationship. Finally the total force Ft on the moving structure is calculated by summing all forces and this is translated in the acceleration at = Ft/m.

3)The values are stored the next time step is determined and the new values at that time step are calculated. The initial assumption is that the time step is dt, unless the structure displaces more then dx. In this case the time step is decreased until the displacement is equal to dx. If the structure approaches the contact within 1um, the resolution in displacement is increased to 0.1um, if within 0.1um it is increased to 0.01um and if within 0.01um it is increase to 0.001um (1nm). The new values are t = t+tstep (new time for coming calculation), xt = xt + tstep*vt (position at new time, based on velocity and position at

old time) and vt = vt + tstep*at (velocity at new time, based on velocity and acceleration at old time). Note that the new acceleration will be calculated in the loop based on the new position and time. Step 2) and 3) are done inside a loop until the specified end time is reached.

4)Plot results

5.3 Results

Two sizes of bi stable switches have been fabricated, “small” and “large”. Typical parameter values are given in Table 5.1.

Table 5.1 Parameter values for large and small bi stable switches (parameters as defined in Figure 5.2)

Parameter	Description	Large	Small	Unit
l	Overlap of comb finger	20	20	μm
w	Width of comb finger	4	4	μm
g	Gap between comb fingers	5	3	μm
d	Tip-base distance combs	15	15	μm
h	Height of combs	80	80	μm
L_h	Total arm length of hinges	500	300	μm
l_h	Length of hinges	100	100	μm
t_h	Thickness of hinges	4	4	μm
t_l	Thickness double clamped beam	11	9	μm
L_l	Length double clamped beam	180	120	μm
x_0	Offset	8	5	μm
x_c	Contact position	10	10	μm
N	Number of moving fingers	300	40	#

5.3.1 Resonance

First the parasitic effects of the experimental setup shown in Figure 5.3 will be discussed. Both inputs to the Lock In form a very large impedance in parallel to the impedance that is being measured, so both inputs will see the correct voltage. Likewise the cable from the source has a low series resistance and a large parallel resistance compared to the impedance to be measured so it is supplied with the intended voltage. The parasitics of the measurement resistor are neglectable. The only important factor is the capacitance of the package Cp that holds the MEMS switch which is in parallel to the capacitance Coff to be measured. The measurement resistance R is much smaller then the impedance of Coff//Cp or Cp alone (empty package). This means that the

voltage over Coff/Cp is almost the same as over Cp alone. Therefore the empty package current can be subtracted from the total current with component to arrive at the current through Coff (or any other component in the package). This is of course only true if both measurements are repeated under the same conditions. This gives an error of approximately 0.01% and this method will be used for the remainder of this chapter. With this method an empty socket capacitance of 1.4pF is found, and a capacitance of 6.7pF for a capacitor with capacitance of 6.8pF (measured with HP LCR meter).

The parasitics in the MEMS switch itself are illustrated in Figure 5.5. The parasitic capacitance values are estimated using a parallel plate approximation of the opposing surfaces of the two parts. The parasitic capacitance in the device layer excludes the intentional (non parasitic) capacitance of the comb actuators. In our case the OFF capacitance is measured, all other pads are grounded and the substrate is floating. The result is that a 3.8pF parasitic capacitance parallel to the capacitance to be measured needs to be taken into account.

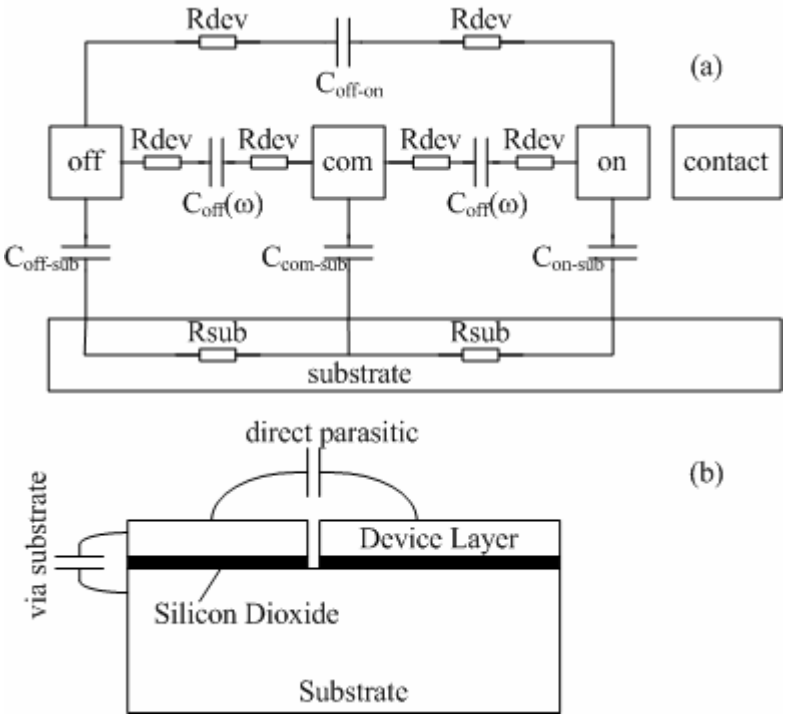

Figure 5.5. (a) Parasitic capacitances on the MEMS switch. Parasitic capacitances arising from the package are not shown. (b) Visual representation of type of parasitics.

With these parasitics the ideal circuit (Figure 5.3) is still true and equation 5.11 for the current can still be used if Cp is added to $C_{off}(\omega)$ and we remember that $C_{off,0}$ (equation 5.12) includes a parasitic capacitance as quantified above. Now the expression for the current will be written in terms of powers of $e^{i\omega t}$ in order to compare with the measured value of the Lock In at multiples of ω. The enumerator of equation 5.11 can be expanded in a Taylor series around zero since $\omega R(C_p+C_{off}(\omega))<1e\text{-}3<<1$. This gives:

$$\mathbf{I} = i\omega(C_p + C_{off,0} + \mathbf{C}_\omega)(1 - i\omega R(C_p + C_{off,0}) - i\omega R\mathbf{C}_\omega)\mathbf{V} \quad (5.15)$$

$\mathbf{C}_\omega$ (equation 5.13) provides the link to the switch dynamics (equation 5.6) if the solution $\mathbf{X}_\omega$.is known. An analytical solution is found making the following approximations:

1) Small displacements around the OFF position (x=0)

1.1) Discard the contact and sticking force term (F_{cs} in equation 5.6).

1.2) Expand the mechanical force $F_{springs}$ (equation 5.3) in a Taylor series around x=0 and discard all second order and higher order terms. We arrive at $F_{springs}(x)=-k*x+O(x^2)$

$$k = k_h + \frac{k_l x_o^{\,2}}{L_h \sqrt{x_o^{\,2} + L_h^{\,2}}} \qquad (5.16)$$

2) Discard the tip to base capacitance contribution (first term in equation 5.2). This makes it possible to write $F_x(V,t) = c_v*V^2$, independent of displacement x with $c_v=N\varepsilon h/g$. Note that due to the current to voltage converting resistor R, the amplitude of the ac voltage over the actuators is not exactly equal to V, but is a function of ω. To be exact, it is

$$V(\omega) = \frac{V}{1 + i\omega R(C_p + C_{off,0})} \qquad (5.17)$$

However, the term in the enumerator is approximately equal to 1 (see above), so V(ω)=V is assumed.

With these approximations equation 5.6 reduces to

$$m\frac{d^2x}{dt^2} = c_v V^2 e^{i2\omega t} - c\frac{dx}{dt} - kx \qquad (5.18)$$

Note that the frequency of the electrical force is doubled with respect to the imposed frequency of the voltage. If we write

$$\mathbf{X}_{\omega} = X(\omega)e^{i(2\omega t+\varphi(\omega))} \qquad (5.19)$$

the solution for X(ω) and φ(ω) is

$$\varphi(\omega) = \arctan\left(\frac{2\omega c}{4m\omega^2 - k}\right)$$
$$X(\omega) = \frac{c_v V^2}{(k - 4m\omega^2)\cos\varphi - 2\omega c \sin\varphi} \qquad (5.20)$$

with resonance at $2\omega=2\omega_0=\sqrt{k/m}$.

Supplementing equation 5.20 in equation 5.13 and equation 5.15, after rearranging and again approximating a (1+ωRC) term by 1 the following theoretical expectation for the current in the first three harmonics is found

$$i\omega(C_p + C_{off,0})V \qquad \text{First harmonic (5.21)}$$

No current in second harmonic

$$i\omega V c_x X(\omega)e^{i\varphi(\omega)} \qquad \text{Third harmonic (5.22)}$$

The first harmonic contains information about the initial capacitance and the third harmonic contains information about the resonance of the movable structure.

The resonance frequency is first determined optically under a microscope (see chapter 3). Then the start- and stop frequency of the sweep can be determined. Next the sweep time, number of steps and time constant of the Lock In need to be chosen. A trade off between measurement time and signal to noise ratio needs to be found. The sweep time and number of steps gives the time per step. The start- and stop frequency and the number of steps determine how much the frequency changes per step. At each new step the Lock In needs to make a transition to a new output value. The time it takes to reach 90% of final output after a step input (the waiting time) is given by a multiple of the time constant. The waiting time must be smaller then the step time, so this determines an upper limit on the time constant. On the other hand, the time constant is inversely proportional to the bandwidth of the low pass filter. That means the higher the time constant the lower the noise. For our situation it was found that 100 sec sweep time, 2048 points and 10 ms time constant gave satisfying results. This sweep time is low enough that it could for example be used in manufacturing for control purposes.

Data are acquired at 1 kHz and imported into Matlab. The measured voltage is calculated from the Lock In output using offset, expansion and sensitivity settings. The samples in one frequency step are averaged and in addition, the data are moving averaged over a 40Hz frequency range.

The OFF actuator capacitance Coff,0 for a small switch based on measurement of the current in the first harmonic is 3.3pF (corrected for 3.8pF MEMS parasitic and 1.8pF empty package parasitic) to be compared with theoretically expected 3.1pF. A comparison of the measured current in the third harmonic with the theoretically expected current for a large bi stable switch is given in Figure 5.6.

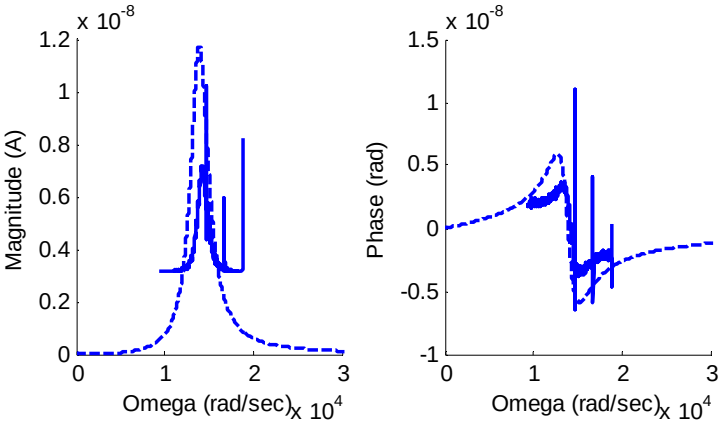

Figure 5.6 Magnitude (in A, left graph) and phase (in rad, right graph) of the third harmonic of the current as a function of ω (rad/sec) for a large bi stable switch. The solid line is the measured data, the dotted line is the theoretical expectation. The theoretical expected value is calculated using the equation for X(ω) and φ(ω) in the mechanical domain and the link to the electrical domain via C(ω) as described in detail above. Note that the theoretically expected spring constant and damping coefficient have been adapted with a factor of 0.68 and 50 respectively in order to shift the position and width of the resonance peak respectively.

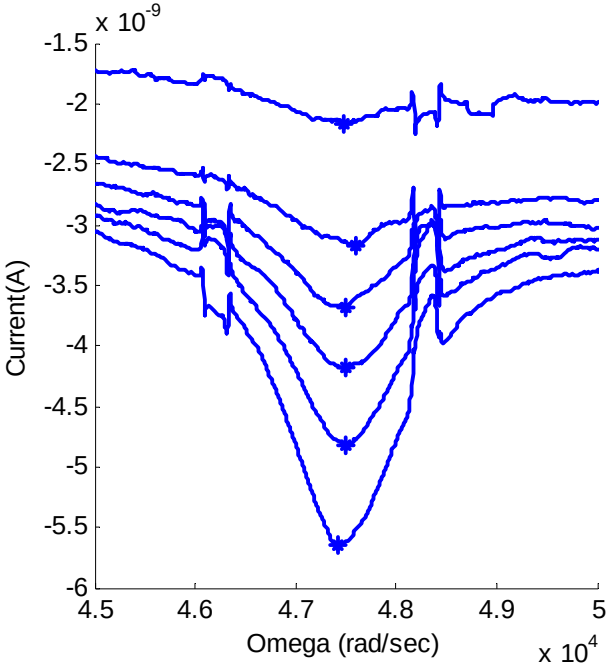

Figure 5.7 Measured in phase component of the current in the third harmonic (in A) as function of omega (rad/sec) for a single small bi-stable switch for various amplitudes of ac excitation voltage. The Vrms amplitude of the excitation voltages are 14.2, 12.7, 11.3, 9.86, 8.44 and 7.03 from bottom to top. The markers indicate the frequency at the minimum current. This frequency changes less then 1% as a function of excitation amplitude.

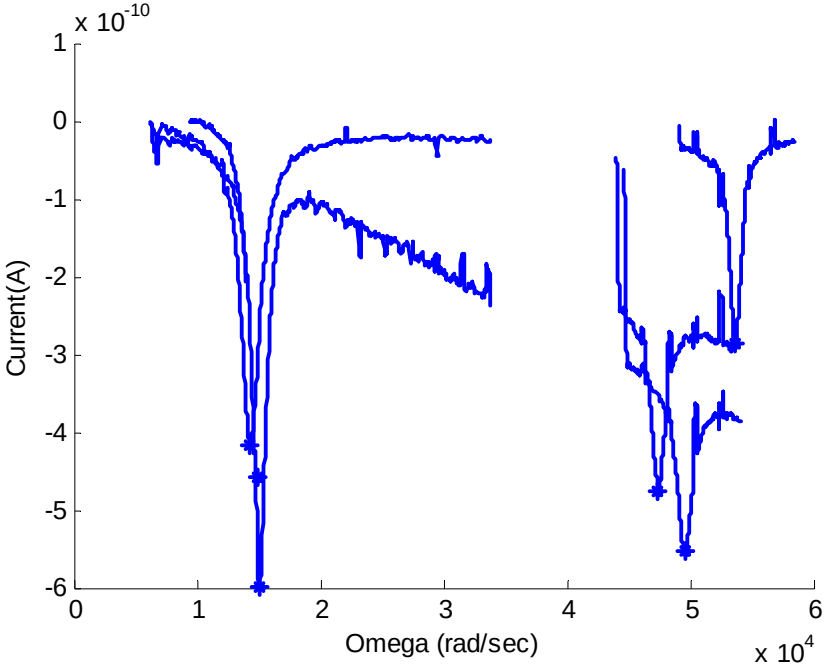

Figure 5.8 Measured in phase component of the current in the third harmonic (in A) as function of omega (rad/sec) for three different large- and small- bi-stable switches. The markers indicate the frequency at the minimum current. Note the small switches show larger deviation in resonance frequency.

Table 5.2 Comparison between the resonance frequency (ω) as determined from the measurements as shown in Figure 5.8 and the actuation voltage (Va) as measured electrically with optical view on the switch. The ratio of the actuation voltage and the resonance frequency is 22.7±0.3 V/10^4rad/s.

Switch	ω(rad/sec)	Va (V)
S1	4.7406e+004	105.8±0.2
S2	5.3606e+004	122.6±0.1
S3	4.9567e+004	110.9±0.1
B1	1.4318e+004	32.4±0.2
B2	1.5037e+004	34.2±0.1
B4	1.4897e+004	34.5±0.3

5.3.2 Bouncing

Measured and simulated bouncing behavior is shown in Figure 5.9.

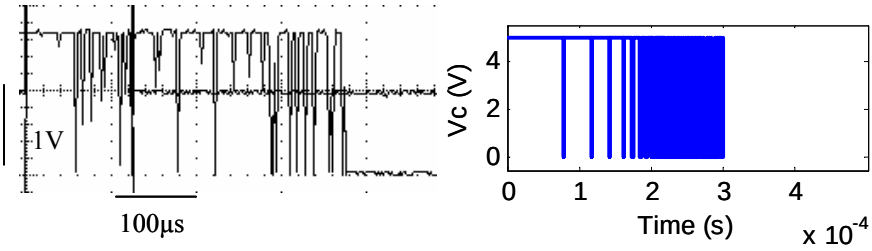

Figure 5.9 Part of a scope screenshot (left) and simulation (right) of the contact voltage (vertical axis in V) as a function of time (horizontal axis). The contact voltage is high in open position and low in closed position. The switch is initially in open position and is actuated with a 250µs voltage pulse starting at t=0. The contact bounces and then closes.

The measurement and simulations are performed as described in section 5.2.3 and 5.2.4. The spring constant k_c was calculated using finite element analysis (pro Engineer) to be 38461 N/m. A sticking force of maximal 15 µN is used based on previous measurements (see chapter 3). All other values used in the simulation are calculated using the theory described in section 5.2.

5.4 Discussion

The dynamical response of the switch to actuation pulses of different widths is shown in Figure 5.10.

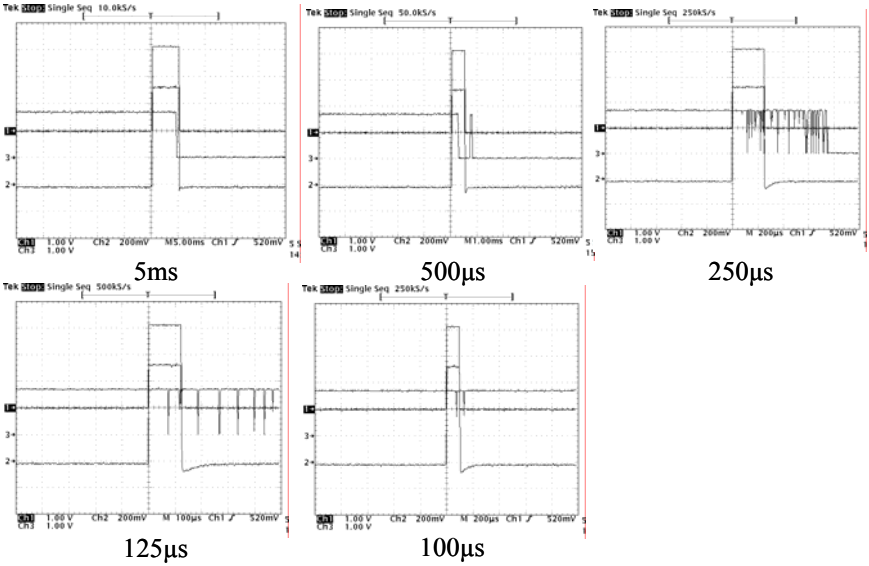

Figure 5.10 Measured switching behavior from OFF to ON for actuation pulse with constant amplitude and different pulse length. The square pulses are a measure for the actuation pulse (pulse width given in text below each graph). The contact voltage indicates the switch response and is the trace that changes from high to low voltage (if the switch closes). Starting from the upper left corner, the observed behavior is switching (5ms pulse) via bouncing (250µs) to barely switching (125µs) and not switching at all (100µs).

The voltage needed to close the switch is not significantly influenced by the pulse width of the actuation pulse over the range as given above. The actuation force is proportional to the square of the voltage and always attractive. If the frequency is high enough it is seen as an effective constant force, which is demonstrated in (Figure 5.11).

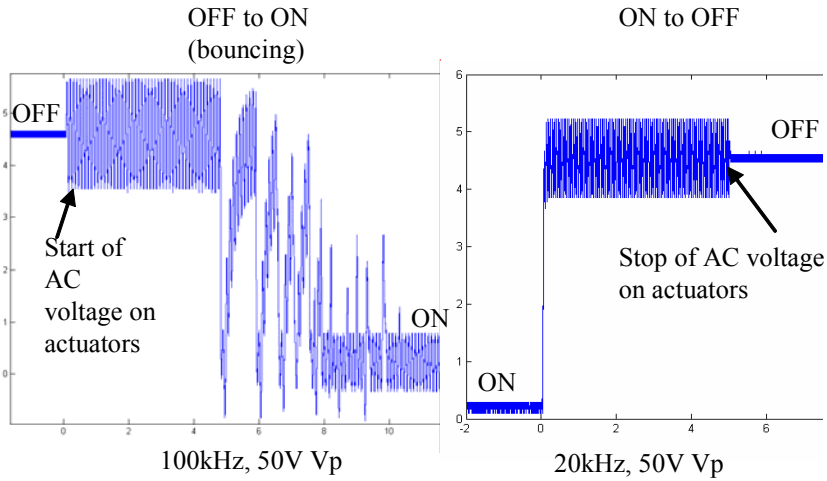

Figure 5.11 Closing (left) and opening (right) of the switch using an ac actuation voltage.

MEMS test, measurement and simulation are active research fields and some work relates to the material presented in this chapter [17,18,19,20,21,22,23,24].

5.5 Conclusion

Reliability theory provides a quantitative basis that enables experimental planning, accelerated testing, lifetime predictions including confidence intervals, and design for reliability. Typical Active Implantable Medical Device Essential Requirements are protection against defibrillation and Magnetic Resonance Imaging (MRI) and electrical surgery compatibility. MEMS reliability is different from IC reliability for a variety of reasons, like the diversity in processes and functions, the lack of large sample sizes and test data and the unknown character of some failure mechanisms. Nevertheless carefully designed MEMS can be highly reliable and good design practices and guidelines have been proposed. Reliability tools like Computer Assisted Design

and Design for Test are progressing. A large range of possible failure mechanisms has been formulated for the MEMS switch, including mechanical, electrical, material, processing and other type of failure mechanisms.

The theory of the dynamics of the MEMS switch has been given. An experimental and theoretical method to describe resonance and bouncing behavior is given. Measurements of resonance peaks not only provide the location of the resonance frequency, but also provide a measure for the degree damping of the structure. The electrical method that is described in this chapter is applicable for automated reliability screening during manufacturing. A 125μs pulse is sufficient to switch from OFF to ON state. The required pulse amplitude is not influenced by the pulse width.

5.6 References

[1] Sze, S M 1988 *VLSI technology* ed Sze, S M Boston McGrawHill 0-07-062735-5

[2] Amerasekera, E A and Campbell, D S 1987 *Failure Mechanisms in Semiconductor Devices* New York John Wiley & Sons 0 471 91434 7

[3] Tobias, P A and Trindade, D C 1995 *Applied Reliability* Chapman & Hall / CRC 0442004699

[4] Shea, H R 2006 Reliability of MEMS for space applications *Proceedings of SPIE - The International Society for Optical Engineering* vol 6111 San Jose, CA, United States International Society for Optical Engineering, Bellingham WA, WA 98227-0010, United States pp 61110

[5] Tai-Ran, H 2006 Reliability in MEMS packaging *2006 IEEE International Reliability Physics Symposium proceedings. 44th Annual* San Jose, CA, USA IEEE pp 5

[6] Stark, B 1999 *MEMS Reliability Assurance Guidelines for Space Applications* ed Stark, B Pasadena, California

National Aeronautics and Space Administration; Jet Propulsion Laboratory California Institute of Technology JPL Publication 99-1

[7] Gad-el-Hak, M 2002 *The MEMS Handbook* ed Gad-el-Hak, M London CRC Press 0-8493-0077-0

[8] Madou, M 1997 *Fundamentals of microfabrication* New York, United States CRC Press LLC 0-8493-9451-1

[9] Maluf, N 2000 *An introduction to microelectromechanical systems engineering* Boston, United States Artech House Inc. 0-89006-581-0

[10] Kovacs, G 1998 *Micromachined Transducers Sourcebook* WCB/McGraw-Hill 0-07-290722-3

[11] Patton, S T and Zabinski, J S 2005 Fundamental studies of Au contacts in MEMS RF switches *Tribology Letters* **18** 215-230

[12] Kwon, H, Choi, D-J, Park, J-H, Lee, H-C, Park, Y-H, Kim, Y-D, Nam, H-J, Joo, Y-C, and Bu, J-U 2007 Contact materials and reliability for high power RF-MEMS switches *IEEE International Conference on Micro Electro Mechanical Systems* IEEE pp 231-234

[13] DeNatale, J and Mihailovich, R 2003 RF MEMS reliability *TRANSDUCERS '03. 12th International Conference on Solid-State Sensors, Actuators and Microsystems. Digest of Technical Papers (Cat. No.03TH8664)* vol vol.2 Boston, MA, USA IEEE pp 943-946

[14] Marxer, C 1997 *Silicon Micromechanics for Applications in Fiber Optic Communication* University of Neuchatel

[15] Marxer, C and Roth, S 2000 *Design Summary Latching Mechanism* Neuchatel Institute of Microtechnology, University of Neuchatel

[16] Fromel, J, Wiemer, M, and Gessner, T 2005 Packaging of MEMS structures in SCREAM technology using anodic bonding *Micro System Technologies* Poing (DE) Franzis Verlag GmbH pp 99-104

[17] Qiu, J, Lang, J H, and Slocum, A H 2004 A curved-beam bistable mechanism *Microelectromechanical Systems, Journal of* **13** 137-146
[18] Junseok, C, Kulah, H, and Najafi, K 2004 An in-plane high-sensitivity, low-noise micro-g silicon accelerometer with CMOS readout circuitry *Microelectromechanical Systems, Journal of* **13** 628-635
[19] Sulfridge, M, Saif, T, Miller, N, and Meinhart, M 2004 Nonlinear dynamic study of a bistable MEMS: model and experiment *Microelectromechanical Systems, Journal of* **13** 725-731
[20] De, S K and Aluru, N R 2004 Full-Lagrangian schemes for dynamic analysis of electrostatic MEMS *Microelectromechanical Systems, Journal of* **13** 737-758
[21] Nieminen, H, Hyyrylainen, J, Veijola, T, Ryhanen, T, and Ermolov, V 2005 Transient capacitance measurement of MEM capacitor *Sensors and Actuators A: Physical* **117** 267-272
[22] Lai, W P and Fang, W 2005 Determining the in-plane and out-of-plane dynamic response of microstructures using pulsed dual-mode ultrasonic array transducers *Sensors and Actuators A: Physical* **117** 186-193
[23] Steeneken, P G, Rijks, T, van Beek, J T M, Ulenaers, M J E, De Coster, J, and Puers, R 2005 Dynamics and squeeze film gas damping of a capacitive RF MEMS switch *Journal of Micromechanics and Microengineering* **15** 176-184
[24] Cagdaser, B and Boser, B E 2005 Resonant drive: Sense and high voltage electrostatic drive using single mems capacitor and low voltage electronics *Proceedings of the IEEE International Conference on Micro Electro Mechanical Systems (MEMS)* Miami Beach, FL, United States Institute of Electrical and Electronics Engineers Inc., Piscataway, NJ 08855-1331, United States pp 142-146

6 Discussion and Outlook of the Bi-Stable MEMS switch

In this chapter the most important bi-stable MEMS switch properties will be recapitalized, an outlook on the topic of controlling MEMS is provided and system level aspects are discussed.

6.1 MEMS switch versus FET

Some specific properties of bi-stable MEMS switches generally are considered as advantages in comparison to FET switch specifications. In this section these properties are reviewed, namely power consumption, DC breakdown, ESD sensitivity and leakage current. Some attention will be given to system level aspects when comparing specifications

6.1.1 Power consumption

The bi stable MEMS switch needs approximately 0.2nJ to change state, compared to 25nJ for a FET. In a fixed state, the bi-stable switch does not consume power while a FET switch needs approximately 2µW. It is interesting to compare the current drain per stim pulse of the two implementations of this concept (with bi-stable MEMS or with FET) at system level. The FET solution needs to be powered all the time to keep the switch state. The current drain to drive the cable capacitance (assumed 1000pF)is a factor of 30 larger then the current required to drive the FET chip itself (3nA). Assuming a 10V stimulation amplitude in a stimulation load impedance of 500Ω with a pulse width of 10ms this can be seen as a 5% overhead on the stimulation current. The lifetime of an implantable device with FET-programmable

electrodes could be increased with 5% by using bi-stable MEMS switches. The number of stim pulses between state changes of the bi-stable switch needs to exceed only 300 pulses to cross the 5% level (bi-stable switching energy as percentage of energy in stim pulses). Since this is a comparison between two non existing technologies and it depends on assumptions this number should be interpreted as a first estimate of the order of magnitude. Even though the energy savings are not enormous they are interesting for implantable devices.

6.1.2 DC Breakdown

Breakdown could occur through the silicon dioxide between SOI device- and handle layer or through the gaps between the structures in the SOI device layer. A literature value for the breakdown of silicon dioxide is 10e7 V/cm [1], a typical oxide thickness is 2µm, so the theoretically expected breakdown voltage is 2000V. The breakdown through an airgap is described by the Paschen curve and for gaps smaller then 4µm by a modified Paschen curve [2]. For an airgap of 11µm filled with air at 1bar pressure the breakdown voltage is approximately 330V. The breakdown between the drain and the source of a FET is in the order of 5 to 20V [1].

6.1.3 Electrostatic Discharge (ESD)

Voltages in the range of 100V to 20kV can exist on materials due to static electrical charges. This voltage may be discharged through oxide breakdown, junction short circuits or cracks between isolation regions. Low voltage electrostatic pulses can damage gate oxides without causing complete breakdown. Non damaging voltage pulse can cause micro cracks that are a reliability hazard. Unprotected MOS components are classified as Class 1 ESD sensitivity (0-1kV) [3].

It can be expected that electrostatic MEMS are sensitive to ESD. A standard for ESD sensitivity testing exists (JEDEC

STANDARD Electrostatic Discharge (ESD) Sensitivity Testing Human Body Model (HBM) JESD22-A114-B. The electrostatic discharge pulses specified in this standard can be generated with special equipment (ESD simulator, NSG 435, Schaffner). Due to the small size of the MEMS device under test special test fixtures are needed to be able to impose this pulse on the MEMS. At this moment it is estimated that the MEMS switch belongs to the same Class 1 as the FET in terms of ESD sensitivity.

6.1.4 Leakage current

The leakage current is the direct current between the two contact members in open state. For the bi-stable MEMS switch no direct current can flow through the air gap between the two contacts (except breakdown current, see above). Current can flow from one contact member through the silicon oxide to the handle layer and back through the oxide to the other contact member. The direct current resistivity of silicon dioxide at 25°C is $1x10^{12}\Omega m$ [1]. Together with pad areas of $8.6x10^{-8}m^2$ and $7.0x10^{-7}m^2$ for the two contact members and an oxide layer of 2μm this gives a total resistance of $2.6x10^{13}\Omega$.

The leakage current through a FET switch is the drain source current with the FET in off state. This can be approximated by the reverse bias current of a diode. The current becomes more or less independent of the voltage for qV/kT=2, corresponding to approximately 0.6V (q is the electron charge, k is Boltzmann constant and T is the temperature). The leakage current of a diode with $2.5x10^{15}cm^{-3}$ doping at 20°C is approximately $7x10^{-10}A$ [1]. For comparison, at a voltage of 0.6V the leakage current through the MEMS switch is $2.3x10^{-14}A$.

6.1.5 MEMS switch vs. FET switch

The MEMS and FET switch properties discussed in the above are summarized in Table 6.1. Size and contact resistance have been added to this table.

Table 6.1 FET- and MEMS switch properties. *Through the air gap, the oxide breakdown is 2000V.

	FET	MEMS	Unit
Power in ON or OFF	2	0	µW
DC Breakdown	5-20	330*	V
ESD	0-1	0-1	kV
Ileakage	$7x10^{-10}$	$2x10^{-14}$	A
Size	550x275	637x550	µmxµm
Contact resistance	20	5	Ω

The MEMS switch retains its setting in the absence of power and therefore, would be safer. The increased lifetime due to lower power consumption is important for implantable devices that cannot be recharged. The lower contact resistance of the MEMS switch leads to additional energy savings. The MEMS switch has a higher break down voltage which corresponds to better intrinsic protection of the switch against high voltages. The MEMS size, although larger then the FET, is within the requirements.

6.1.6 Recommendations

The bi-stable MEMS switch as benchmarked in the previous sections versus a FET switch could be further improved. The size could be further reduced by increasing the actuation voltage (see also next section on MEMS control). Increased isolation resistance would be possible by working with “Silicon On Anything” and selecting a good insulator as the substrate. The breakdown voltage between open contacts could be increased by increasing the distance between contact members. This results in a larger force that has to be overcome (if the rest of the switch is kept constant). Combined with a higher actuation voltage this would be possible. Ruthenium, Rhodium and Gold/Nickel are contact metals that are generally used for micro contacts. Which one functions best can only be determined experimentally for this particular design. The

design can then be improved by eliminating experimentally identified failure mechanisms.

6.2 MEMS control

Small size is an important device metric, required to be able to reach small veins and more in general to minimize the foreign body impact. Consequently we have made the bi stable MEMS switch as small as possible, while still having a reliable contact behavior. Apart from the choice of contact metal and contact topology, the micro contact reliability is determined by the contact force, which is directly related to the switching force in our design. The smaller the structure, the smaller the area available for the electrostatic actuators and hence the larger the voltage must be in order to generate the required switching force. This leads to a required actuation voltage in the order of 150V to 200V. There is a need for a system to control the state of the bi stable electrostatic MEMS switch and a means to generate the actuation voltage from a lower supply voltage. It can be stated that this need is in general true for (electrostatic) MEMS devices. It is clear that small size is also an important requirement for such a system, not only for implantable applications, but for many other applications as well. The availability of Small Smart Modules will increase the ease of applicability of MEMS components and are of great interest to the MEMS community. This section will provide and outlook on ways to interconnect MEMS with an IC and ways to generate high voltage in various levels of integration.

6.2.1 MEMS IC interconnect

One of the main aspects of incorporating a MEMS component into a smart module is connecting the MEMS to an integrated circuit and possibly some discrete components. The end user of the smart module interfaces with this multi component (sub)

system at an application oriented level and does not need to be concerned with MEMS component level details. The outlook on MEMS IC interconnect is split in three conceptually different classes: first a separate MEMS die and IC next to each other, second a separate MEMS die and IC stacked on top of each other and three MEMS-IC integration.

6.2.1.1 MEMS next to IC

A typical smart module has electrical interconnects to the outside and internal electrical interconnects between MEMS and IC. Movable MEMS structures are protected from damage and dust by a seal. A hermetic seal is required when a controlled and stable environment is necessary for functional reasons. In that case it should be possible to electrically connect structures inside the MEMS package without disturbing the long-term stability of the environment created inside the cavity. The various options for creating a hermetic seal and feedthroughs have been reviewed earlier [4]. Briefly, the hermetic seal can be made by direct bonding, anodic bonding, bonding using an intermediate layer and thin film encapsulation. The feedthroughs can be “Under the lid”, extending out of the package in lateral direction in the plane of the substrate and lid or “Through the lid”, extending out of the package in vertical direction, perpendicular to the plane of the substrate and lid. For the “MEMS next to IC” concept the MEMS die and IC are placed next to each other on an interconnection substrate to which each of the chips is interconnected individually. This can for example be done on a hybrid circuit substrate[5]. Wirebonding and injection molding in lead-frame based packages of thin film encapsulated MEMS has been reported in [6].

6.2.1.2 MEMS – IC stacking

To save area but still keep separate processes for functionally different parts, the MEMS die and IC can also be stacked in the

third dimension. A small hermetically sealed MEMS die with feedthroughs like described above could be placed on top of a larger IC and electrically interconnected to it by conventional wirebonding. If the IC is smaller then the MEMS die the order of stacking can be reversed. If both parts have comparable area, space can be saved by having surface array interconnects between the two. One extreme case is described in [7] in which the MEMS structures are electrically interconnected and transferred to the IC by using an intermediate carrier substrates, a dissolved wafer like approach and a self aligned interconnection system that is robust for differences in height.

There are some examples of MEMS structures that are hermetically sealed with a silicon wafer. If the sealing process is CMOS compatible and there exists a way to make electrical interconnects between lid and MEMS inside the cavity at the same time, an IC could be used as the lid. Sealing and electrical interconnection at the same time have been demonstrated using the same metal as is used for the sealing [8,9,10] and with the use of mechanical press contacts between metallization on the lid and substrate[11,12,13].

IC stacking and wirebonding is common practice in the semiconductor industry to achieve the small packaging volumes required for mobile phone applications as for example done by ASE (http://www.asetwn.com.tw). The trend is clearly towards putting more and more functionality in a smaller space, leading to various concepts like System In Package[14,15], System On Chip or Integration in Substrates [16,17] and also area array interconnects[18]. The wafer bonding techniques in combination with high density electrical interconnects lead in the direction of 3D chip[19,20,21] and the semiconductor industry is investing in the MEMS market[22]. If these interconnects are through the wafer, multiple die stacks can be made. Through wafer interconnects through the MEMS die also allow interconnect to the IC with minimal loss of space while still having the front

MEMS side in contact with the outside environment[23]. There are many ways to make these as reported in literature. The MEMS transfer process described above can be repeated several times and extended to 3D packages[24]. Power transistors with through wafer vias made using a laser ablation process, 3D – metalization and -lithography are described in [25]. The Fraunhofer institute has developed an InterChip Via Technology (http://www.izm.fraunhofer.de) and many other techniques have been published [26,27,28,29,30,31,32,33].

6.2.1.3 MEMS IC integration

In this concept it is possible to make MEMS structures and integrated circuits on the same substrate by using compatible fabrication processes. This may lead to process complexity and may compromise performance[23]. On the other hand this approach solves the interconnection between MEMS and IC at the circuit manufacturing level. One example is a thin film encapsulated surface micro machining process completely compatible with a standard BiCMOS process[6]. In [34] a bulk micromachining process can be performed on the same substrate as a CMOS process by using deep trench isolation technology. A CMOS compatible pressure sensor is described in [35] and there are many others[36]. When placed next to each other in one substrate only the area used for interconnects is saved compared to the first category, assuming negligible area is consumed by the integrated interconnections. There are also processes that allow manufacturing of the MEMS structures on top of CMOS structures [37]. One MEMS IC integrated process allows manufacturing of the IC on top of the MEMS structure in the same substrate[38]. One other group has reported a new process to create MEMS and (simple) IC structures at the same time, rather then doing a MEMS process on a CMOS wafer or the other way around[39].

6.2.2 High Voltage MEMS control

In many cases design trade offs for electrostatic MEMS applications result in actuation voltages higher then the available supply voltage. For the moment this will be referred to as high voltage. In addition there are non-MEMS applications for example in the automotive and display industry that also require a high voltage. Therefore there is a need to generate a high voltage from a low(er) voltage. An outlook on methods to generate high voltage and ways to integrate high voltage generation is given in this section.

6.2.2.1 High voltage generation

Charge pumps can be used to generate a high voltage. If one considers a charged capacitor as a bucket full with electrons, the high voltage is generated by pumping more electrons in this bucket. In the case of switched capacitors, a number (N) capacitors (with capacitance C) that are connected in parallel are charged to a voltage V. The capacitors are then switched in series resulting in a total capacitance C/N charged to N*V (in the ideal case). If this series of capacitors is discharged in a load with a capacitance C_2<<C/N, the load will see approximately N*V in voltage. A somewhat similar approach consists out of a circuit of diodes and capacitors, a DC input voltage and a single switch. With every switch charge redistributes over the capacitors and the diodes force it to flow into the next level of capacitor, adding to the voltage at the output. The output voltage that these circuits can achieve depends (amongst others) on the loss of charge into parasitic capacitors of the circuit, the leakage rate in relation to the switching speed, the switching speed of the components and the voltage to start with. A Cockcroft-Walton voltage multiplier uses the same diode capacitor scheme but and AC input voltage [40].

Resonance effects can generate high amplitudes out of small driving force under the correct conditions. In electricity the LC

resonant circuit is a well known example. When the circuit is switched at the right time, a large overshoot is generated that can be used to charge a capacitor. In the micro electro mechanical domain a resonating mechanical spring-mass system can generate high voltages. In Coulomb damped resonators operated at constant charge, the voltage across the capacitor plates increases linearly with separation [41].

Transformers are in general use to change the ac voltage from primary to secondary. Piezo transformers perform the same function via a mechanical coupling between primary and secondary side and electrical mechanical transduction by the Piezo effect. Integrated transformers are being reported in literature, but not with very high gains [42]. A flyback converter is an easy way to develop a high voltage from a low voltage input. The output voltage is not determined by the turns ratio of the transformer. It is not really a transformer. Instead, energy is stored in the inductor as a magnetic field during the primary “on” phase and then delivered to the secondary during the secondary “flyback” phase. Typical flyback converter topologies have a ferromagnetic material as a core to increase the inductance of the windings as well as an output diode to prevent current during the “on” phase. Voltage step up circuits are available from for example Maxim. The MAX1771 generates voltages up to 300V using an external coil (http://www.maxim-ic.com).

6.2.2.2 Integration of high voltage generation

We have stated before that small size is an important requirement for many applications, including the ones that need a high voltage. Therefore there is a need for integration of the above mentioned principles since integration is the solution with the smallest size. An integrated circuit that can handle high voltage and has integrated high voltage generation capability would be preferred. There are many semiconductor manufacturers that have developed high voltage processes. A

family of 100V Bipolar CMOS DMOS processes on SOI has been presented in 2000 [43]. Processes up to 500V available as foundry service are described in [44]. These processes can also be compatible with low voltage processes on the same substrate, in order to make high voltage circuits that can interface with the low voltage world [45,41]. Integrated high voltage generation in a System In Package (SIP) containing a programmable microcontroller, a programmable DC/DC converter, a multi output HV interface and electrostatic MEMS actuators is described in [46]. A fully integrated high voltage CMOS DC-DC up converter for ultrasonic transmitters is presented in [47].

6.3 System level aspects

A smartlead as introduced in chapter 3 needs more then a packaged MEMS switch to function as a complete system. The two main aspects are smartlead packaging and communication between smartlead and IPG. The most straight forward solution for the packaging is to use a hermetic metal housing and feedthroughs as they are used today for chronic implantable medical devices. The communication part is most conveniently done by dedicating one electrical connection between smartlead and IPG to this purpose. The more electrodes are addressed over this wire, the less important this dedicated wire becomes.

Adding more electrodes is aimed at addressing the need to simplify the clinical procedure and improve therapy. It is clear that the required increased system complexity to be able to address the electrodes may not lead to reduced overall system reliability.

6.4 Conclusion

The bi-stable MEMS switch has advantages in comparison to a FET switch in the area of power consumption, DC breakdown

voltage, leakage current and contact resistance. The MEMS switch retains its setting in the absence of power and therefore, would be safer. The MEMS size, although larger then the FET, is within the requirements.

There is a general need for a small smart system to control MEMS and a means to generate a high actuation voltage from a lower supply voltage. The availability of Small Smart Modules will increase the ease of applicability of MEMS components, which is of great interest to the MEMS community. An outlook has been provided on three conceptually different ways for MEMS IC interconnect, namely MEMS die and IC next to each other, a separate MEMS die and IC stacked on top of each other and MEMS-IC integration. Several ways of (integrated) high voltage generation have also been given.

A lot of MEMS switch material is being published or appears as result of new searches and there are several companies active in the field of MEMS switches ([48,49,50,51,52,53,54,55,56] http://www.teravicta.com ; http://www.radantmems.com ; http://www.nais-e.com/relay/mems ; http://www.mems.mech.tohoku.ac.jp ;). Further developments could be in the area of chip scale implantable medical devices and micro electrodes.

6.5 References

[1] Sze, S M 1981 *Physics of Semiconductor Devices* ed Sze, S M New York John Wiley & Sons 0-471-05661-8

[2] Oberhammer, J 2004 *Novel RF MEMS Switch and Packaging Concepts* Microsystem Technology; Department of Signals, Sensors and Systems; Royal Institute of Technology

[3] Amerasekera, E A and Campbell, D S 1987 *Failure Mechanisms in Semiconductor Devices* New York John Wiley & Sons 0 471 91434 7
[4] Receveur, R A M, Zickar, M, Marxer, C, Larik, V, and De Rooij, N F 2006 Wafer level hermetic package and device testing for a SOI-MEMS switch for biomedical applications *Journal of Micromechanics and Microengineering* **16** 676-683
[5] Chae, J, Kulah, H, and Najafi, K 2004 An in-plane high-sensitivity, low-noise micro-g silicon accelerometer with CMOS readout circuitry *Journal of microelectromechanical systems* **13** 628-635
[6] Aigner, R, Opperman, K-G, Kapels, H, and Kolb, S 2001 "Cavity-Micromachining" Technology: Zero-Package Solution for Inertial Sensors *The 11th International Conference on Solid-State Sensors and Actuators* vol 11 Piscataway, NJ, United States IEEE pp 186-189
[7] Despont, M, Drechsler, U, Yu, R, Pogge, H B, and Vettiger, P 2003 Wafer-scale microdevice transfer/interconnect: from a new integration method to its application in an AFM-based data storage system *Transducers 2003* **2003** 1907-1910
[8] Tilmans, H A C, Van De Peer, M, and Beyne, E 2000 The indent reflow sealing (IRS) technique - A method for the fabrication of sealed cavities for MEMS devices. *Journal of microelectromechanical systems* **9** 206-217
[9] Elger, G, Shiv, L, Heschel, M, Veneau, J F, and Glukh, K 2004 Low Cost Hermetic Wafer-Level Packaging of Magnetic Proximity MEMS Switches *IMAPS*
[10] Kilian, A, Elger, G, Hase, A, Shiv, L, Heschel, M, and Kuhmann, J 2003 Hermetic, small form factor package for edge emitting opto-electronic devices *IMAPS*
[11] Hedenstierna, N, Habibi, S, Nilsen, S M, and Kvisteroy, T 2003 Bulk Micromachined Angular Rate Sensor Based on

the 'Butterfly'-Gyro Structure *Micro Mechanics Europe Workshop* Delft, The Netherlands Delft University of Technology pp 175

[12] Jakobsen, H, Lapadatu, A, and Kittilsland, G 2001 Anodic Bonding for MEMS *Symposium on Semiconductor Wafer Bonding* Pennington, NJ, United States The Electrochemical Society

[13] WO 2004/013898 A2 PCT/US2003/023255 Pashby, G. and Slater, T. G. 12-2-2004 *Sealed integral MEMS switch* Siverta Inc.

[14] Smolders, A B, Pulsford, N J, Philippe, P, and Van Straten, F E 2004 RF SiP: The next wave for wireless system integration *IEEE Radio Frequency Integrated Circuits Symposium, RFIC, Digest of Technical Papers* Fort Worth, TX, United States Institute of Electrical and Electronics Engineers Inc., Piscataway, United States pp 233-236

[15] Imec Advanced packaging technologies to bridge the interconnect technology gap 2005 http://www.imec.be

[16] Chanchani, R, Bethke, D T, Webb, D B, Sandoval, C, and Wouters, G 2005 Integrated Substrate Technology and its RF characterization *Micro System Technologies* Poing (DE) Franzis Verlag GmbH pp 289-298

[17] Garchon, G, Jenei, S, Carbonell, L, van Hove, M, Decoutere, S, De Raedt, W, Maex, K, and Beyne, E 2003 High Q RF Inductors on standard silicon realized using wafer level packaging techniques

[18] 2004 *Chip Sandwich means more memory for mobile ICs* Electronic Design Europe vol November/December, pp 6-6

[19] Thompson, T E 2006 *Wafer Bonding Reaches New Highs ... and Lows!* Chip Scale Review vol 2006,

[20] Lammers, D 2006 *Sematech targets infrastructure for 3-D chips* EETimes vol 2006, pp 1-2

[21] Nunes, R 2005 *Automated Triple-Stack Wafer Bonding* MicroNews vol 2005, Yole Developpement pp 6-6

[22] Yole Developpement and QinetiQ 2004 *MEMSonIC 04*
[23] Cheng, C H 2005 *Electrical through-wafer interconnect for integrated sensors and actuators* Stanford Univeristy
[24] Pogge, H B, Yu, R, Despont, M, Drechsler, U, and Vettiger, P 2003 A Versatile 2D/3D SoC/SoP Device Fabrication Technology *Micro System Technologies* pp 256-263
[25] de Samber, M, van Grunsven, E, Rutjes, C, Grob, T, Kettelarij, H, and van Veen, C 2004 Through wafer vias for power transistors *European Microelectronics and Packaging Symposium, Prague 16th to 18th June 2004*
[26] Alavi, M, Scheithauer, H, and Sandmaier, H 2004 *New chip interconnection technology for smar cards and smart labels* MSTNews vol 2004, pp 16-17
[27] Benkart, P, Munding, A, Kaiser, A, Bschorr, M, Heittmann, A, Hubner, H, Pfleiderer, H-J, Kohn, E, and Ramacher, U 2005 3-Dimensional Chip Integration Scheme *Micro System Technologies* Poing (DE) Franzis Verlag GmbH pp 281-288
[28] Crawley, D, Nikolic, K, Forshaw, M, Ackermann, J, Videlot, C, Nguyen, T N, Wang, L, and Sarro, P M 2003 3D molecular interconnection technology *Journal of Micromechanics and Microengineering* **13** 655-662
[29] Nga, P P, Boellaard, E, Burghartz, J N, and Sarro, P M 2004 Photoresist coating methods for the integration of novel 3-D RF microstructures *Journal of microelectromechanical systems* **13** 491-499
[30] Nguyen, N T, Boellaard, E, Pham, N P, Kutchoukov, V G, Craciun, G, and Sarro, P M 2002 Through-wafer copper electroplating for three-dimensional interconnects *Journal of Micromechanics and Microengineering* **12** 395-399
[31] Videlot, C, Ackermann, J, Fages, F, Nguyen, T N, Wang, L, Sarro, P M, Crawley, D, Nikolic, K, and Forshaw, M 2004 Polymer interconnections for 3D-chip stacking

technology: Directional volume patterning of flexible substrates with conducting polymer wires *Journal of Micromechanics and Microengineering* **14** 1618-1624

[32] Iscoff, R 2000 *New Process Forms Die Interconnects by Vertical Wafer Stacking* Chip Scale Review vol 2000,

[33] Li, X, Abe, T, Liu, Y, and Esashi, M 2001 High density electrical feedthrough fabricated by deep reactive ion etching of pyrex glass *Unknown*

[34] Yan, G, Zhu, Y, Wang, C, Zhang, R, Chen, Z, Liu, X, and Wang, Y Y 2004 Integrated bulk-micromachined gyroscope using deep trench isolation technology *International Conference on Micro Electro Mechanical Systems* vol 17 pp 605-608

[35] Pakula, L S, Yang, H, Pham, H T M, French, P J, and Sarro, P M 2004 Fabrication of a CMOS compatible pressure sensor for harsh environments *Journal of Micromechanics and Microengineering* **14** 1478-1483

[36] Ouellet, L 2003 Low-temperature MEMS processing for intelligent MEMS over CMOS *CMC Technical Session - Symposium on microelectronics research & development in canada (MR&DCAN 2003)*

[37] Bifano, T G, Bierden, P A, Cornelissen, S, Dimas, C E, Lee, H, Miller, M, and Perreault, J A 2002 Large-scale metal MEMS mirror arrays with integrated electronics *The International Society for Optical Engineering* vol 4755 The International Society for Optical Engineering pp 467-476

[38] Partridge, A 2003 *A lateral Piezoresistive Accelerometer with Epipoly Encapsulation* Stanford University, CA, United States

[39] Draper, B L, Okandan, M, Mani, S S, and Bennett, R S 2004 A novel method of fabricating integrated FETs for MEMS applications *Microelectromechanical Systems, Journal of* **13** 500-504

[40] Jieh-Tsorng, W and Kuen-Long, C 1998 MOS charge pumps for low-voltage operation *IEEE Journal of Solid-State Circuits* **33** 592-597

[41] Mitcheson, P D, Green, T C, Yeatman, E M, and Holmes, A S 2004 Architectures for vibration-driven micropower generators *Microelectromechanical Systems, Journal of* **13** 429-440

[42] Vasic, D, Sarraute, E, Costa, F, Sangouard, P, and Cattan, E 2005 Piezoelectric micro-transformer based on SOI structure *Sensors and Actuators A: Physical* **117** 317-324

[43] Van Der Pol, J A et al. 2000 A-BCD: An economic 100V RESURF silicon-on-insulator BCD technology for consumer and automotive applications *IEEE International Symposium on Power Semiconductor Devices and ICs (ISPSD)* Toulouse Institute of Electrical and Electronics Engineers Inc. pp 327-330

[44] TSMC High Voltage Technology 2006 http://www.tsmc.com;

[45] Richard, J F, Lessard, B, Meingan, R, Martel, S, and Savaria, Y 2003 High Voltage Interfaces for CMOS/DMOS Technologies *The IEEE Northeast Workshop on Circuits and Systems*

[46] Saheb, J-F, Richard, J F, Meingan, R, Sawan, M, and Savaria, Y 2005 System integration of high voltage electrostatic MEMS actuators *International IEEE-NEWCAS Conference* IEEE pp 155-158

[47] Chebli, R and Sawan, M 2004 A CMOS high-voltage DC-DC up converter dedicated for ultrasonic applications *IEEE International Workshop on System-on-Chip for Real-Time Applications* IEEE pp 119-122

[48] Oberhammer, J and Stemme, G 2004 S-shaped film actuator for low-voltage high-isolation MEMS metal contact switches *Proceedings of the IEEE International Conference on Micro Electro Mechanical Systems (MEMS)*

Maastricht, Netherlands Institute of Electrical and Electronics Engineers Inc., Piscataway, United States pp 637-640

[49] Masters, N D and Howell, L L 2003 A self-retracting fully compliant bistable micromechanism *Journal of microelectromechanical systems* **12** 273-280

[50] US 6,307,169 B1 Sun, X-Q, Parsey, J. M., Huang, J-H, and Xu, J-H 2001 *Micro-Electro Mechanical Switch* Motorola Inc.

[51] Oberhammer, J and Stemme, G 2004 S-shaped film actuator for low-voltage high-isolation MEMS metal contact switches

[52] Eloy, J C 2004 *New Emerging MEMS devices* MicroNews vol 2004, pp 4-5

[53] US 6,388,359 B1 Duelli, M., Friedrich, D., and Hichwa, B. 2004 *Method of actuating MEMS switches* Optical Coating Laboratory Inc.

[54] Pruitt, B L, Woo-Tae, P, and Kenny, T W 2004 Measurement system for low force and small displacement contacts *Microelectromechanical Systems, Journal of* **13** 220-229

[55] Coutu, J, Kladitis, P E, Leedy, K D, and Crane, R L 2004 Selecting metal alloy electric contact materials for MEMS switches *Journal of Micromechanics and Microengineering* **14** 1157-1164

[56] Brazzle, J D, Taylor, W P, Ganesh, B, Price, J J, and Bernstein, J J 2005 Solution hardened platinum alloy flexure materials for improved performance and reliability of MEMS devices *Journal of Micromechanics and Microengineering* **15** 43-48

7 Final Conclusions

A large range of microsystems is being investigated for implantable applications. Sensors, micro electrodes, drug and gene delivery devices, micro machined ultrasound transducers, MOEMS, micro actuators, surgical tools, micro surface topology, micro fabricated bio degradable scaffolds and other examples have been presented. These micro systems find application in a wide range of clinical areas including cardiology, neurology, ophthalmology, orthopedics, drug delivery (for various clinical areas), surgery, endocrinology, tissue engineering etcetera. There are 105 active and 70 commercial end items from a total of 142. The majority of the 37 passive end items (25 of 37) are prototypes or animal research devices created by academic organizations. From the 105 active end items, 18 (13% of total number of end items) are classified as products, all made by commercial organizations. Note also that from these 18 products, there are only 2 for chronic use. There is still considerable potential for permanent implantable micro system products to come, judged by the number of end items in clinical- (17), animal- (13) and proto- (20) phase in this category. The path from academic research to commercialization, clinical trials and market introduction of permanently implantable products is long, however, as indicated by the average year of first publication of end items that are still in the animal- (1994, n=7) or clinical- (1993, n=11) phase. The major technology-market combinations are Sensors for Cardiovascular, Drug Delivery for Drug Delivery and Electrodes for Neurology and Ophthalmology applications. Together these form 51% of all end items. Pressure sensors are the most common type of sensors and there is just one product (considered to be an implantable micro system) in the neurological area. Hermetic housings are traditionally made from

titanium, tantalum or niobium. Micro machined ceramic packages, glass sealed packages and polymer encapsulations are also used. Glass to metal seals are used for feedthroughs. Interconnection techniques like flip chip, wirebonding or conductive epoxy as used in the semiconductor packaging and assembly industry are also applied for manufacturing implantable devices. Coatings are used to improve the interface of the implant with the body organs with polymers or metal as coating material. Much development effort is put in implantable batteries. As an alternative, rechargeable batteries were introduced or concepts in which energy is provided from the outside based on inductive coupling. Long term developments aiming at autonomous power are for example based on electrostatic conversion of mechanical vibrations. Communication with an implantable device is usually done through an inductive link although optical means also have been reported. Entirely passive circuits that can be wirelessly probed to communicate information from inside to outside the body have been described. A list of biocompatible and biostable materials does not exist, since the mechanisms involved depend on many details, like material processing, shape, finish, post treatment and impurities but also on the place and duration of use. There is a large range of materials commonly used in micro fabrication used for implantable microsystems including silicon, polymers and metals.

A bi-stable micro electro mechanical switch has been designed and prototyped with a measured initial contact resistance of approximately 5Ω. Breakdown voltage between the two contact members in OFF state is 300V, while breakdown between actuators and contact member occurs at 150V. The energy needed to change state is estimated to be 0.2nJ. The switch is bi-stable, meaning that it consumes no energy in either the ON or the OFF state. The total size of the structure including bondpads and actuators is 1374μmx1320μm. Advantages over FET

switches in terms of power consumption, contact resistance and breakdown voltage have been achieved. With measurements on both mono-stable and bi-stable test structures we have demonstrated that our theory compares well with experiment. All measured results were within 10% of the theoretical expectations. Furthermore we have demonstrated that it is possible to create an initial contact resistance below 5Ω with a contact force in the order of 10μN.

A process for creating hermetic sealing with feedthroughs through the lid using wafer level glass to silicon anodic bonding has been presented. Each contact is electrically isolated in the SOI device layer and individually surrounded by a sealing ring. Structures bonded at 250 kg, 230 V, 365 ºC pass thermal and mechanical stress tests according to MIL-STD-883 and meet the requirements for biomedical applications for these aspects. Numerical analysis shows that the thermal stresses in the glass silicon stack are a factor of 20 lower then the bond strength, which is confirmed by shear strength measurements to be in the order of 20 MPa. Contact measurements carried out in an N_2 atmosphere inside the wafer level package demonstrate that ruthenium covered contacts are robust for 10^6 cycles, which is a factor of 100 more then gold coated contacts.

Reliability theory provides a quantitative basis for addressing this topic. Typical Active Implantable Medical Device Essential Requirements are protection against defibrillation and Magnetic Resonance Imaging (MRI) and electrical surgery compatibility. MEMS reliability is different from IC reliability for a variety of reasons, like the diversity in processes and functions, the lack of large sample sizes and test data and the unknown character of some failure mechanisms. Nevertheless carefully designed MEMS can be highly reliable and good design practices and guidelines have been proposed. A large range of possible failure mechanisms has been formulated for the MEMS switch, including mechanical, electrical, material, processing and other

type of failure mechanisms. The theory of the dynamics of the MEMS switch has been given. An experimental and theoretical method to describe resonance and bouncing behavior is given. Measurements of resonance peaks not only provide the location of the resonance frequency, but also provide a measure for the degree of damping of the structure. The electrical method that is described is applicable for automated reliability screening during manufacturing. A 125μs pulse is sufficient to switch from OFF to ON state. The required pulse amplitude is not dependant on the pulse width.

The bi-stable MEMS switch has advantages in comparison to a FET switch in the area of power consumption, DC breakdown voltage, leakage current and contact resistance. The MEMS switch retains its setting in the absence of power and therefore, would be safer. The MEMS size, although larger then the FET, is within the requirements.There is a general need for a small smart system to control MEMS and a means to generate a high actuation voltage from a lower supply voltage. An outlook has been provided on three conceptually different ways for MEMS IC interconnect, namely MEMS die and IC next to each other, a separate MEMS die and IC stacked on top of each other and MEMS-IC integration. Several ways of (integrated) high voltage generation have also been given. Since the MEMS switch field is active and includes commercial players means that there are real advantages to gain. Further possible future developments could be in the area of chip scale implantable medical devices and micro electrodes.

Acknowledgements

During the years I have had the pleasure to work with many people who have contributed to this thesis. Thanks to Professor Nico de Rooij of the Institute of Microtechnology (IMT) of the University of Neuchatel for putting me on the publishing path with the suggestion to submit an abstract for MEMS 2004 and for the always warm welcome at the IMT. Thanks to Cornel Marxer, Michael Zickar and Francois Duport for all the MEMS design and processing done at the COMLAB at IMT. Without samples no measurements! My time spend at the IMT and in the cleanroom was very pleasant. In particular I would like to recall here the HF etching with “das Siebli”. Thanks also to Wilfried Noell of IMT and Paul Weiss of Colybris for valuable discussions and to all the other IMT scientists for pleasant encounters.

Part of this work has been done in the context of Medtronic Quest Project L2006.000 Smartlead and The Swiss Innovation Promotion Agency KTI/CTI Project Nr. 7250.2 LSPP-LS Chip Scale Implantable Medical Device: Bi Stable Micro Electro Mechanical Switch for Smartlead (Mediclic). The management team of the Medtronic Bakken Research Center (BRC), in particular my departmental manager Vincent Larik, have provided the work environment in which these type of projects are possible. Thanks also to Mark Hjelle, Keith Miesel and Jo Lissens (all of Medtronic) for their support. Special thanks to Fred Lindemans, VP and general manager of the Medtronic BRC for supporting my ambition to write a thesis, for taking the time to review my manuscripts and provide constructive critical comments and sponsoring the printing of this thesis.

Rob Leinders, thanks for spending time with me in the lab, performing measurements on these strange devices (for an IC design engineer) and Richard Houben for valuable discussion. Thanks to the interns Ruben Burgers, Roel Woering and

Lennaert Klerk for their contributions. Thanks to R.C. Hamlen and L. Nygren from Medtronic for capacitance calculations and ruthenium deposition and R.F. Wolffenbuttel and L.A. Rocha from Delft University of Technology for performing the relative capacitance measurements. This thesis has been improved by the gratefully acknowledged proofreading of Pierre André Grandjean, Technical Fellow and Bakken Fellow at Medtronic. For those that are accidentally not mentioned here: thank you too.

Last but not least I would like to thank my lovely Cecile for her support and patience during the many hours spend on this at home during the past years in which we also expanded our family. Maurice, Luc, Pascalle and Chris thanks for providing distraction.

Bibliography

Invited topical review paper (peer reviewed):

R.A.M Receveur, F.W. Lindemans and N. F. De Rooij, Micro System Technologies for Implantable Applications, Journal of Micromechanics and Microengineering 2007.

Peer reviewed papers:

R. A. M. Receveur, M. Zickar, C. Marxer, V. Larik, and N. F. De Rooij. Wafer level hermetic package and device testing for a SOI-MEMS switch for biomedical applications. Journal of Micromechanics and Microengineering 16:676-683, 2006.

(selected by the editors of the Institute of Physics IOP as featured article, IOP select article and included in highlights of 2006)

R. A. M. Receveur, C. R. Marxer, R. Woering, V. C. M. H. Larik, and N. F. deRooij. Laterally Moving Bistable MEMS DC Switch for Biomedical Applications. Microelectromechanical Systems, Journal of 14 (5):1089-1098, 2005.

Conference proceedings:

R. A. M. Receveur, C. Marxer, N. F. De Rooij, and M. Zickar. Wafer Level Hermetic Package and Feedthrough for SOI-MEMS switch. Micro System Technologies 2005. Reichl H. Poing, Germany:Franzis Verlag GmbH. 353-359, 2005. 10-05-2005.

R. Receveur, C. Marxer, F Duport, R. Woering, V. Larik, and N. F. De Rooij. A laterally moving bi-stable MEMS DC switch for biomedical applications. International Conference on Micro Electro Mechanical Systems. Piscataway, NJ, United States:IEEE. (17):854-856, 2004.

Invited oral presentations

Rogier Receveur; Micro-mechatronics in bio-medical applications; School of Mechatronics and Microsystems; April 10 2003; Delft University of Technology, Delft, The Netherlands

M. Zickar, W. K. Noell, R. A. M. Receveur, V. Larik, and N. F. De Rooij. 8x8 bi-stable Relay Array for Implantable Applications. International workshop on wearable micro- and nanosystems for personalized Health. 2006. 01-30-2006. http://www.phealth-2006.com

R.A.M. Receveur, Micro fabricated switch for implantable electrical stimulation application, Biocompatible Electronics, May 9-10, 2007 Neu-Ulm, www.hanser.de/biocompatible-electronics

Posters presentations

Michael Zickar, Wilfried Noell, Rogier Receveur, Vincent Larik, Paul Weiss, Nico de Rooij; Chip Scale Implantable Medical Device: Bi-stable Micro Electro Mechanical Switch for Smartlead ("MEDICLIC"); CTI Medtech Event 2005; 6 september 2005; Bern, Switzerland

Michael Zickar, Wilfried Noell, Rogier Receveur, Vincent Larik, Paul Weiss, Nico de Rooij; Chip Scale Implantable Medical Device: Bi-stable Micro Electro Mechanical Switch for Smartlead ("MEDICLIC"); CTI Medtech Event 2006; 30 august 2006; Bern, Switzerland

Book chapter:

S. Audet, J. Carney, G. Haubrich, E. Herrmann, V. Larik, R. A. M. Receveur, E. Scott, and G. Vaughn. Industrial Applications: Medical and Health Care. In: Comprehensive Microsystems, edited by Y. B. Gianchandani, O Tabata, and H. Zappe,Reed Elsevier, to be published

Magazine article:

M. R. S. Hill and R. A. M. Receveur. Technological Developments sustain the trend in medical product miniaturization. Reed Elsevier. International Hospital Equipment & Solutions (September), 2006.

Patents:

US7190245
Multi-stable MEMS switches and methods of fabricating same
Issued March 13, 2007

US 7,228,177
Chip Scale biostable interconnect for permanent implantable medical devices
June 5, 2007

US2005/0115811 Application No. 10/973,117
MEMS switching circuit and method for an Implantable Medical Device
October 26, 2004 filing date

US Application No. 11/066,820
Wafer Level Hermetically Sealed MEMS device with FeedThrus for Biomedical Applications
February 25, 2005 filing date

Biography

Rogier Alphons Maurice Receveur was born in Capelle aan den IJssel, The Netherlands, on February 9 1969 and holds a master degree in applied physics from Delft University of Technology, Delft, The Netherlands from 1993.

He has worked at Océ Technologies and is now a Senior R&D Engineer at Medtronic Bakken Research Center, Maastricht, The Netherlands. His research interests include micro systems and sensors for biomedical applications.

Ir. Receveur is a member of the Netherlands' Physical Society (NNV), the Royal Dutch Society of Engineers (Kivi), the European Society for Engineering and Medicine (ESEM), the Dutch Micro- and Nano- Network (MINACNED) and the European Microsystems Network (NEXUS).